Univerzita Tomáše Bati ve Zlíně
Fakulta technologická

Doctoral Thesis

Polymerní speciální a multifunkční folie

Polymer Special and Multifunctional Films

Autor: **Ing. Bc. Alice Tesaříková Svobodová**
Studijní program: Chemie a technologie materiálů (P2808)
Studijní obor: Technologie makromolekulárních látek (2808V006)
Školitel: doc. Ing. Dagmar Měřínská, Ph.D.

Zlín, 2018

Published by **Tomas Bata University in Zlín** in the **Doctoral Thesis Edition.**
The publication was issued in 2018.

Klíčová slova: *polymerní folie*, *nanokompozity, mechanické vlastnosti, bariérové vlastnosti*

Key words: *polymeric films, nanocomposites, mechanical properties, barrier properties*

The full text of the dissertation is available in the library of Tomas Bata University in Zlín.

ABSTRAKT

Předložená doktorská práce je zaměřena na přípravu, vlastnosti a využití polymerních speciálních a multifunkčních folií. Je zde nastíněna problematika přípravy a zlepšení některých vybraných vlastností, jako například mechanických a bariérových. Polymerní folie však nejsou nutně jen bariérové a mnohé z nich nalezneme nejen v potravinářském průmyslu, ale i v jiných oblastech průmyslové výroby. Doktorská práce se tedy věnuje nejen foliím s vylepšenými bariérovými vlastnostmi, ale i foliím vyrobeným z recyklovaného materálu.

Disertační práce se skládá ze dvou částí. Teoretická část je věnována stručnému popisu polymerních, vícevrstvých, multifunkčních folií a použitým polymerním matricím ze skupiny polyolefinů, jejich kopolymerů a vinylových polymerů. V práci jsou také popsány výrobní postupy a metody použité k hodnocení vybraných vlastností folií. Hlavní pozornost je věnována nanoplnivům a jejich použití v polymerních foliích.

Druhá část práce předkládá výsledky získané během doktorského studia formou krátkého shrnutí jednotlivých publikovaných článků. Výzkumné práce v plném znění jsou k dispozici v samém závěru práce.

ABSTRACT

Doctoral thesis is focused on preparation, properties and utilization of polymer special and multifunctional films. Issues of preparation and enhancement of selected properties, such as mechanical or barrier, are outlined. However, polymer films are not necessarily applied only as barriers. A variety of them may be emploed in the the food industry or in the other areas of industrial production as well. Therefore, doctoral thesis focuses not only on films with improved barrier properties, but also on films produced from recycled materials.

Thesis is divided into two main parts. Theoretical part is devoted to brief description of polymeric, multilayer, multifunctional films and applied polymer matrices from the group of polyolefins, their copolymers and vinyl polymers. The paper also describes manufacturing processes and methods used to evaluate selected film properties. Major focus is placed on nanoparticles and their application in polymeric films.

The second part presents the results obtained during the doctoral study in the form of a short summary of published articles. Full-text research is to be seen at the end of the paper.

ACKNOWLEDGMENTS

I would like to thank everyone who contributed to accomplish this research and thesis.

First and foremost, I would like to express my deepest gratitude to my supervisior, assossiate professor Dagmar Měřínská for her excellent guidance, care, patience, and for providing a motivating atmosphere.

I would also like to thank my family for the continuous support and standing by me through the good times and bad.

CONTENT

THEORETICAL BACKROUND

1 INTRODUCTION TO POLYMER SPECIAL AND MULTIFUNCTIONAL FILMS

Special and multifunctional polymer films have become well-established in many types of manufacturing industries. Polymer films are predominantly used as packaging materials, some may be even applied as auxiliary materials in the industry. Although plastics are not the only packaging material, they have gradually replaced more traditional packaging materials, such as metal, glass and wood. It has been estimated that approximately 75 % of all films produced in Europe are used in the packaging industry[1].

Polymeric films usage is associated with product protection against the climatic influences, aggressive gases and aerosols, against the UV radiation, oils, fats, acids and bases, but also against microbial attacks. Not surprisingly, the food industry is one of significant consumers of polymer films. Film materials from polyolefins and their copolymers, polyesters, polyamides, polystyrene and vinyl polymers are those the most used due to their specific properties [2].

Application of fillers into polymer films provides additional possibilities to enhance the properties of packaging materials. Especially nanoparticles in polymeric matrix can substantially improve some of the properties and consequently the properties of the final product films, even with the minimum of nanofibre content. If matrix is formed by polymer component and filler with at least one dimension in nanoscale, the final product is referred to as a nanocomposite. Nanofillers may occur in the form of nanoculars, nanopowders or nanotubes [3, 4].

Clay materials contain nanoparticles in the form of nanopowders and are applied in the plastics and building industry, and also in the ceramics and agriculture.

If nanofibres exfoliation is gained in polymer matrix, clay nanoparticles may significantly affect the properties of prepared polymer, enhance mechanical properties and reduce the gas and water vapor permeability [5, 6].

As it was already mentioned above, polymeric films may not necessarily act only as a barrier, but may also be used as waterproof films used in the building industry. Individual layers of floor coverings between the foils may be arranged as well. What is more, the alternative to replace some of these multilayer films with recycled materials attracts growing attention. Application of recycled PVB as a possible substitution for PVC in these products appears to be a significant opportunity to reduce the amount of these waste materials in landfills [7, 8].

2 POLYMER FILMS

Polymeric material films are flat units with a thickness of about 2 μm. Common features of these polymeric films include barrier properties, resistance to high and low temperatures, mechanical resistance, weldability and printability. Properties required by the packaging industry are often impossible to meet by only one specific polymeric material.

A suitable solution is a polymeric film comprising multiple layers of different polymer types providing desired properties, especially barrier ones.

By combining two or more polymers, it is possible to achieve enhanced foil properties, such as tensile and impact strength, ductility and flexibility. Polymeric films are characterised by their chemical composition, the order and thickness of individual layers. A layer in a direct contact with food must suit the properties of health-conscious material, such as PE, PP and EVA. On the other hand, materials as PVC or PVB may be applied for non-food applications. Outer layers must perform certain specific traits, such as resistance against the UV radiation, abrasion and water. Internal adhesive layers, often being referred to as "tie - layers", are mostly ionomers, EVA, EMAA and melamine hydrides in a very thin layer of about 4 g / m². The cost of used polymeric materials is also a very important criterion of the individual film layer choice [5, 9, 10].

2.1 Main materials of polymer films

Carrier materials form a skeleton or the basis of all polymeric films. These include polyethylene, polypropylene, EVA, Surlyn, ethylene-octene copolymer, PVC and PVB.

Polyethylene (PE)

It is the most popular polyolefin produced by ethylene polymerization. It was prepared by heating diazomethane by Hans von Peckmann for the first time in 1898. Nevertheless, the history of polyethylene production dates back to 1935. Until 1953 it was manufactured only in a high-pressure way. In 1953 Ziegler's catalyst was applied to enable polyethylene production at normal pressure [11]. Today, PE is one of the most common packaging materials. Several types of polyethylene have been distinguished differing in the macromolecule structure (chain branching) and density, which is reflected in its properties. Mostly HDPE, LDPE and LLDPE are applied in the packaging industry [12, 13].

Polypropylene (PP)

Discovery of polypropylene is associated with Professor Natta from Polytechnic in Milan in 1954. Special polymerization initiator, known as stereospecific catalyst, was employed to polymerize propylene. Natt's discovery was closely connected with Professor Ziegler's work on low-pressure ethylene polymerization.

Structural composition of polypropylene influences its resistance at higher temperatures. Softening point of pure polypropylene is 176 °C. Conventional commercial product has a softening point slightly lower, at approximately 165 °C. Polypropylene is also remarkable for its excellent electro-insulating and dielectric properties [14, 15].

Chemical resistance of polypropylene is related to its chemical structure. Polypropylene is insoluble in organic solvents. In chlorinated and aromatic solvents, polypropylene can be dissolved at higher temperatures. Polypropylene is also resistant to acids and alkalis. Addition of stabilizers may prevent unfavourable effects of air oxygen and ozone [16, 17].

Ethylene vinyl acetate copolymer (EVA)

Ethylene vinyl acetate (EVA) is produced by radical copolymerization of branched ethylene (LDPE) with vinyl acetate in a temperature range from 180 to 250 °C and the pressure of 140 MPa. Its crystallinity decreases with an growing vinyl acetate content. That improves toughness, flexibility and adhesion of the material to the heat. Ideal content of vinyl acetate is considered to be up to 20%. In such conditions EVA acquires properties similar to those of softened PVC. EVA is mainly used for the production of stretch and shrinking films, packaging materials, hoses, lacquers, adhesives and may substitute for softened PVC. Films made from EVA copolymer can be welded at the temperatures between 105 and 135 °C. Ethylene vinyl acetate can be dissolved in ketones and aromatic or chlorinated hydrocarbons [15, 16].

Surlyn

DuPont launched Surlyn A, which is a trade name for a copolymer of ethylene with vinylcarboxylic acids, such as methacrylic acid (EMAA) or acrylic acid (EAA) with free carboxyl groups converted to salts derived from metals of groups I or II. It is a flexible polymer with properties similar to polyethylene LDPE. However, these copolymers perform higher strength and toughness, enhanced hot grip and better adhesion to other materials [15].

EOC

In addition to commonly used types of polyolefins, special polymers have also been attracting the attention of the professional public. Ethylene-octene copolymer (EOC) is one of them, suitable particularly for the use in the combination with aforementioned polymers, especially PP. Ethylene-octene copolymer developed by Dow Chemical Company (Delaware, USA) with metallocene catalysts is being recognized thanks to its eminent properties both in the research and industry [4-6]. The presence of octen in EOC comonomer affects the level of crystallinity and provides a greater flexibility. EOC may be considered as polyolefin (POE) and octane content in copolymer typically ranges from 17 to 45 wt. % [18-20].

Polyvinyl chloride (PVC)

PVC is thermoplastic, slightly branched (< 10 branches per molecule) polymer. Chlorine atom in the molecule increases intermolecular attracting forces causing both the stiffness and hardness of the polymer. PVC powder lasts temperatures of 60-65 °C on a long-term basis. It softens at temperatures of about 80 °C and warming above 100 °C causes a slow decomposition together with removing hydrogen chloride (HCl). Stabilizers may cease HCL releasing even at temperatures exceeding 160 °C. PVC properties depend on its viscosity, which is defined by K-value. This value divides PVC into a hard (K = 56-65) and soft type (K = 65-80). The higher K value is, the better mechanical properties of the film are gained, but the worse it could be processed. Plasticized PVC is used to produce waterproofing foils and floor coverings [21, 22].

Polyvinyl butyral (PVB)

PVB is the most significant polymer of polyvinylacetals formed as a condensation product of the reaction of polyvinyl alcohol and aldehydes. Foils made of polyvinylacetals perform an excellent adhesion to metals and glass thanks to hydrophilic vinyl alcohol and vinyl acetate units.

Concerning applications, PVB may be divided into 3 groups - showing low, medium and hight viscosity. High viscosity type is utilized as an adhesive interlayer of safety glasses. Extrusion temperatures reach more than 150 °C. Generated foils are highly plastic and adhesive [23, 24].

2.2 Multilayer films

Characteristics of simple and multilayer barrier films

Common features of polymeric films include barrier properties, resistance to high or low temperatures, transparency, translucency, mechanical resistance, weldability and printability. As mentioned earlier, film properties required by the packaging industry are not often possible to guarantee by only one polymeric material. Polyolefins, polyvinylchloride, polystyrene, polyamides, polyvinyl alcohol and polyesters are used as polymer materials suitable for single (homogeneous) films for both food and non-food applications [5, 25]. *Combining two or more polymeric materials may enhance some properties, such as* tensile and impact strength, ductility, flexibility, chemical and heat resistance, water vapor permeability and processability. Characteristic properties of multi-layered films are defined by their chemical composition and the order and thickness of individual layers. It is necessary to follow certain principles to determine the order of each layer. Layers in a direct contact with food must be produced of non-toxic materials (PE, PP, PETP); on the other hand, materials based on PS, PVC, PVDC may be applied in non-food utilizations. Outer layers must correspond with other specific requirements, such as the resistance against the UV radiation, abrasion,

solvents, oils and water. Internal adhesive layers known as "tie - layers" are mostly ionomers, EVA, EMAA and melamine hydrides applied in a very thin layer of about 4 g / m². Economic reasons limit the use of recycled materials in barrier foils only to restricted quantities. Unfortuately, the price of polymeric materials is still a significant criterion for individual film layer choice [25, 26].

As it has been mentioned earlier, suitable solutions are the films *containing multiple layers of different types of polymers*, in which the individual layers provide desired properties, in particular the barrier ones [27, 28].

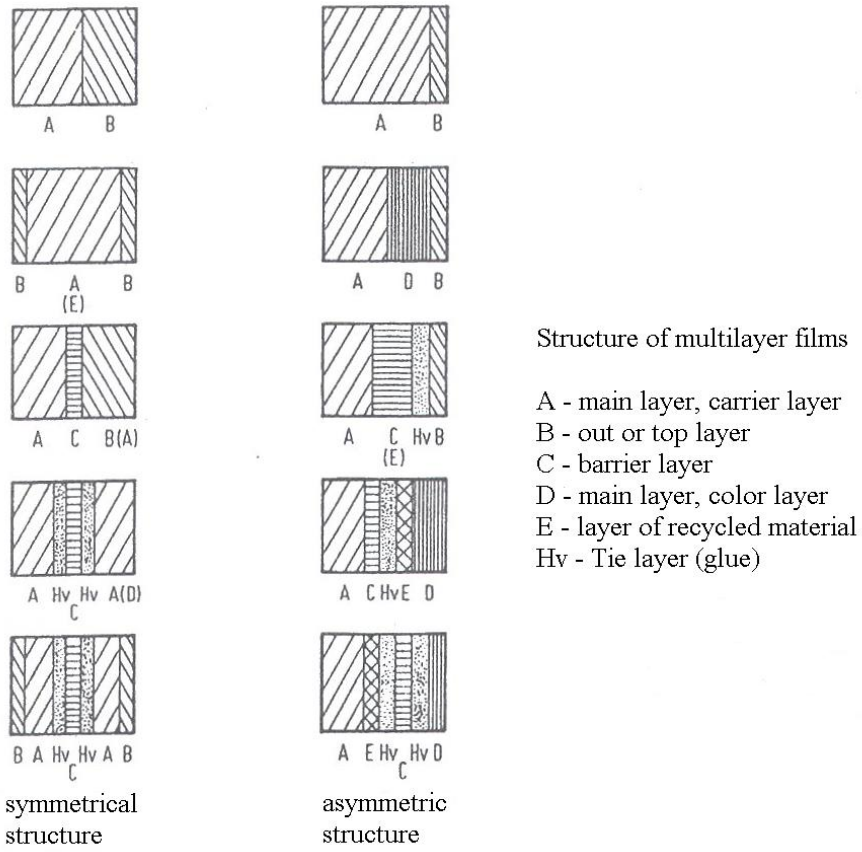

Fig. 1. Structures of Multilayer Films [Weldability of Barrier Films. BP, TBU 2007].

2.3 Multifunctional films

Films made from several polymer types are considered as multifunctional. The examples could be blown films, such as polyethylene. Biaxially oriented polyethylene phthalate films are mostly used in the packaging industry, electrotechnics and as separation films. Multifunctional rolled foils are produced either as polymeric or monomeric. Thin films could be made of polyethylene or polyvinyl chloride by rolling. Special foils are referred to as reflective, protective and ironing foils. Most of these films could be produced in two types, plot or print, and can be laminated as well.

In the packaging industry, usage of laminated materials has been increas. Films provide required barrier and mechanical properties. That is why flooring and waterproofing films can also be included among laminated foil products [10, 29].

2.4 Waterproofing films

PVC films are mainly used as roof or foundation insulation to protect buildings from water, radon and other liquids. It is also employed in the construction of swimming pools, dams or other water structures requiring waterproofing protection.

PVC waterproofing foils are either homogeneous (unvarnished) applied especially as the roof insulation or heterogeneous (reinforced - sandwiched), where a layer of reinforcement is found between PVC, such as a non-woven fabric, textile grid or glass-fiber insert. Their purpose is to increase strength and dimensional stability [30].

Important properties of PVC waterproofing films include high tensile strength, good elasticity and ductility at low temperatures, dimensional stability, weldability and a long service life [31].

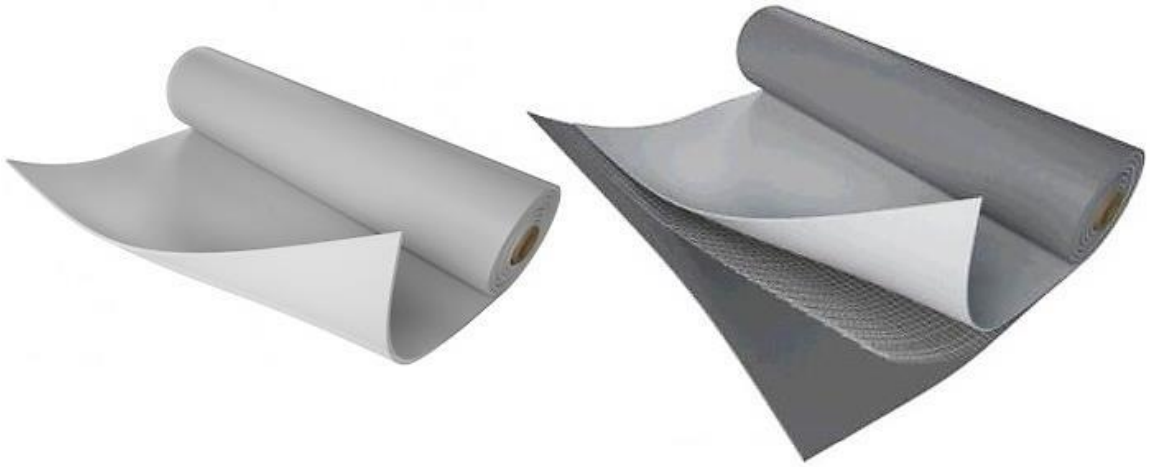

Fig. 2. Waterproofing PVC films – homogeneous (left), heterogeneous with PES grille (right) *[Fatra Napajedla]*.

2.4.1 Recycled PVB films

Thousands tons of PVB films are annually produced to manufacture laminated safety glasses (LSG) for the automotive industry. Such an enormous PVB film production generates waste that might be divided into three groups:

- waste from the film production known as a non-compliant material;
- LSG production waste, trimming = *trim*;
- recycled LSG waste.

The largest share of PVB waste belongs to the category of waste from VBS production. Possibility of using trimmings or automotive glass waste is another step for the future research [32].

Trim

PVB film is highly elastic and shrink-proof, showing good adhesion. Thus, PVB films are also larger than real glass surface in safety glass production. If a film is cut exactly on the edge of glass before adjusting the film to glass, the final film edges show visible imperfections in a subsequent heat treatment.

Sheet cuts of laminated pre-laminated glasses range from 1 to 20 cm depending on the type and geometry of laminated glass and shape of prepared PVB film. Within the current production technology, the amount of trimmings generated in automotive glasses is between 7 to 10% of the total amount of processed film. The amount of pure trim to be recycled depends on the number of new and recycled LSG produced. As the annual production of cars in Europe is 15 millions, recycling capacity reaches from 1.5 to 2 thousand tons [33].

Two methods of separating glass from PVB to recycle glass from VBS may be used:

- dry method,
- wet method.

Dry method

Principle of dry separation is mechanical wiping of the glass from the film. Currently in the Czech Republic, Sklopan Teplice deals with this separation, but the first company that started to employ this technology was ZIPPE Industrielanlage. Pure glass is obtained within this type of separation.

Recycled PVB films contain glass residues, from 0.5 to 4%, depending on the pulp size. However, purity requirements for PVB films are higher for the residual glass, only around 0.02%. This purity is fulfilled only by trim and recycling wet method.

Wet method

A wet process of separation provides a more acceptable solution to separate PVBs from glass with maintaing a relatively good quality of both materials. This method offers more effective removal of glass shards. Basic aqueous solution together with increasing temperature causes the interference of hydrogen bonds. These bonds are responsible for the size of adhesive bonds between residual hydroxyl groups on polymer chain and polar glass.

Higher water content substantially changes PVB mechanical, physical and chemical properties. Water acts as a softener, separates and delays molecules from each other causing temporary matte appearance of the film.

An acceptable option for using recycled PVB films is their combination with PVC of similar properties. Plasticized PVC is most commonly used in the production of floor coverings or waterproofing foils. This suggests that it would be possible to used recycled PVB to reduce costs and amounts of landfilled PVB [19, 56].

3 NANOFILLERS

As it has been mentioned above, fillers used in manufacturing nanocomposites have at least one dimension in a nanometer size. If only one dimension is in nanometers, then it is a particle in the form of sheets or wafers. If two dimensions are in nanometers, it is the structure of nanotubes. And in case of three nanometric dimensions, isodimensional particles are concerned [34].

Clay minerals are mixed natural materials, composed of finely grained minerals. If they contain adequate amount of water, they are plastic. They harden after firing and drying. Clays mostly contain phyllosilicates, which are silicates with a layered structure. Clays may also incorporate other minerals or organic matter, which may not necessarily affect their properties [35]. Clay minerals are divided into two basic groups:

Clay minerals - together with phyllosilicates, there are also minerals of allophane group, hydroxides, oxo-hydroxides and oxides providing clays with plasticity and harden them after drying and firing. Unlike phyllosilicates, these minerals represent only a small part of clays.

Accompanying minerals – form a part of clay but do not belong to the above mentioned group of clay minerals [36].

Phyllosilicates - basic coordination polyhedron which forms phyllosilicate structure is referred to as *tetrahedra* [TO_4] (tetrahedral network). T denotes the central cation of tetrahedrons, most often Si^{4+}, followed by Al^{3+}, Fe^{3+} or Ge^{3+} and *octahedra* [MA_6] with M denoting Fe^{2+}, Mg^{2+}, Mn^{2+}, Ca^{2+}, Li^{+}. A is anion as phyllosilicates contain some anions represented by O, OH or F [37, 38].

Networking

Connection of either two tetrahedral networks or tetrahedral and octahedral networks may occur in phyllosilicate structures.

Combination of two tetrahedral networks is realized between basal oxygen in the network:

- directly through the weak van der Wals forces.
- through the involment of cations creating a coordination polyhedron together with the basal oxygen. Newly created bond has an ionic character.
- using hydrating cations. The final bond is much weaker than in the previous type since the controlling factor is the interaction between basal oxygens of hydrating clusters via hydrogen bonding [37, 39].

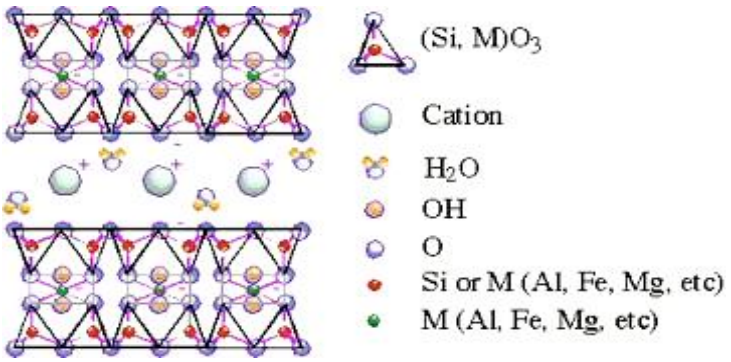

Fig. 3. Basic structure of clay minerals [37].

3.1 Montmorillonite (MMT)

Montmorillonite is one of the most important minerals of diocadedric smectite class, silicate class and phyllosilicate subclass. Montmorillonite is typical with tetrahedral positions with almost no or very insignificant degree of Al substitution for Si. Chemical formula of montmorillonite is *(Na,Ca)0,3(Al,Mg)2Si4O10(OH)2·n(H_2O)* [40].

MMT could be white, gray or pink with yellow or green shades. MMT crystals are built from compact or lamellar substances. MMT hardness is between 1 and 2, its density is 2.35 g / cm^3. If MMT crystals are mixed with water, they can significantly increase their original volume [41, 42].

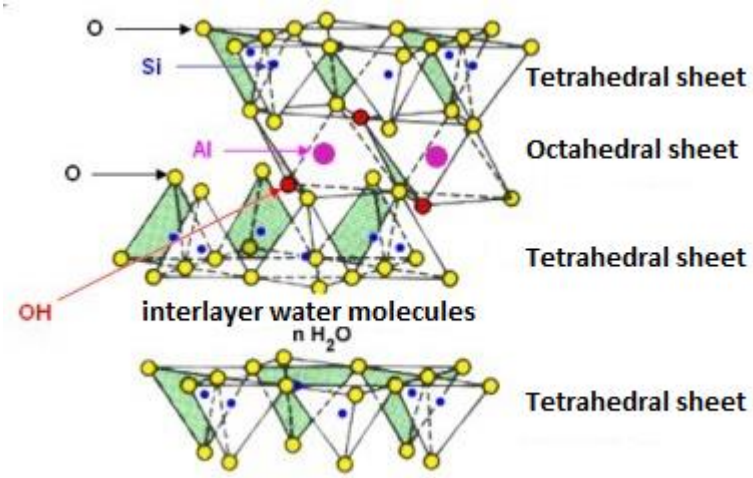

Fig. 4. Montmorillonite structure [38].

Montmorillonite modification

Clay modification enables properties customization for required applications. In the case of this study, MMT was intercalated with organic molecules in a process known as *organophillization* [43].

Organophillization is a process of blending MMT with organic substance which iniciates an intercalation of the compound between the layers and thus increases the distance d between the individual networks. The initial distance *d* between the plates is 9-12Å. Two main ways of intercalation are distinguished [44, 45].

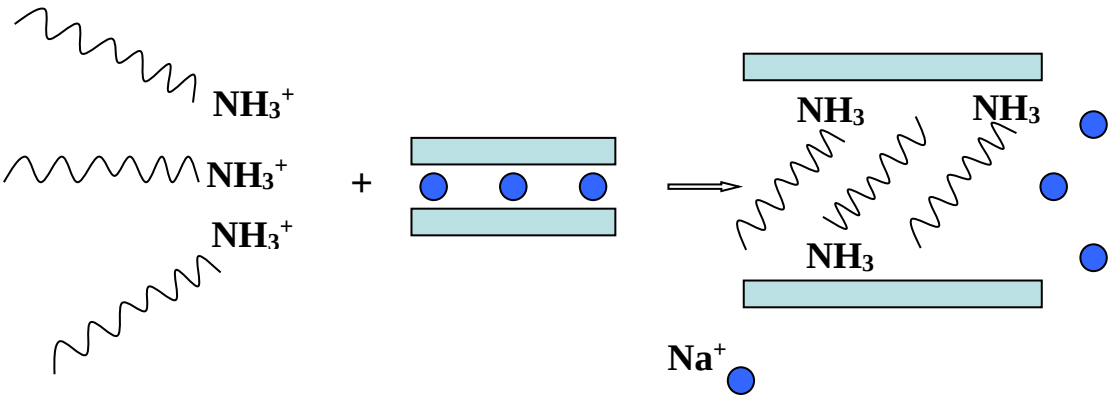

Fig. 5. Pattern of the ion-exchange reaction [45].

Ion-exchange method

Ion-exchange method is based on the ability of MMT to absorb certain cations and to retain them in an exchange state. The ion-exchange reaction is affected by the action of other cations in the aqueous solution. That is why, it is often referred to as a "wet" path. As salt is formed during the reaction, the final product must be washed [46, 47].

Ion-dipole interaction

Since the early 1990s, Nanocor has been developing a procedure using ion-dipole intercalation. This mechanism is based on the interaction of dipoles of given organic compounds and the interlayer cation. Ion-dipole intercalation is usually performed in the melt of intercalating agent (the phase of washing the by-product is eliminated). Therefore, ion-dipole intercalation is often referred to as a "dry" path [48, 49].

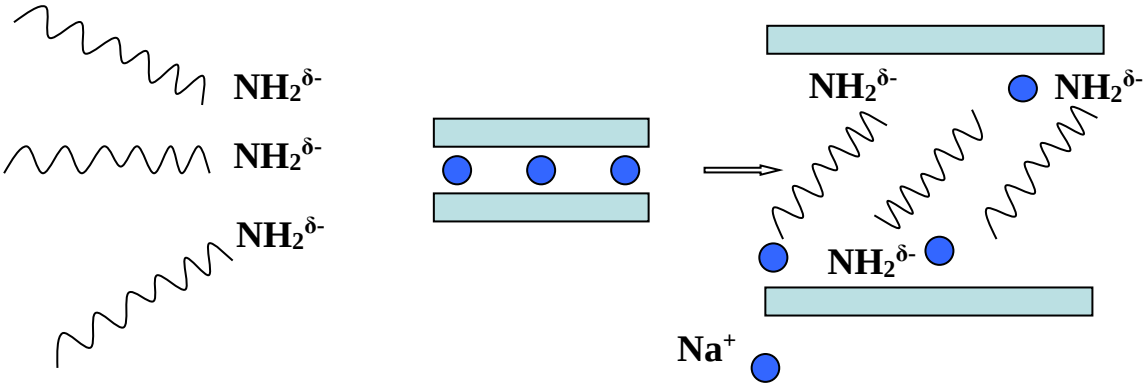

Fig. 6. Pattern of the ion-dipole interaction [45].

Organic compounds that serve as intercalation agents are mostly substances containing amine-groups (alkylamines) [50].

3.2 Compounding

Compounding is the most important step in the preparation of polymeric nanocomposites. As it has already been mentioned, it is the incorporation of modified nanofiller into polymer matrix in polymer melt. In order to achieve desired properties, both the composition parameters and chronology of individual steps in the process must be respected [3, 51]. Compounding should provide nanocomposite polymer system where nanoparticles will be perfectly dispersed and homogenized in polymer matrix. During compounding, none of the system components must be degraded. As can be seen in Fig. 7, specific terms are used to label the level of perfection of nanofiller mixing - intercalation, delamination and exfoliation of nanofibers in polymer matrix [52, 53].

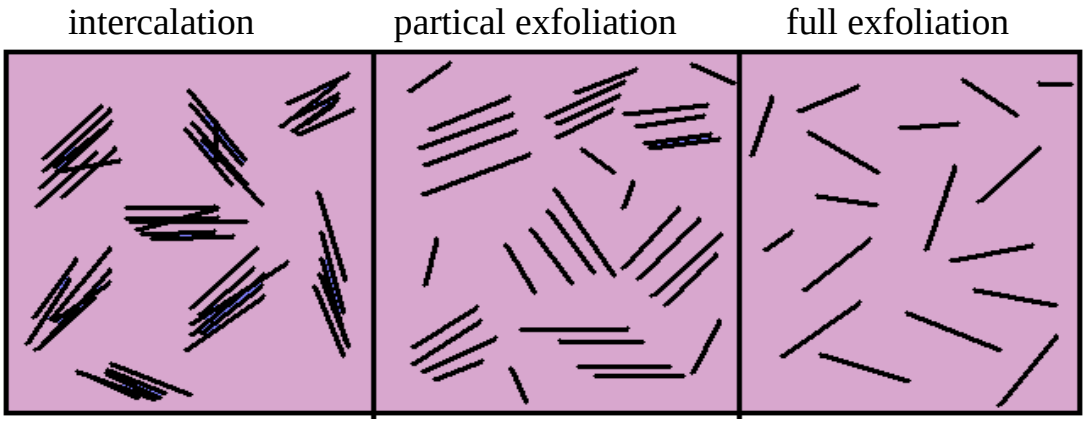

Fig. 7. Degrees of exfoliation of nanofillers in polymer matrix [38].

Requirements for a high level of nanofiller exfoliation in polymeric matrix may be fulfilled in the preparation of nanocomposites based on polar polymers, such

as polyurethane, polyamide or polyester. What is more, PVC and nanofiller compounding lead to enhancing of nanocomposite properties [54-56].

Due to hydrophobic nature of polyethylene and polypropylene chains, compounding is more complicated than in the previous cases. In addition to nanofiller modification, compatibilizers, such as PP or PE enhancing affinity to the surface of clay montmorillonite, are added to these types of polymers. PP and PE compatibilizers are fundamentally the same polymers modified by chain-linked polar substituents. These substituents could be styrenes, methyl methacrylates, hydroxyl groups or most often maleic anhydride. Content of polar groups and compatibilizer concentrations in the mixture may vary. Exfoliation of nanofibers in polymeric matrix is improved with an increasing polarity of the mixture. However, at the same time properties of such polymer matrix may be deteriorated due to a change in the system layout [57, 58]. Regularly, up to 5 wt. % of compatibilizer is added. Considering EVA nanocomposites preparation, compatibilizer is not applied due to a higher polarity of polymer matrix affected by the content of vinyl acetate groups [59, 60].

Level of exfoliation depends on the influence of chemical or structural properties and also on the used composing device. During the process of compounding, there is an effort to provide the system with the energy or forces to disintegrate montmorillonite monocots to individual plates and to disperse them homogeneously in polymer matrix.

Complete, perfect exfoliation of nanofiller in polymer matrix is the key factor in the preparation of nanocomposites with desired properties. Within further research of nanocomposites it has been found that nanomaterials may significantly influence also other properties, such as thermal stability, degradation and gas permeability. As an example may serve a case of reduced permeability for gases. It is assumed that oriented exfoliated nanoparticles prolong the distance of the gas passage through films [61, 62].

4 TECHNOLOGY OF FILM PRODUCTION

Extrusion, blowing and rolling are the most common methods of film production. Extrusion is a manufacturing process in which plastic melt is continuously extruded through a profiling device (extrusion head) into free space. Extrusion technology is used to produce finished and semi-finished products, foil or board. This production process employs a screw extruders as a part of production lines. In this study, EOC samples were extruded.

Blown film production technology is based on the process that a parison with a wall thickness of from 0.5 to 2 mm is still in its plastic state inflated by compressed air (magnification from 2 to 5 times) and at the same time stretched by a pulling device (up to 5 times longitudinal stretching). Blown film of a wall thickness from 0.015 to 0.3 mm is then cooled and wound.

Blow molding produces LDPE, HDPE and PP, PVC, PA and PETP films, multi-layer films of different material compositions. Today, seven or twelve-layer films may be produced using this method [63, 64].

Most often, foil top version is applied for blowing multilayer foils. Extruder is fitted with a blow head. Extruded foil with a predetermined overpressure (0.15 to 1 kPa) is blown and cooled by air which is fed through the cooling ring and uniformly blows the film over the entire circumference. Obtaining uniform thickness is conditioned by cooling. The air is fed to the foil sleeve through the extrusion head and the blown sleeve is gradually cooled and eventually flattened between the folding plates. Afterwards, the line closes the pull-out and winding device. Extraction speed may be controlled and so influences thickness and longitudinal orientation of the film. The film can be trimmed either on one or both sides. PE, PP, EVA and SRL samples were blown in this study [16, 65, 66].

Rolling is a method of continual shaping of plastic material in a plastic state in a slot created by a pair of rollers rotating against each other. The passage of the molded mass is uniformed. The feed material is compressed, accelerated, retracted and released between the rollers. The course of these changes is influenced by the type and state of molded material fed into the slot, by the peripheral speed of the rollers and slip value, temperature of cylinders and other qualities. Rolled-up materials are malleable and adhesive. They could be easily removed from the rolls. Softened PVC is a typical example of a plastic manufactured by rolling. To produce softened PVC foils, type of material is selected primarily according to the requirements of the final PVC mixture properties [25, 67, 68].

5 CHARACTERIZATION OF FILMS PROPERTIES

5.1 Sample preparation

Polymer matrix of PP, PE, EVA and Surlyn samples containing nanoparticles were mixed on Scientific LTE 20-40 twin-screw extruder and subsequently granulated. Extrusion head temperature was set to 210 °C for PP, 160 °C for PE and EVA and 200 °C for Surlyn, the speed was 150 minutes per minute. Extruded string was cooled in a water bath and then granulated.

Samples with LDPE and EOC were prepared using the same process. PVC and PVB samples were prepared in two steps. Firstly, PVC and PVB mixture was stirred on a two-screw extruder BUSS with the head temperature of 160 °C (in co-operation with Fatra, a.s.). Resulting string was granulated and the granules were mixed with nanofibers using a kneader of FT UTB in Zlín at the temperature of 150°C. Finally, plates of 125 x 125 x 2 mm were molded.

5.2 Sample evaluation

Mechanical properties

Mechanical properties were measured on Galbadini Quasar 25. Two-sided vane shaped specimens were tested respecting EN ISO 527-3 (64 0604) at two tearing rates - the initial velocity was 1 mm / min in 2% module. Then the speed was increased to 100 mm / min until causing a fracture.

Dynamic mechanical analysis (DMA)

DMA measurements were performed on 20x5x2 mm samples from pre-shaped DMA Perkin Elmer plates. E module and tan δ (tan delta = E "/ E ') were determined ranging from 1 to 200 Hz in a 2 Hz step and at the temperatures between -100 °C and + 100 °C.

Barrier properties (GTR, OTR)

Barrier properties were established using Julabo TW8 and CSN 64 0115 standard volume method. Test bodies were in the shape of a circle with a diameter of 80 mm. Pressure was set to 2 bars and temperature to 35 °C. N2, O2 and CO2 were measured and obtained values were subsequently recalculated according to ASTM D 3985-05.

Transmission electron microscopy (TEM)

Ultra-thin sections were prepared using Leica Ultra-Cryo-Microtome at -100 °C. Transmission electron microscopy was performed on JEM 200 CX at the accelerated voltage of 100 kV.

Differential scanning calorimetry (DSC)

DSC test was performed on Mettler Toledo DSC 1 with an external cooling unit. The rate of cooling and heating varied in particular cases (5, 10, 15 and 20 °C per minute) and the temperature ranged from -90 °C to 140 °C.

X-ray diffraction analysis (XRD)

X-ray diffraction analysis was performed using URD diffractometer in the laboratories of FT UTB. This method was chosen to determine the intercalation or exfoliation of the filler in the blends. Measurements were performed at the voltage of 40 kV and current of 30 mA. The area observed to prove the presence of clay fillers was from 2 ° to 8 ° 2 θ.

Accelerated degradation

Accelerated aging test was performed in Xenotest Alpha. UV radiation was applied with reference to the conditions defined in EN ISO 4892. Temperature was 38 °C, filters simulating daylight emitted 60 Wh / m and 50% RH was set. One measurement cycle lasted for 46 days and simulated one-year degradation.

Fourier transmission spectroscopy (FTIR)

FTIR test was performed on some samples (those after accelerated aging test) using FTIR spectrometer AVATAR 320 (Nicolet) with wavelengths between 4000 and 500 cm^{-1}. Spectral change between 1810 cm^{-1} and 1681 cm^{-1} was observed due to material degradation during the irradiation.

Hardness

Hardness test was performed using Shore A hardness tester respecting the Czech national standard ČSN EN ISO 868. Measurements were realized under the standard conditions at laboratory temperature of 20 °C using film remainders of 50x20x2 mm. A test body, thick in total 6 mm, consisted of three two-millimeter foils placed on top of each other. Determination was based on pressing the hardness tip into softened material. Instantaneous hardness values (1 s after a contact between the support foot and the test body) were recorded. Five measurements were performed at different locations of each test body.

6 SHORT EVALUATION OF STUDIED POLYMER FILMS

6.1 Characterization of films with nanofillers

Initially, test films were prepared from polypropylene, polyethylene, EVA and Surlyn (SRL). Based on measured mechanical and barrier properties, polyethylene, specifically LDPE, was selected for further testing and preparation of nanocomposite suitable as a part of multilayer polymeric film.

6.1.1 PP, PE, EVA and Surlyn films

As can be seen in Table 1, the values of pure PP, PE and Surlyn materials are higher than the values of the same materials enriched with fillers. Particularly for PP, added nanofillers significantly reduced tensile strength. The only exception may be materials containing EVA with the values slightly higher for filled samples. Concerning elongation at break, the largest percentage of elongation was obtained at materials filled with EVA. EVA samples with 5% Cloisite 93A nanofiller showed the best traction elongation properties. Fillers content in PP did not significantly deteriorate ductility. Tensile modulus reached higher values for the samples filled with PE and Surlyn. Within the samples with EVA, the increase of the modulus was rather insignificant.

In addition to mechanical properties, barrier properties of these films were measured. XRD and TEM analyses were performed and water vapor permeability was tested.

Based on obtained results, LDPE was determined as a representative of polyethylenes. It is widely used in the production of blown multilayer films.

Optimal conditions for the preparation of blending with nanofiller were established and subsequently, two representatives of nanofillers were selected for further testing and modifications - Cloisite 93A and Dellite 67.

Apart from commonly used polyolefins in the packaging insustry, such polyethylene and polypropylene, there occurred an opportunity to test mixing these nanofillers into non-traditional polymers, such as EOC. EOC is a new polyolefin elastomer, developed by Dow Chemical Company (Delaware, USA) employing metallocene catalysts. As it has valuable properties, it attracts growing attention of both the research and industry. The presence of octene in EOC comonomer affects the level of crystallinity and provides greater flexibility of copolymer. EOC may be considered as elastomeric polymer. Typically, octene content in copolymer is between 17 and 45 wt. % [8 - 12].

Table 1. Mechanical properties of nanocomposites

Composition	**Tensile strenght (MPa)**	**Elongation (%)**	**Tensile modulus (MPa)**
PP/93A	8,6	601,1	307,6
PP/67	8,6	619,1	313,9
PP	28,5	948,4	320,5
PE/20A	13,3	862,1	142,3
PE/30B	13,2	833,7	145,7
PE	15,9	790,3	117,3
EVA/93	20,5	1171,0	42,1
EVA/67	20,1	1112,1	38,6
EVA	19,5	1173,4	26,9
SRL/93	22,6	461,9	206,6
SRL/67	23,1	449,7	206,9
SRL	30,4	555,9	167,8

After the initial testing of the selected polymers, a representative of commercially commonly used materials, low density polyethylene, was chosen. In accordance with literature and past experience, LDPE is one of the most widely applied materials in the production of multilayer films. It may also be filled with nanofibres to enhance some of the material properties.

6.1.2 EOC films

Ethylene-octene copolymer may be used in the packaging industry, either alone or in the combination with PE or PP. Therefore, its barrier properties for N_2, O_2 and CO_2 were measured.

Gas permeability results for EOC-17 and EOC-45 copolymer / nanocomposite clay can be seen in Fig. 8. Compared with pure materials, filled EOC systems show lower throughput for all monitored gases. The best combination seems to be filling by 5 wt. % Cloisite 93, which is also confirmed by the results of mechanical properties and TEM.

If these two ethylene-octene copolymers are compared, EOC-17 exhibits significantly better properties for all gases. This may be due to fewer octane groups and higher crystallinity.

It may be concluded that Cloisite 93 nanoparticles enhances barrier properties of EOC polymer matrix. Gas permeability decreases after nanotube application in EOC matrix, with ideally 5 wt. %.

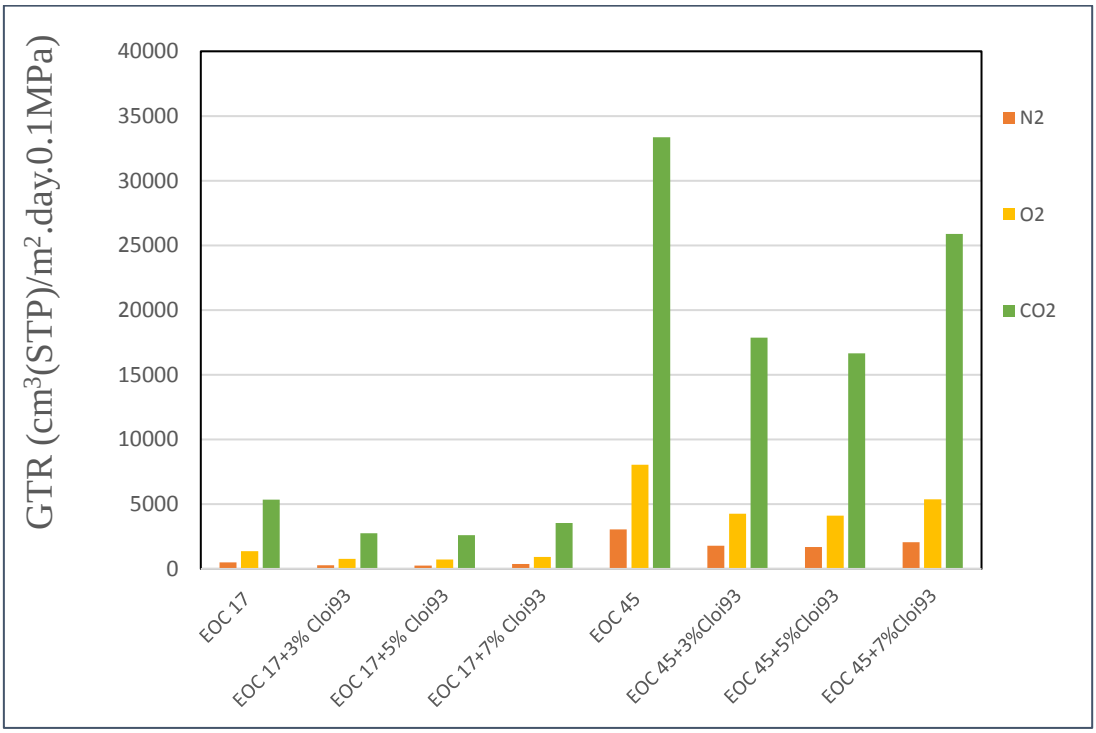

Fig. 8. Barrier properties of EOC samples - N_2, O_2 and CO_2.

This effect may be initiated by better distribution and dispersion of nanofiller in polymer matrix and by better exfoliation of MMT nanoparticles in polymer matrix. However, it has been known that the ideal orientation of MMT plates in polymer matrix during the samples molding is impossible to achieve.

Molded samples, films, are pressed into very thin plates. Thickness of the molded film is about 50 μm and the size of MMT plates is in nanometers. That is why, the orientation of MMT plates in polymer matrix cannot be excluded.

Comparison of the nanofibers distribution in EOC-45 matrix with variable clay contents can be seen in Fig. 9. Distribution is approximately the same in both cases. However, as the figures show, if EOC-45 contains 5 and 7 wt. % of nanoparticles in polymer matrix, exfoliation is worse.

It is evident that the concentration of 5 wt. % of nanofibers in polymer matrix leads to more significant exfoliation of filler nanoparticles in polymer. While at the concentration of 7 wt. %, nanoparticles may form agglomerates and filler exfoliation is imperfect.

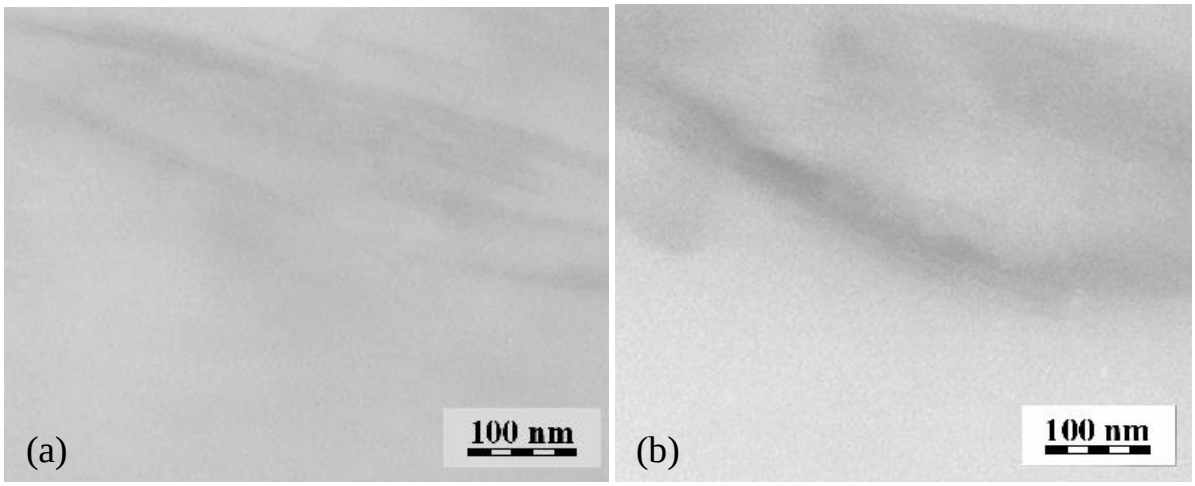

Fig. 9. TEM pictures: (a) EOC-45 (Engage 8842) with 5 wt. % Cloisite 93, (b) EOC-45 (Engage 8842) with 7 wt. % Cloisite 93.

6.1.3 PVC/PVB films

Tables 2 and 3 compare the results of mechanical properties for PVC / PVB and recycled PVC / PVB systems. According to mechanical properties, 80% PVB filling seems to be the optimal ratio for both systems. These results have confirmed the previous measurements of PVC / PVB mixtures with decreasing mechanical properties in the range from 10% to 50% and increasing from 60% to 90% again.

Table 2. Mechanical properties of PVC/PVB blends

Composition PVC/PVB	**Tensile strength (MPa)**	**Elongation (%)**
100% PVC	15,78	352,82
10 % PVB	11,87	242,26
20 % PVB	10,44	192,48
30 % PVB	10,09	185,68
40 % PVB	12,43	183,10
50 % PVB	13,62	210,64
60% PVB	15,96	227,62
70% PVB	17,27	231,12
80% PVB	18,57	236,92
90% PVB	17,89	228,38
1000% PVB	18,37	218,22

From the mechanical properties point of view, PVC / PVB ratio of 20:80 is optimal. However, mechanical properties may not be the only criterion. Therefore, further properties, such as hardness, dimensional stability, thermal and light degradation were measured as well.

Table 3. Mechanical properties of recycled PVC/PVB blends

Composition PVC/PVB rec.	**Tensile strength (MPa)**	**Elongation (%)**
100% PVC	15,78	352,82
10 % PVB	12,54	240,79
20 % PVB	10,62	186,63
30 % PVB	10,75	185,61
40 % PVB	11,13	181,06
50 % PVB	13,92	201,42
60% PVB	15,41	216,35
70% PVB	17,29	217,17
80% PVB	18,83	221,50
90% PVB	17,21	199,41
1000% PVB	17,84	178,65

DSC analysis was conducted to define polymer miscibility. Glass transition temperatures (T_g) of pure (non-blended) plasticized PVC and PVB were established. T_g of plasticized PVC was -29.5 °C and T_g of PVB 16.8 °C.

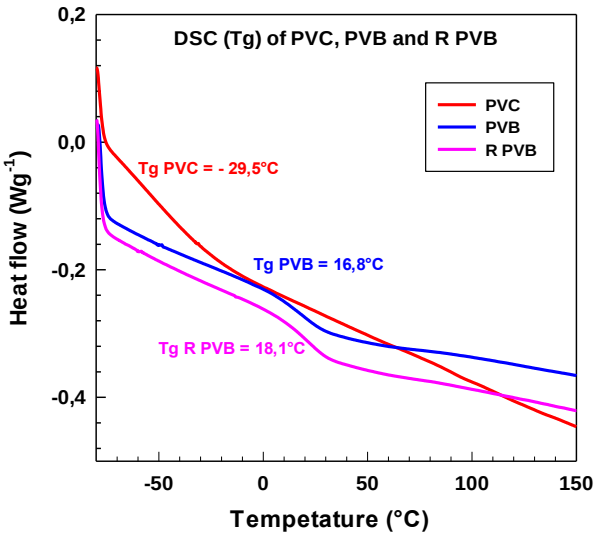

Fig. 10. Glass transition temperatures of pure PVC, PVB and recycled (R) PVB polymers determined by DSC analysis.

Obtained curves are shown in Fig. 10. Furher experiments focused on T_g values of selected blends. Polymer immiscibility was determined by two glass transition points, at a ratio of 20% and 80% of PVB. The glass transitions at temperatures of -40.6 °C (PVC part) and 28.2 °C (PVB part) were determined in a blend containing 20% of pure PVB and -29.6 °C (PVC part) and 18.1 °C (PVB part) in a blend consisting of 80% of pure PVB.

This study clarifies suitability of recycled PVB application in the industry, especially in PVC blends. Not only may recycled PVB be acquired at acceptable cost, unlike PVB, it also performs decent mechanical properties and is not degraded during its lifetime.

7 AIMS OF THE DOCTORAL THESIS AND THEIR FULFILMENT

The aim of the doctoral thesis is to prepare polymer special multifunctional films.

Partial aims of the work include:

- *Research of polymer materials* – this goal has been achieved.

Various types of polymeric matrix and clay nanoparticles were selected in the first part of the thesis. Based on measured properties, particularly barrier and mechanical properties, polyethylene (LDPE) was selected for further detailed testing.

Published as **Mechanical Properties of PE, PP, Surlyn and EVA Clay/Nanocomposites for Packaging Films.**

- *Mapping the possibilities of using prepared polymer films* – this goal has been achieved.

In the next part of the thesis, the attention was attracted to PE foils and their copolymers. For example, EOC copolymer with different octene content was tested.

Results were published as **Ethylene-Octene Copolymers/Organoclay Nanocomposites: Preparation** and **Properties and Influence of Clay Nanofillers on Properties of Ethylene-Octene Copolymers.**

- *Preparation of polymeric films containing nanofibers and waste filler* – this goal has been achieved.

Next part of the work focused on LDPE films containing nanofillers. Possibility of using these foils in the packaging industry was studied. The base film prepared this way was used as one of the layers of a 5-layer film of industrially manufactured foil.

In addition, films have been prepared containing other nanoparticles, such as nano Ag and nano Fe. Polymeric matrix was formed by LDPE.

Co-author of utility model - Multilayer packaging film with antimicrobial effects and method of their production from 14. 12. 2015

Another part of the work has been devoted to polymer blends preparation. This includes materials of similar composites that are well miscible. Results of PVC and PVB mixtures blending will be published as **Basic Properties of PVC/PVB Pure and Recycled Material Blends and Their Preparation.**

Co-author of utility model - Polyvinyl butyral recyclate for the preparation of polymer blends and polymer mixtures containing it from 15. 9. 2016

Co-author of utility model - Universal pad used in construction from 24. 7. 2017

- *Determination of selected evaluation methods for particular types of polymeric films* – this goal has been achieved.

Evaluation methods to characterize properties of special and multifunctional films were selected. Specifically, barrier properties, morphology, mechanical properties, XRD and FTIR for barrier films with nanofillers and mechanical properties and hardness for multifunctional films PVC/PVB.

The purpose of preparing polymeric films is to obtain such a film composition that it would be feasible to manufacture it industrially.

LIST OF PAPERS

I. Ethylene-Octene Copolymers/Organoclay Nanocomposites: Preparation and Properties

Alice Tesarikova, Dagmar Merinska, Jiri, Kalous and Petr Svoboda
Published in *Journal of Nanomaterials* [online]. 2016, Article ID 6014064, 13 pages
Accessible of: http://dx.doi.org/10.1155/2016/6014064

II. Influence of Clay Nanofillers on Properties of Ethylene-Octene Copolymers

Alice Tesarikova, Dagmar Merinska, Jiri Kalous and Petr Svoboda
Published in *Polymer Composites* [online]. 2017, Article ID 14544276, DOI: 10.1002/pc.24568
Accessible of: http://onlinelibrary.wiley.com/doi/10.1002/pc.24568/abstract

III. Basic Properties of PVC/PVB Pure and Recycled Material Blends and Their Preparation

Alice Tesarikova, Dagmar Merinska, Jiri Kalous, Jana Orsavova, Michael Tupy and Jaroslav Cisar
Submitted for publication in *Polymer Bulletin*

IV. Mechanical Properties of PE, PP, Surlyn and EVA Clay/Nanocomposites for Packaging Films

Alice Tesarikova and Dagmar Merinska
Published in *Book of Abstract – Time of Polymer (TOP) and Composites 2014,* Aip Conf. Proc. 1599, 178-181, DOI 10.1063/1.4876807

SUMMARY OF PAPERS

Articles in this paper are mainly focused on the possibility of using nanoparticles, especially MMT, as a part of polymer films. Selected types of MMT and polymers, possibility of successful mixing at different concentrations and the evaluation of basic physical and mechanical properties were compared. In addition to nanofibers use in various polymeric matrices, possibilities of films production from waste materials, especially PVB, have been investigated.

Paper I. The copolymer of ethylene, namely ethylene-octene (EOC), was been chosen for further study of nanofibers use in polymer films. Two different types of EOC (EOC-17 and EOC-45, depending on the content of octene groups) and one type of MMT - Cloisite 93 (in three different concentrations of 3, 5 and 7 wt. %) were studied. Increase in EOC tolerance to nanoparticles was achieved by the addition of maleinated PE (5 wt. %). Material was homogenized on a twin-screw extruder and the foils were extruded through a wide slot head. Such polymeric films were tested for their barrier and mechanical properties, morphology and degradation of nanocomposites. Results of barrier properties of ethylene-octene copolymers proved significantly better properties of EOC-17 (17% of octene groups in copolymer) for all gases. This facts may be due to a lower octane content and higher crystallinity. It could be concluded that Cloisite 93 nanoparticles may improve barrier properties of EOC polymer matrix. Because after applying nanoil (ideally 5 wt. %) into EOC matrix, gas permeability decreased.

Paper II. Next study of polymer films applying results of the previous research of EOC copolymers was based on another type of MMT (Dellite 67). The influence of nanoparticles on octene group content in EOC was determined. Based on previous measurements, 5% concentration of nanoparticles in polymeric EOC matrices was chosen. Samples were homogenized on a twin-screw extruder and subsequently extruded through a wide-slotted head. Degree of exfoliation (intercalation) of nanofiller in polymer matrix, barrier and mechanical properties and degradation of the films due to the UV radiation were tested and compared with previous studies. Distributions of nanofibers in EOC-17 and EOC-45 matrix with 5% clay content were compared. TEM analysis results suggested that EOC blending with nanoparticles was successful. Although distribution of nanoparticles in EOC-17 matrix was comparable, exfoliation was slightly better in EOC 17 with 5 wt. % Dellite 67 in polymer matrix. TEM results confirmed XRD conclusions, which proved significantly improved exfoliation of nanocomposite in EOC-45. In general, the best results were achieved with MMT exfoliation in EOC-45 with 5% Dellite 67.

Paper III. In addition to the use of nanoparticles in polymer matrix, further possibilities to prepare films from recycled PVB was investigated. The basis of polymer matrix was formed by PVC with different PVB content (pure and recycled) from 0 to 100%. Films were rolled on a two-roll laboratory machine and samples were subsequently pressed to maintain the same thickness. Possibility of applying recycled PVB from automotive glass as a substitution for PVC was examined. Appropriate PVB concentration in PVC matrix was assessed mainly based on the evaluation of mechanical properties, hardness and reflective elasticity. Filling of 80% of PVBs, both recycled and non-recycled, appeared to be optimal (considering mechanical properties). These results confirmed previous measurements of PVC / PVB mixtures with mechanical properties deterioration from 10% to 50% of PVB values and enhancing again from 60% to 90%.

Applyling the results of individual nanofilling measurements it may be emphasized that it is necessary to consider possible complications in preparation related to different polarities of clays and matrix used for clay nanocomposites with polyolefinic matrix. Although the exfoliation was imperfect, properties were significantly better if compared with pure matrix, especially mechanical and barrier properties. Usage of nanoparticles and other waste materials in PVC / PVB films may be another step for the future research.

Paper IV. The study of nanocomposites focused on polymer films preparation from polyethylene (PE), polypropylene (PP), surlyn (SRL), ethylene vinyl acetate (EVA) and different types of MMT. Due to various polymers and clay application, maleinized types of these materials had to be added to enhance miscibility. Foils were blown on a laboratory blower. Results were compared with pure foils; barrier properties, morphology and mechanical properties were evaluated. Results showed that the use of nanoparticles at 5% concentration in ethylene copolymers (Surlyn and EVA) appears to be a suitable option for further testing.

CONTRIBUTION TO SCIENCE AND PRACTICE

The most important contributions of the doctoral thesis to science and practice can be summarized as follows:

- Better understanding of the preparation of polymer films, multilayer films, nanocomposites with clay nanofillers; developing of an optimalized technologic prossesing.
  - *Outputs gathered within this part of the thesis can be used under preparation of polymeric, special and multifunctional films.*

- The successful preparation of multilayer polymer film with better possibility of recycling.
  - *The mixture for pre- production of multilayer PE film was also prepared. Based on previous measurements, testing and production requirements, polyethylene LDPE LD 100 AC, Modified Cloisite 93A clay in 5 wt. % concentration (modified in Synpo Pardubice) and Priex 15005 as compatibilizer were selected for pre- production. A five-layer blown film with a thickness of 0.070 mm (70 μm) from the prepared mixture was made in Invos Svárov.*

- The development of novel special antibacterial films.
  - *Nano Ag and nano Fe in polymer matrix and encapsulated essential oils on the surface of the foil were prepared and evaluated (cooperation with UPOL Olomouc, Synpo Pardubice and Invos Svárov)*
  - *The output: Utility model - Multilayer packaging film with antimicrobial effects and method of their production - from 14. 12. 2015.*

- The formulation of using of recycled PVB in multifunctional films.
  - *This part of the work notably contributed to description of recycled PVB which are suitable to using in polymer multifunctional films.*
  - *The output: Utility model - Polyvinyl butyral recyclate for the preparation of polymer blends and polymer mixtures containing it - from 15. 9. 2016.*

- The formulation of using of recycled waste of waterproofing films in special aplications.
  - *The last part of the work also contributed to description of recycling proces of PES waste as a part of waterproofing film which are suitable to using in other polymer special and multifunctional films and in building industry.*
  - *The output: Utility model - Universal pad used in construction - from 24. 7. 2017.*

REFERENCES

1. Sonawane, S.S., et al., *Nanocomposites for Food Packaging Applications.* Research Journal of Chemistry and Environment, 2011. **15**(2): p. 721-723.
2. Busolo, M.A. and J.M. Lagaron, *Oxygen scavenging polyolefin nanocomposite films containing an iron modified kaolinite of interest in active food packaging applications.* Innovative Food Science & Emerging Technologies, 2012. **16**: p. 211-217.
3. Carvalho, J.W.C., C. Sarantopoulos, and L.H. Innocentini-Mei, *Nanocomposites-Based Polyolefins as Alternative to Improve Barrier Properties.* Journal of Applied Polymer Science, 2010. **118**(6): p. 3695-3700.
4. de Azeredo, H.M.C., *Nanocomposites for food packaging applications.* Food Research International, 2009. **42**(9): p. 1240-1253.
5. Andersson, C., *Composite Multilayer Coatings for Improved Barrier Properties of Packaging Board.* Composite Laminates: Properties, Performance and Applications, 2010: p. 83-119.
6. Feldman, D., *Polymer barrier films.* Journal of Polymers and the Environment, 2001. **9**(2): p. 49-55.
7. Moreno, S.H. and S.C.S. de la Torre, *Applications of Nanocomposites in Architecture and Construction.* Contexto-Revista De La Facultad De Arquitectura Universidad Autonoma De Nuevo Leon, 2017. **11**(14): p. 59-71.
8. Khunova, V., et al., *The Effect of Interfacial Modification on the Properties of Reactively Processed Polypropylene/Clay Nanocomposites.* Composite Interfaces, 2011. **18**(4): p. 357-370.
9. Ayuse, C.F., et al., *High Oxygen Barrier Polyethylene Films.* Polymers & Polymer Composites, 2017. **25**(8): p. 571-581.
10. Decker, J.J., et al., *Polyethylene-based nanocomposites containing organoclay: A new approach to enhance gas barrier via multilayer coextrusion and interdiffusion.* Polymer, 2015. **61**: p. 42-54.
11. Wang, K.H., et al., *Morphology and physical properties of polyethylene/silicate nanocomposite prepared by melt intercalation.* Journal of Polymer Science Part B-Polymer Physics, 2002. **40**(14): p. 1454-1463.
12. Abedi, S., et al., *Highly exfoliated PE/Na+MMT nanocomposite produced via in situ polymerization by a catalyst supported on a novel modified Na+MMT.* Polymer Bulletin, 2013. **70**(10): p. 2783-2792.
13. Araujo, E.M., et al., *Thermal and mechanical properties of PE/organoclay nanocomposites.* Journal of Thermal Analysis and Calorimetry, 2007. **87**(3): p. 811-814.

14. Zehetmeyer, G., et al., *Morphological, optical, and barrier properties of PP/MMT nanocomposites.* Polymer Bulletin, 2013. **70**(8): p. 2181-2191.
15. Tesarikova, A. and D. Merinska, *Mechanical Properties of PE, PP, Surlyn and EVA/Clay Nanocomposites for packaging films.* Times of Polymers (Top) and Composites 2014, 2014. **1599**: p. 178-181.
16. Merinska, D., A. Kalendova, and A. Tesarikova, *Barrier Properties of PE, PP and EVA (Nano) composites - the Influence of Filler Type and Concentration.* Times of Polymers (Top) and Composites 2014, 2014. **1599**: p. 186-189.
17. Mittal, V., *Barrier Properties of Polyolefin Nanocomposites.* Barrier Properties of Polymer Clay Nanocomposites, 2010: p. 93-115.
18. Tesarikova, A., et al., *Ethylene-Octene Copolymers/Organoclay Nanocomposites: Preparation and Properties.* Journal of Nanomaterials, 2016.
19. Bagheri-Kazemabad, S., et al., *Morphology and properties of polypropylene/ethylene-octene copolymer/clay nanocomposites with double compatibilizers.* Polymers for Advanced Technologies, 2014. **25**(10): p. 1116-1121.
20. Svoboda, P., *Influence of Branching Density in Ethylene-Octene Copolymers on Electron Beam Crosslinkability.* Polymers, 2015. **7**(12): p. 2522-2534.
21. Amberg-Muller, J.P., et al., *Migration of phthalates from soft PVC packaging into shower and bath gels and assessment of consumer risk.* Journal Fur Verbraucherschutz Und Lebensmittelsicherheit-Journal of Consumer Protection and Food Safety, 2010. **5**(3-4): p. 429-442.
22. Fankhauser-Noti, A., S. Biedermann-Brem, and K. Grob, *PVC plasticizers/additives migrating from the gaskets of metal closures into oily food: Swiss market survey June 2005.* European Food Research and Technology, 2006. **223**(4): p. 447-453.
23. Ambrosio, J.D., et al., *Preparation and Characterization of Poly (Vinyl Butyral)-Leather Fiber Composites.* Polymer Composites, 2011. **32**(5): p. 776-785.
24. Zhang, X.H., et al., *The mechanical properties of Polyvinyl Butyral (PVB) at high strain rates.* Construction and Building Materials, 2015. **93**: p. 404-415.
25. Cui, Y.B., et al., *Gas barrier properties of polymer/clay nanocomposites.* Rsc Advances, 2015. **5**(78): p. 63669-63690.
26. Priolo, M.A., et al., *Influence of Clay Concentration on the Gas Barrier of Clay-Polymer Nanobrick Wall Thin Film Assemblies.* Langmuir, 2011. **27**(19): p. 12106-12114.
27. Sadeghi, F. and A. Ajji, *Structure, Mechanical and Barrier Properties of Uniaxially Stretched Multilayer Nylon/Clay Nanocomposite Films.* International Polymer Processing, 2012. **27**(5): p. 565-573.

28. Attaran, S.A., A. Hassan, and M.U. Wahit, *Materials for food packaging applications based on bio-based polymer nanocomposites: A review.* Journal of Thermoplastic Composite Materials, 2017. **30**(2): p. 143-173.
29. Wrona, M., et al., *Antioxidant packaging with encapsulated green tea for fresh minced meat.* Innovative Food Science & Emerging Technologies, 2017. **41**: p. 307-313.
30. Chen, K., S. Schunemann, and H. Tuysuz, *Preparation of Waterproof Organometal Halide Perovskite Photonic Crystal Beads.* Angewandte Chemie-International Edition, 2017. **56**(23): p. 6548-6552.
31. Liao, X.Q., et al., *Flexible, Cuttable, and Self-Waterproof Bending Strain Sensors Using Microcracked Gold Nanofilms@Paper Substrate.* Acs Applied Materials & Interfaces, 2017. **9**(4): p. 4151-4158.
32. Mrkvickova, L., J. Danhelka, and S. Pokorny, *Characterization of Commercial Polyvinylbutyral by Gel-Permeation Chromatography.* Journal of Applied Polymer Science, 1984. **29**(3): p. 803-808.
33. Valasek, P. and M. Muller, *Recyclation of Waste Microparticles in Interaction with Polymeric Matrix - Multiphase Composite.* 12th International Scientific Conference Engineering for Rural Development, 2013: p. 238-243.
34. Bahranowski, K., et al., *Influence of purification method of Na-montmorillonite on textural properties of clay mineral composites with TiO2 nanoparticles.* Applied Clay Science, 2017. **140**: p. 75-80.
35. Coskunses, F.I. and U. Yilmazer, *Preparation and Characterization of Low Density Polyethylene/Ethylene Methyl Acrylate Glycidyl Methacrylate/Organoclay Nanocomposites.* Journal of Applied Polymer Science, 2011. **120**(5): p. 3087-3097.
36. Cao, M.L. and Y.F. Yu, *Synthesis and Characterization of Montmorillonite Inorgano-Intercalation Compound Assisted by Microwave Irradiation.* Journal of Wuhan University of Technology-Materials Science Edition, 2010. **25**(3): p. 444-448.
37. Kubisova, H. and D. Merinska, *Polyolefin/clay nanocomposites: Comparing mechanical and barrier properties.* Ivth International Conference on Times of Polymers (Top) and Composites, 2008. **1042**: p. 178-180.
38. Kubisova, H., D. Merinska, and P. Svoboda, *Polyethylene and Poly(propylene)/Clay Nanocomposites.* Macromolecular Symposia, 2009. **286**: p. 210-217.
39. Erdmann, E., et al., *Effect of the Organoclay Preparation on the Extent of Intercalation/Exfoliation and Barrier Properties of Polyethylene/PA6/Montmorillonite Nanocomposites.* Journal of Applied Polymer Science, 2010. **118**(4): p. 2467-2474.

40. Liu, Y.Z., et al., *Co-intercalation of Montmorillonite by Poly(oxypropylene) Amine Hydrochlorides with Different Chain Length.* Acta Chimica Sinica, 2012. **70**(7): p. 911-916.
41. Alikhani, M. and M.R. Moghbeli, *Ion-exchange polyHIPE type membrane for removing nitrate ions: Preparation, characterization, kinetics and adsorption studies.* Chemical Engineering Journal, 2014. **239**: p. 93-104.
42. Khan, A.H., M. Nurnabi, and P. Bala, *Studies on thermal transformation of Na-montmorillonite-glycine intercalation compounds.* Journal of Thermal Analysis and Calorimetry, 2009. **96**(3): p. 929-935.
43. Rama, M.S., et al., *Exfoliation of clay layers in polypropylene matrix using potassium succinate-g-polypropylene as compatibilizer.* Composites Science and Technology, 2010. **70**(10): p. 1550-1556.
44. Merinska, D., et al., *PP/MMT Nanocomposite: Mathematic Modelling of Layered Nanofiller.* Journal of Nanomaterials, 2012.
45. Merinska, D., et al., *Processing and Properties of Polyethylene/Montmorillonite Nanocomposites.* Journal of Thermoplastic Composite Materials, 2012. **25**(1): p. 115-131.
46. Jeong, C.J., et al., *Preparation of exfoliated montmorillonite nanocomposites with catechol/zwitterionic quaternized polymer for an antifouling coating.* Polymer Engineering and Science, 2015. **55**(9): p. 2111-2117.
47. Kim, S., et al., *Ionic conductivity of polymeric nanocomposite electrolytes based on poly(ethylene oxide) and organo-clay materials.* Colloids and Surfaces a-Physicochemical and Engineering Aspects, 2008. **313**: p. 216-219.
48. Lee, S.D., et al., *Catalytic performance of ion-exchanged montmorillonite with quaternary ammonium salts for the glycerolysis of urea.* Catalysis Today, 2014. **232**: p. 127-133.
49. Sun, H.G., et al., *Surface modification of natural Na-montmorillonite in alkane solvents using a quaternary ammonium surfactant.* Colloids and Surfaces a-Physicochemical and Engineering Aspects, 2013. **426**: p. 26-32.
50. Song, L., et al., *Study on the solvothermal preparation of polyethylene/organophilic montmorillonite nanocomposites.* Journal of Materials Chemistry, 2002. **12**(10): p. 3152-3155.
51. Kim, Y.C., *Effect of maleated polyethylene on the crystallization behavior of LLDPE/clay nanocomposites.* Polymer Journal, 2006. **38**(3): p. 250-257.
52. Cui, L., et al., *Polyethylene-montmorillonite nanocomposites: Preparation, characterization and properties.* Macromolecular Symposia, 2007. **260**: p. 49-57.
53. Besco, S., M. Modesti, and A. Lorenzetti, *Influence of processing parameters on the structure of melt blended polyethylene/organoclay nanocomposites produced by a masterbatch route.* Polymer Engineering and Science, 2013. **53**(4): p. 689-698.

54. Ren, C.Y., et al., *Preparation of multifunctional supported metallocene catalyst using organic multifunctional modifier for synthesizing polyethylene/clay nanocomposites via in situ intercalative polymerization.* Polymer, 2010. **51**(15): p. 3416-3424.
55. Dolez, P.I., M. Weltrowski, and E. David, *Study of the Parameters Controlling Nanoparticle Dispersion for Nanocomposite Geomembrane Applications.* Geotechnical Frontiers 2017: Waste Containment, Barriers, Remediation, and Sustainable Geoengineering, 2017(276): p. 107-116.
56. Costantino, A., et al., *Morphology-performance relationship of polypropylene-nanoclay composites processed by shear controlled injection moulding.* Polymer International, 2013. **62**(11): p. 1589-1599.
57. Teymouri, Y. and H. Nazockdast, *The effect of process parameters on physical and mechanical properties of commercial low density polyethylene/ORG-MMT nanocomposites.* Journal of Materials Science, 2011. **46**(20): p. 6642-6647.
58. Lei, F., et al., *Exfoliation of organic montmorillonite in iPP free of compatibilizer through the multistage stretching extrusion.* Polymer Bulletin, 2014. **71**(12): p. 3261-3273.
59. Wei, L.M., T. Tang, and B.T. Huang, *Synthesis and characterization of polyethylene/clay-silica nanocomposites: A montmorillonite/silica-hybrid-supported catalyst and in situ polymerization.* Journal of Polymer Science Part a-Polymer Chemistry, 2004. **42**(4): p. 941-949.
60. Ziabka, M., *Study of Mechanical Properties of Polymer Composites Containing Silver Nanoparticles for Middle Ear Prostheses.* Composites Theory and Practice, 2016. **16**(1): p. 42-46.
61. Santamaria, P., J.I. Eguiazabal, and J. Nazabal, *Dispersion and Mechanical Properties of a Nanocomposite with an Organoclay in an Ionomer-Compatibilized LDPE Matrix.* Journal of Applied Polymer Science, 2011. **119**(3): p. 1762-1770.
62. Ren, C.Y., et al., *The Role of Polymerizable Organophilic Clay During Preparing Polyethylene Nanocomposite via Filling Polymerization.* Journal of Applied Polymer Science, 2010. **117**(3): p. 1646-1657.
63. Myshkin, N.K., S.S. Pesetskii, and A.Y. Grigoriev, *Polymer Composites in Tribology.* Proceedings of Viii International Scientific Conference (Balttrib' 2015), 2016: p. 142-145.
64. Hundakova, M., et al., *Structure and antibacterial properties of polyethylene/organo-vermiculite composites.* Solid State Sciences, 2015. **48**: p. 197-204.
65. Martinez-Sanz, M., A. Lopez-Rubio, and J.M. Lagaron, *Nanocomposites of ethylene vinyl alcohol copolymer with thermally resistant cellulose nanowhiskers by melt compounding (I): Morphology and thermal properties.* Journal of Applied Polymer Science, 2013. **128**(5): p. 2666-2678.

66. Battisti, M.G. and W. Friesenbichler, *PP-Polymer Nanocomposites with Improved Mechanical Properties Using Elongational Flow Devices at the Injection Molding Compounder.* Proceedings of Pps-29: The 29th International Conference of the Polymer - Conference Papers, 2014. **1593**: p. 195-198.
67. Hosseinkhanli, H., et al., *Thermal, Mechanical, and Barrier Properties of Polyethylene/Surlyn/Organoclay Nanocomposites Blown Films Prepared by Different Mixing Methods.* Journal of Vinyl & Additive Technology, 2015. **21**(1): p. 60-69.
68. Kichatov, B.V. and A.M. Korshunov, *Development of an Extrusion Die With Rollers for Foaming Polymers.* Polymer Engineering and Science, 2015. **55**(10): p. 2256-2269.

LIST OF TABLES AND FIGURES

Tables

Figures

LIST OF ABBREVIATIONS

UV	Ultraviolet radiation
PE	Polyethylene
PP	Polypropylene
PS	Polystyrene
PVC	Polyvinyl chloride
PVB	Polyvinyl butyral
EVA, EVAC	Ethylene-vinyl acetate
SRL	Surlyn
EMAA	Copolymer ethylene with methacrylic acid
TIE	Adhesive layer
g/ m²	Gram per square meter
g	Gram
m²	Square meter
LDPE	Low density polyethylene
g/ cm³	Gram per cubic centimeter
cm³	Cubic centimeter
O_2	Oxygen
N_2	Nitrogen
CO_2	Carbon dioxide
EOC	Ethylene-octene copolymer
Na^+	Sodium Cation
MPa	Megapascal
Pa	Pascal
cm	Centimeter
m	Meter
mm	Millimeter
NC	Nanocomposite
MMT	Montmorillonit
ČSN EN ISO	Czech national standard
ASTM	American technical standard
TEM	Transmission electron microscopy
XRD	X-ray diffraction analysis
DMA	Dynamic mechanical analysis
cm^{-1}	Reciprocal centimeter

CURRICULUM VITAE

Personal information

Name: Ing., Bc. Alice Tesaříková Svobodová
Adress: Kojetínská 1420, 767 01 Kroměříž
Nationality: Czech
Affiliation: Department of Polymer Engineering
Faculty of Technology, TBU in Zlin
Vavrečkova 275, 760 01 Zlin, Czech Republic
E-mail: svobali@seznam.cz

Education

2013 – until now *Ph.D., Chemistry and Material Technology*
Tomas Bata Univerzity in Zlin, Czech Republic
Faculty of Technogy
Degree: Technology of macromolecular materials

2012 – 2014 *B. Sc., Specialization in Education*
Tomas Bata Univerzity in Zlin, Czech Republic
Faculty of Humanities
Degree: Teaching of special subjects for secondary schools

2009 – 2011 *M. Sc., Chemistry and Material Technology*
Tomas Bata Univerzity in Zlin, Czech Republic
Faculty of Technogy
Degree: Technology and Management

2006 – 2009 *B. Sc., Chemistry and Material Technology*
Tomas Bata Univerzity in Zlin, Czech Republic
Faculty of Technogy
Degree: Chemistry and Material Technology

Work experience

2016 – until now Teacher of special subjects at secondary school

2013 – 2017 Research worker
Tomas Bata Univerzity in Zlin, Czech Republic
Faculty of Technogy

2006 – 2016 Teacher of special subjects at elementary school

1990 – 2005 Professional dentist

Research experience and projects

Research projects:
MPO - FR TI 4/623 (6/2011-6/2015)

Nanostructured packing materials of specific utility properties with facile recyclation
Member of project team
Utility model - Multilayer packaging film with antimicrobial effects and method of their production from 14. 12. 2015

TAČR - TA03010799 (1/2012-1122015)
Usage of nanomaterials and natural extracts as funtional substances in the development of active packing materials with barrier, antimicrobiotic, protective and oxygen absorbing effect
Member of project team

TAČR - TH 01030054 (1/2015-12/2017)
Possibilities of PES shredded material and further technological waste processing
Member of project team
Utility model - Polyvinyl butyral recyclate for the preparation of polymer blends and polymer mixtures containing it from 15. 9. 2016
Utility model - Universal pad used in construction from 24. 7. 2017

IGA/FT/2014/014
Enhancements of utility and processing properties due to processing parametres adjustments and additives
Project investigator

IGA/FT/2015/007
Enhancements and possible adjustments of utility, processing properties and applicable potential of polymeric materials by examining processing parametres and additives
Member of project team

IGA/FT/2016/009
Methods of natural and synthetic polymers and assessment of their properties based on utility manufacturing processes
Member of project team

IGA/FT/2017/007
Enhancements and possible adujstments of natural and synthetic polymeric materials
Member of project team

Courses
Jan 2015 Basics of IR spektroscopy - Training Course

LIST OF PUBLICATIONS

Articles in journals with impact factors

1. **TESARIKOVA, A.,** D. MERINSKA, J. KALOUS a P. SVOBODA. Ethylene-Octene Copolymers/Organoclay Nanocomposites: Preparation and Properties. *Journal of Nanomaterials* [online]. 2016, Article Number 6014064, DOI: 10.1155/2016/6014064, 13 pages
   Available from: http://dx.doi.org/10.1155/2016/6014064

2. **TESARIKOVA, A**., D. MERINSKA, J. KALOUS a P. SVOBODA. Influence of Clay Nanofillers on Properties of Ethylene-Octene Copolymers. *Polymer Composites* [online]. 2017, Article Number 14544276, DOI: 10.1002/pc.24568
   Available from:
   http://onlinelibrary.wiley.com/doi/10.1002/pc.24568/abstact

3. **TESARIKOVA A**., D. MERINSKA, J. KALOUS, J. ORSAVOVA, M. TUPY a J CISAR. Basic Properties of PVC/PVB Pure and Recycled Material Blends and Their Preparation.
   Submitted in Polymer Bulletin.

Articles in book of abstracts in Web of Science database

1. **TESARIKOVA, A**., MERINSKA, D. Mechanical Properties of PE, PP, Surlyn and EVA/Clay Nanocomposites for Packaging Films. *Book of conference 7th International Conference on Times of Polymers and Composites (TOP), Ischia, ITALY, Jun 22-26, 2014.*
   Book Series: AIP Conference Proceedings, 2014, vol. 1599, p. 178-181.

Articles in a national journal

1. KALENDOVÁ A., D. MĚŘÍNSKÁ, **A. TESAŘÍKOVÁ** a M. ŠLOUF. Studium jilových nanokompozitů z hlediska propustnosti pro plyny. *Plasty a kaučuky 2014, č. 11-12, s. 335-338, ISSN 0322-7340.*

2. **TESAŘÍKOVÁ A.,** D. MĚŘÍNSKÁ, J. KALOUS a P. SVOBODA. Možnosti přípravy a hodnocení vybraných vlastností ethylen-okten/jíl nanokompozitů. *Plasty a kaučuky 2016, č. 3-4, s. 68-72, ISSN 0322-7340.*

Conferences with a book of abstracts

1. MERINSKA, D., KALENDOVA, A. a **A. TESARIKOVA**. Barrier Properties of PE, PP and EVA Nano(composites) – the Influence of Filler Type and Concentration. *Book of conference 7th International Conference on Times of Polymers and Composites (TOP), Ischia, ITALY, Jun 22-26, 2014.*
   Book Series: AIP Conference Proceedings, 2014, 1599, 186-189.

2. TUPY M., **A. TESARIKOVA**, D. MERINSKA a V. PETRANEK. Use of Nanoclay in Various Modified Polyolefins.
   Book of conference: ICPMSE 2014- XII International Conference on Polymer Materials Science and Engineering, Venice, Italy, November 13 - 14, 2014.
   World Academy of Science, Engineering and Technology, International Science Index 95, International Journal of Chemical, Nuclear, Metallurgical and Materials Engineering, 2014, vol. 8, No. 11, p. 1102-1105, ISSN: 1307-6892.

3. TUPY, M., D. MERINSKA, **A. TESARIKOVA**, Ch. CARROT, C. PILLON a V. PETRANEK. Mechanical Properties of Recycled Plasticized PVB/PVC Blends. *Book of conference*: *ICCCM 2014, International Conference on Chemistry of Construction and Materials Istanbul, Turkey, September 29-30, 2014.* International Science Index Vol. 8, No. 9, Part XIV, pp. 1845-1850
   World Academy of Science, Engineering and Technology. International Journal of Civil, Architectural, Structural and Construction Engineering, Vol. 8, No. 9, pp. 924-932, 2014, ISSN: 1307-3892.

Conference proceedings

1. **TESARIKOVA A**., A. KALENDOVA a D. MERINSKA. (Bio) Polymer Packaging films and their Properties. *Conference: 18th International Conference on Circuits, Systems, Communications and Computers (CSCC 2014), Santorini Island, Greece, July 17-21, 2014.*

2. **TESARIKOVA A**., D. MERINSKA a L. BENICEK. Selected Properties of LDPE, PP and Surlyn/Clay Nanocomposites Barrier Films. *Conference: AMWC 2015, Advanced Materials World Congress, Stockholm, Sweden 23-26. August 2015.*
   Abstrakt publikován online v "The VBRI Press in 2015", DOI: 10.5185/amwc.2015.
   Available from: www.vbripress.com/amwc.

3. MERINSKA D., **A. TESARIKOVA**. The Influence of the Clay and Compatibilizator Concentration on the PE, PP and PE/EVA Copolymer Properties**.** *Conference: AMWC 2015, Advanced Materials World Congress, Stockholm, Sweden, 23-26. August 2015.*
   Abstrakt published online "The VBRI Press in 2015", DOI: 10.5185/amwc.2015.
   Available from: www.vbripress.com/amwc.

4. **TESARIKOVA A**., D. MERINSKA a M. TUPY. Mechanical Properties of PVC/PVB Mixture with Wood Waste. *Konference: 4th International Conference on Materials Engineering for Advanced Technologies, London, United Kingdom, June 27-28, 2015.*

5. **TESARIKOVA A**., D. MERINSKA a M. TUPY. Preparation and Evaluation of Mechanical Properties of Filled PVC/ PVB Blends/Clay and Calcium Carbonate. *Conference: ANNIC, Applied Nanotechnology and Nanoscience International Conference, Barcelona, Spain, Nov. 9-11., 2016.*

6. **TESARIKOVA A**., D. MERINSKA a M. TUPY. Preparation and Evaluation of Basic Properties of PVC/PVB/clay Nanocomposites. *Conference: 5th International Conference on Nanotechnology and Materials Science, Dubai, UAE, October 16-18., 2017.*

PAPER I

Ethylene-Octene Copolymers/Organoclay Nanocomposites: Preparation and Properties

Alice Tesaříková, Dagmar Měřínská, Jiří Kalous, Petr Svoboda

Journal of Nanomaterials, 2016, DOI: 10.1155/2016/ 6014064

Hindawi Publishing Corporation
Journal of Nanomaterials
Volume 2016, Article ID 6014064, 13 pages
http://dx.doi.org/10.1155/2016/6014064

Research Article

Ethylene-Octene Copolymers/Organoclay Nanocomposites: Preparation and Properties

Alice Tesarikova,[1] Dagmar Merinska,[1,2] Jiri Kalous,[1,2] and Petr Svoboda[1]

[1]*Department of Polymer Engineering, Faculty of Technology, Tomas Bata University in Zlin, Nam. T. G. Masaryka 275, 762 72 Zlin, Czech Republic*
[2]*Centre of Polymer Systems, University Institute, Tomas Bata University in Zlin, Nad Ovcirnou 3685, 760 01 Zlin, Czech Republic*

Correspondence should be addressed to Petr Svoboda; svoboda@ft.utb.cz

Received 29 September 2015; Revised 8 December 2015; Accepted 10 December 2015

Academic Editor: Antonios Kelarakis

Two ethylene-octene copolymers with 17 and 45 wt.% of octene (EOC-17 and EOC-45) were compared in nanocomposites with Cloisite 93A. EOC-45 nanocomposites have a higher elongation at break. Dynamical mechanical analysis (DMA) showed a decrease of tan δ with frequency for EOC-17 nanocomposites, but decrease is followed by an increase for EOC-45 nanocomposites; DMA showed also increased modulus for all nanocomposites compared to pure copolymers over a wide temperature range. Barrier properties were improved about 100% by addition of organoclay; they were better for EOC-17 nanocomposites due to higher crystallinity. X-ray diffraction (XRD) together with transmission electron microscopy (TEM) showed some intercalation for EOC-17 but much better dispersion for EOC-45 nanocomposites. Differential scanning calorimetry (DSC) showed increased crystallization temperature T_c for EOC-17 nanocomposite (aggregates acted as nucleation agents) but decrease T_c for EOC-45 nanocomposite together with greatly influenced melting peak. Accelerated UV aging showed smaller C=O peak for EOC-45 nanocomposites.

1. Introduction

Polymer nanocomposites have been interesting already for a longer period of time. They represent the group of systems where polymer matrix is mixed with a certain type of nanofiller. One of the fillers is a type from layered silicate minerals when the thickness of the individual leaves is in nanometer size. The most frequently used type of nanoclay is montmorillonite (MMT) [1–5]. It is a layered mineral belonging to a group of clay minerals with octahedral and tetrahedral nets in the ratio of 2 : 1. Because of the problems with the exfoliation of its agglomerates in the polymeric matrix, MMT is used not pure but modified by the process known as organofilization or intercalation, that is, the insertion of a suitable organic compound into MMT interlayer [6–9]. The result of this step brings a broader D-spacing as well as a reduction of dispersing forces between the individual platelets of montmorillonite. The role of MMT nanoplatelets in the polymer matrix can be considered from various points of views. Generally, the first one is the original effect of the filler—especially the improvement of mechanical properties [10–13]. The advantage of nanofillers lies in the ability to create this improvement by much lower loading in comparison with common fillers. Another quality of nanoleaves is their positive impact on the orientation of long thick platelets in polymer matrix during compounding (mainly at extrusion/blowing of packaging films), where they create by their orientation a gas barrier to the gas transmission. Thus, the gas permeability is lower. The principle of this phenomenon is shown in Figure 1, where the imagination of an ideal situation—perfect exfoliation of the filler particles together with the perfect orientation of all MMT platelets in polymer matrix—is presented.

Next to the commonly used polyethylene (PE) or polypropylene (PP) matrices from the group of the polymer also some a little bit special types of these polymer matrices

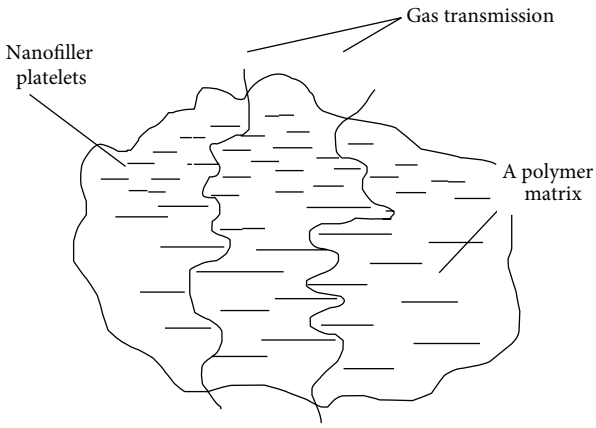

Figure 1: Improved barrier properties of nanocomposites.

are studied. One of them can be an ethylene-octene copolymer (EOC) and alternatively its blends with other polymer matrices, mostly PP [1–3].

The ethylene-octene copolymer (EOC), a new polyolefin elastomer, developed by Dow Chemical Company (Delaware, USA) with metallocene catalysis, is interesting by its properties and is attracting a lot of attention from both research and industry [14–16]. EOC is an ethylene based elastomer, so it brings an excellent compatibility with polyolefins, such as polyethylene and PP [17–20]. The presence of the octene comonomer in EOC causes a lower level of crystallinity and a higher flexibility in the copolymer. EOC can be considered as an elastomeric polymer, and usually the octene content in the copolymer varies under 20 wt.% [21, 22]. Blends of PP/EOC may provide enhanced impact properties and can be used, for example, in extruded or molded automotive exterior and interior parts, housing appliances, and other low-temperature applications. Pelletized EOC exhibits easy handling, mixing, and processability. Based on these properties, EOC is currently being used as an impact modifier of PP to replace ethylene propylene rubber (EPR) and ethylene propylene diene rubber (EPDM) [19, 23, 24].

As it was mentioned above, EOC significantly improves the impact strength, but it causes a decrease of the tensile strength and stiffness of PP [25–27]. Therefore, PP/EOC/mineral filler-based composites have been studied in order to enhance the toughness and stiffness of PP simultaneously. These systems are double-phased [23–25]. Mineral fillers with high aspect ratio, that is, clay nanofillers, have been found to increase stiffness and strength to the thermoplastic polyolefins; they provide a greater possibility for energy transfer from one phase to another [28–31].

However, comparative evaluation of the mechanical and thermal properties of composites based on PP, EOC, and mineral fillers is still limited.

The aim of this work was to add more information about the properties of EOC copolymer with clay nanofiller in order to evaluate the influence of used nanofiller and its concentration on the EOC copolymer. EOC matrix with nanoclay was chosen because this polymer matrix can be considered as one of tie layers of multilayer packaging films with the better end of use properties.

2. Materials and Methods

2.1. Materials. Polymer matrices used as carrier materials were ethylene-octene copolymers: Engage 8842 and Engage 8540 (both of DuPont DOW Elastomers, Europe GMBH, Switzerland)—linear formula $(CH_2CH_2)_x[CH_2CH[(CH_2)_5CH_3]]_y$ (see Figure 2).

To increase compatibility between the polymer matrix and the filler maleinized polyethylene (PE-MA) Priex 12043 (ADDCOMP Holland BV) in 5 wt.% concentration was used.

EOC-45 (Engage 8842) is an ultralow density copolymer (see Table 1) that offers exceptional properties of an ultralow density elastomer with the added potential of handing this polymer in pellet form. It has excellent flow characteristics and provides superb impact properties in blends with polypropylene (PP) and polyethylene (PE).

EOC-17 (Engage 8540) is a polyolefin elastomer that is well suited for foam applications and offers excellent performance for profile extrusion of tubing and hoses.

Organically modified montmorillonite (MMT) with trade name Cloisite 93A (Southern Clay Products, Inc.) was used. This type of nanoclay is modified by organic branches of type: dimethyl, hydrogenated tallow, 2-ethylhexyl, and quartenary ammonium methylsulfate; this type is recommended for nonpolar polymer matrices.

The quantity of the above-mentioned nanofiller added to the polymeric matrix was 3, 5, or 7 wt.%.

2.2. Sample Preparation. Polymers with the fillers were compounded in twin-screw extruder Scientific LTE 20-40; screw diameter was 20 mm and L/D ratio was 40/1. The temperatures of the individual heating zones and the extrusion head were set from 170°C to 205°C, the rotation speed of screws was 300 rpm, and the rotation speed of volumetric feeding screw was 20 rpm. The extruded strands were air-cooled and then transferred using a knife mill back to a pelletizer Scherr SGS-50E.

Specimens for measurement of properties were prepared by compression molding and cutting. Blends in the form of pellets were placed between two PET sheets preventing the contact with air and thus oxidative degradation. The material was pressed in a mold with size 125 × 125 × 2 mm (for platelets). The pressing time was 5 minutes for platelets (thickness approximately 2 mm) and 3 minutes for films (thickness about 50 μm); pellets are molded without a frame, only between two plates of the machine. After that, the mold with material was placed into a water-cooled hydraulic press and cooled down to room temperature.

2.3. Evaluation of Prepared Samples

2.3.1. Mechanical Properties. Tensile tests are among the most widely used test methods. The test specimen is deformed unidirectional until the break. Tensile testing was performed on tear machines with a range of campaign. Tensile test

Table 1: List of applied polymer materials (information from data sheets).

Name	Abbreviation	Octene content (wt.%)	Density (g/cm^3)	T_m (°C)
Engage 8540	EOC-17	17	0.908	104
Engage 8842	EOC-45	45	0.857	38

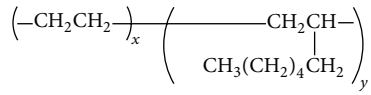

Figure 2: The structural formula of the ethylene-octene copolymer.

measures the deformation of the sample and the force required for deformation.

Tensile tests were measured at the Faculty of Technology in Tomas Bata University in Zlin (FT TBU). On tensile testing machine Galbadini Quasar 25, EN ISO 527-3 (64 0604), was used; for the speed of tearing 2 initial speed was 1 mm/min to the module 2%, and then the speed was increased to 100 mm/min until rupture. For tensile strength, elongation at break and tensile modulus were measured and evaluated.

2.3.2. Dynamic Mechanical Analysis (DMA). $\tan\delta$ (tan delta) damping which is the tangent of the phase angle and the ratio of E''/E' for room temperature in range 1–200 Hz with step 2 Hz and for temperature in the range −100°C to +100°C with at 1 Hz and amplitude 50 μm were measured. DMA measurements were performed on samples of size 20 × 5 mm made from premolded panels on the device DMA Perkin Elmer in laboratories of FT UTB Zlin.

2.3.3. Gas Barrier Properties (GTR). Observed nanocomposite molded films with the thickness of about 50 μm and diameter 80 mm at a pressure 2 bar and a temperature of 35°C were used for the measurement of N_2, O_2, and CO_2 permeability on the equipment known as Julabo TW8 based on CSN 64 0115, method of a constant volume. The conversion of the results according to standard ASTM D 3985-05 was performed.

2.3.4. XRD Analysis. In FT TBU laboratories, X-ray diffraction analysis (XRD) was also performed. The instrument diffractometer URD 6 was used. Measurements were done in the reflection mode in the 2θ range of 2–30° at a voltage of 40 kV and 30 mA with a step size of 0.0263°. Information from X-ray analysis, complemented by TEM, provides us with information on the morphology of the nanocomposites.

2.3.5. Transmission Electron Microscopy (TEM). Dispersion of the clays in polymer matrix and nanostructures was observed through microscopic investigations.

Samples of 40 × 20 mm made from molded plates were sent to IMC Prague, where TEM observation was performed. Ultrathin sections prepared on special ultracryomicrotome LEICA at −100°C were used as samples, temperature of the knife was −50°C, and thickness was of about 50 nm. Transmission electron microscopy was performed on a JEM 200 CX at an accelerated voltage of 100 kV.

2.3.6. Thermal Analysis: Differential Scanning Calorimetry (DSC). The samples on the Mettler Toledo DSC 1 with an external cooling unit and purging the chamber with nitrogen gas were observed. The rate of cooling and heating was 20°C per minute and the temperature range was −90°C to 150°C.

2.3.7. Accelerated Weathering Test. Samples about 5 × 15 cm for accelerated UV degradation test according to EN ISO 4892—2nd ingestion device—Xenotest Alpha were prepared. The measurement conditions were as defined in above-mentioned standard (temperature was 38°C, irradiance 60 Wh/m^2 filters simulating daylight, and RH 50%). One measurement cycle (46 days) simulates the degradation of one year.

2.3.8. Fourier Transform Infrared Spectroscopy (FTIR). The test on the FTIR spectrometer AVATAR 320 (Nicolet) which is a standard single-beam FTIR spectrometer operating in the range of wave numbers 4000 to 500 cm^{-1} was performed. FTIR instrument is controlled via a PC using the software Omnic. The measurement by the ATR (attenuated reflection method) was carried out.

3. Results and Discussion

3.1. Mechanical Properties. Polymer/clay nanocomposites have been studied for longer period of time as materials that could be used in packaging industry. Two types of Engage (ethylene-octene copolymer)/clay nanocomposites in this paper are reported. This work is particularly focused on the mechanical, barrier, and morphology properties.

Table 2 presents the mechanical properties of two types of EOC with nanofiller Cloisite 93 in the polymer matrix. As can be seen, the values of the tensile strength of EOC are the same in comparison to materials enriched by filler Cloisite 93. It can be assumed that the presence of filler in samples, compared to the neat ones, does not have a significant effect on the change of mechanical properties.

Figure 3 illustrates tensile stress as a function of strain for pure EOC-17 (45) and EOC with 5% of Cloisite 93; in Table 2 the values for filler contant 3, 5, and 7 wt.% are listed. EOC-17 exhibits yield point and higher values of stress. This is caused by the presence of lamellar crystals. Higher content of octene groups in EOC-45 causes much lower presence of crystals and the crystals are not lamellar but very small "spot-like" [17]. This unique morphology is responsible for lower modulus (higher softness), absence of yield point, and better elasticity (which is illustrated in Table 2). Presence of nanoclay caused higher stress value, in case of EOC-17 during the whole test; in case of EOC-45 it caused higher elongation. For example, the yield point of EOC-17 increased by addition of 5 wt.% of nanoclay from 7.41 to 9.28 MPa (see Figure 3(a)). During the tensile test the orientation of crystals caused increase in stress for all samples.

Table 2: Tensile tests of pure EOC-17, EOC-45, and filled EOC-17 and EOC-45 with 3, 5, and 7 wt.% of nanoclay Cloisite 93.

Composition	Tensile strength (MPa)	Std. dev.	Ductility (a.u.)	E modulus (MPa)
EOC-17 pure	30.950	2.4	10.8237	25.34
EOC-17 + 3% Cloisite 93	26.767	2.4	9.0378	24.56
EOC-17 + 5% Cloisite 93	28.458	2.5	9.1541	24.65
EOC-17 + 7% Cloisite 93	25.117	2.6	8.3711	24.38
EOC-45 pure	6.950	0.4	18.5486	2.16
EOC-45 + 3% Cloisite 93	6.208	0.4	17.4329	2.53
EOC-45 + 5% Cloisite 93	7.400	0.3	19.4329	4.62
EOC-45 + 7% Cloisite 93	5.258	0.5	11.5429	3.43

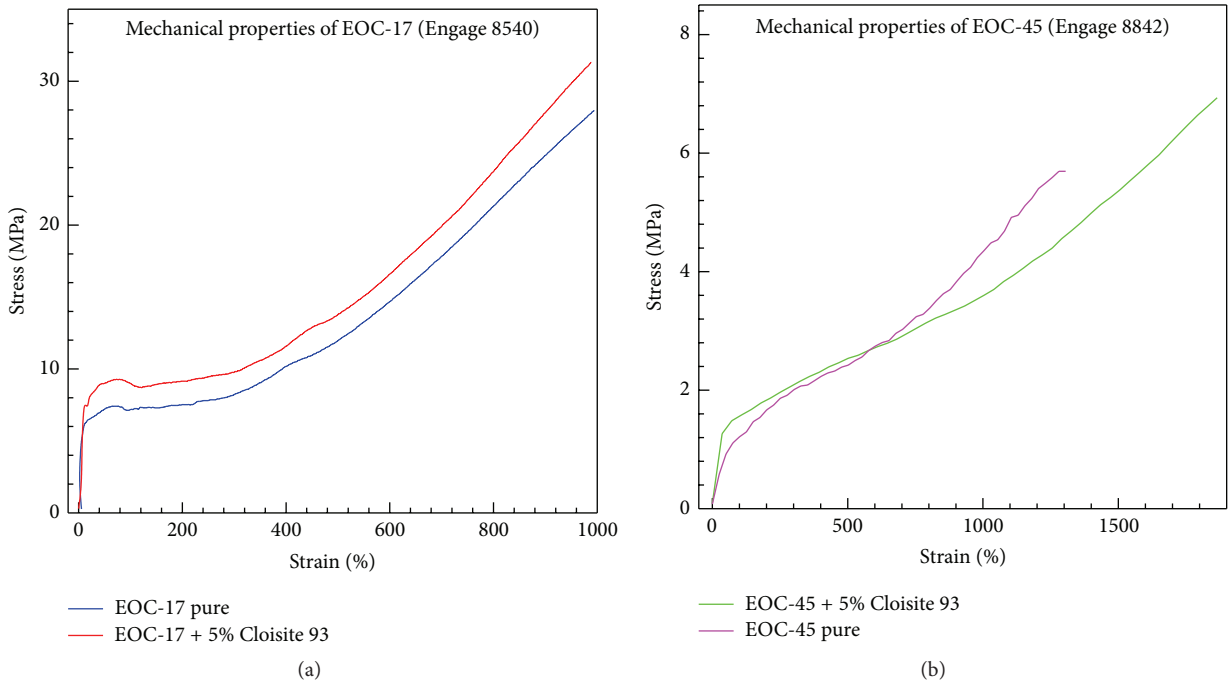

Figure 3: Mechanical properties of (a) EOC-17 (Engage 8540) with 5 wt.% Cloisite 93 and (b) EOC-45 (Engage 8842) with 5 wt.% Cloisite 93.

After the tensile test we have measured also the residual strain. EOC-45 samples exhibit better elasticity (lower value of residual strain). The composites have only slightly worse elasticity (slightly higher values of residual strain).

Measuring distance is as follows: l_0 = initial distance, l_1 = distance at maximum extension, and l_2 = distance after 24 hours of relaxation (see Table 3).

Table 3: Residual strain of pure EOC-17, EOC-45 and filled EOC-17, EOC-45 with 5 wt.% of nanoclay Cloisite 93.

Composition	l_0 (mm)	l_1 (mm)	l_2 (mm)
EOC-17 pure	10	80	60.1
EOC-17 + 5% Cloisite 93	10	90	60.5
EOC-45 pure	10	140	30.2
EOC-45 + 5% Cloisite 93	10	145	30.5

3.2. Dynamic Mechanical Analysis (DMA). Pure EOC-17 and its blends with Cloisite 93 show a linear decrease of tan delta (tan δ) with increasing frequency. The addition of Cloisite 93 causes tan δ to drop significantly at high frequencies whereas the low frequencies are affected only marginally.

However, EOC-45 is behaving differently, the addition of Cloisite 93 leads to increased tan δ, and the increase is higher when compared to pure EOC-45. What remains the same is the marginal effect of Cloisite 93 within low frequencies and much stronger interaction at high frequency. Also the percentage of Cloisite 93 does not affect final values of tan δ; EOC-45 possesses a high percentage of octene chains (45 wt.%) compared to 17 wt.% of EOC-17. As we can see in Figure 4, the driving force for different mechanical behavior is interaction with Cloisite 93.

Results and curves of tan delta versus frequency were very similar for 3, 5, and 7 wt.% Cloisite 93; therefore, we used results of the dependence on the frequency and the temperature only for 5 wt.% concentration level. According to our previous experience the 5% nanoclay filling is optimal.

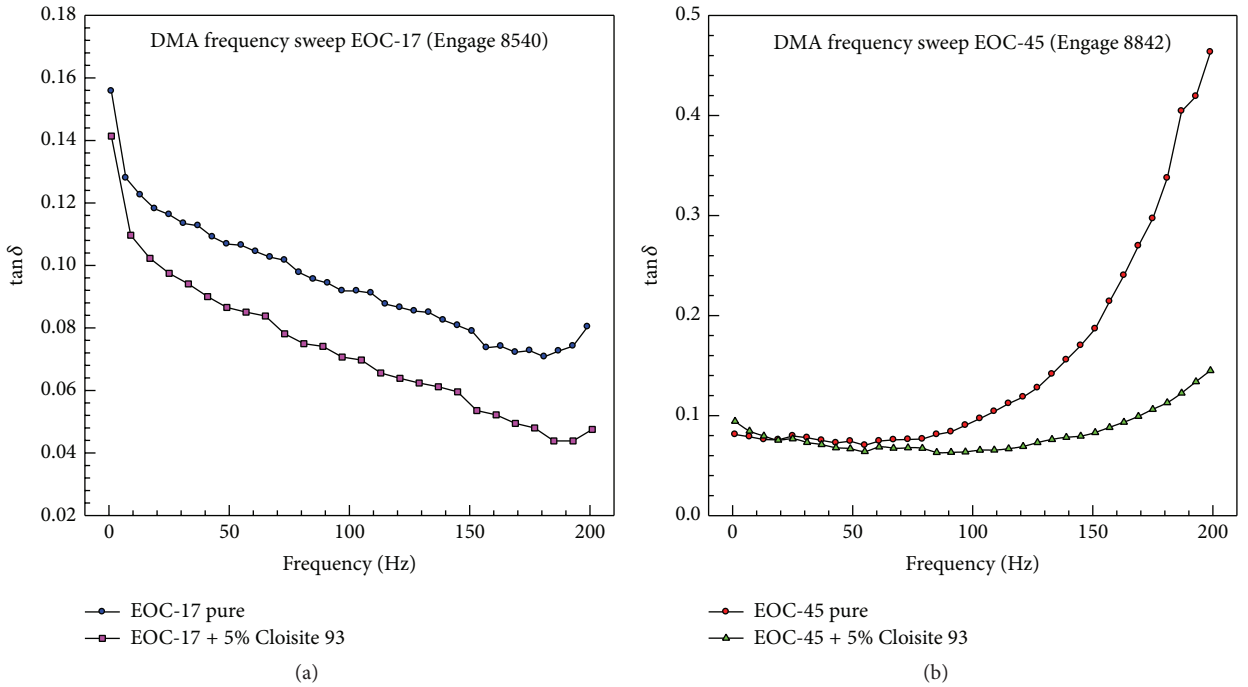

Figure 4: DMA graphs of (a) EOC-17 (Engage 8540) with 5 wt.% Cloisite 93 and (b) EOC-45 (Engage 8842) with 5 wt.% Cloisite 93 at room temperature.

Table 4: Dependence of tan delta and E' modulus on the temperature for pure EOC-17, EOC-45, and filled EOC.

Composition	Temperature (°C)						
	−90	−60	−30	0	30	60	90
				tan δ			
EOC-17 pure	0.0893	0.0215	0.0626	0.1106	0.1669	0.1885	0.0579
EOC-17 + 5% Cloisite 93	0.0312	0.0205	0.0576	0.0931	0.1482	0.2000	0.1262
EOC-45 pure	0.1314	0.1370	0.2551	0.0701	0.0824	—	—
EOC-45 + 5% Cloisite 93	0.0742	0.0978	0.2413	0.0762	0.0987	—	—
				E' modulus (MPa)			
EOC-17 pure	1258	1197	871	356	147.6	47.09	19.10
EOC-17 + 5% Cloisite 93	1552	1460	1078	498	237.7	77.31	28.59
EOC-45 pure	537	436	26.4	8.21	4.01	—	—
EOC-45 + 5% Cloisite 93	841	701	59.9	19.4	9.79	—	—

tan δ was lower for both of the EOC filled nanocomposites. At lower frequencies the EOC-45 and EOC-45 nanocomposites exhibit lower value of tan δ (better elasticity). This is caused by lower crystallinity and also by defect that the crystals are "spot-like" while in EOC-17 there are normal lamellar crystals. At frequencies higher than 100 Hz we found increase of tan δ for EOC-45. The test was performed at room temperature which is rather close to melting point. The macromolecules lose the ability to return to original shape during the high-frequency test. The nanofiller decreases the amount of deformation; therefore the tan δ values are lower (see Figure 4).

The dependency of E' modulus on temperature is similar for both materials and nanocomposites (Figure 5 and Table 4). After reaching glass transmission temperature, modulus shows sharp drop and both compounds possess higher modules in almost whole temperature range with the exception of temperature close to melting point. Strengthening effect of Cloisite is stronger in EOC-17 nanocomposite when compared to EOC-45, in addition to increased modulus, glass transition and melting temperatures are slightly shifted to higher temperatures.

Both nanocomposites show similar behavior in tan δ; temperature dependency Cloisite 93 increases tan delta. Mentioned increase is more significant at the peak position of the curve. The compound of EOC-17 with 5 wt.% Cloisite 93 loses tan delta much less compared to pure EOC-17, and when the temperature approaches melting point, it retains significantly higher tan δ. On the other hand, EOC-45 with Cloisite 93 loses tan delta at the same rate as pure EOC-45,

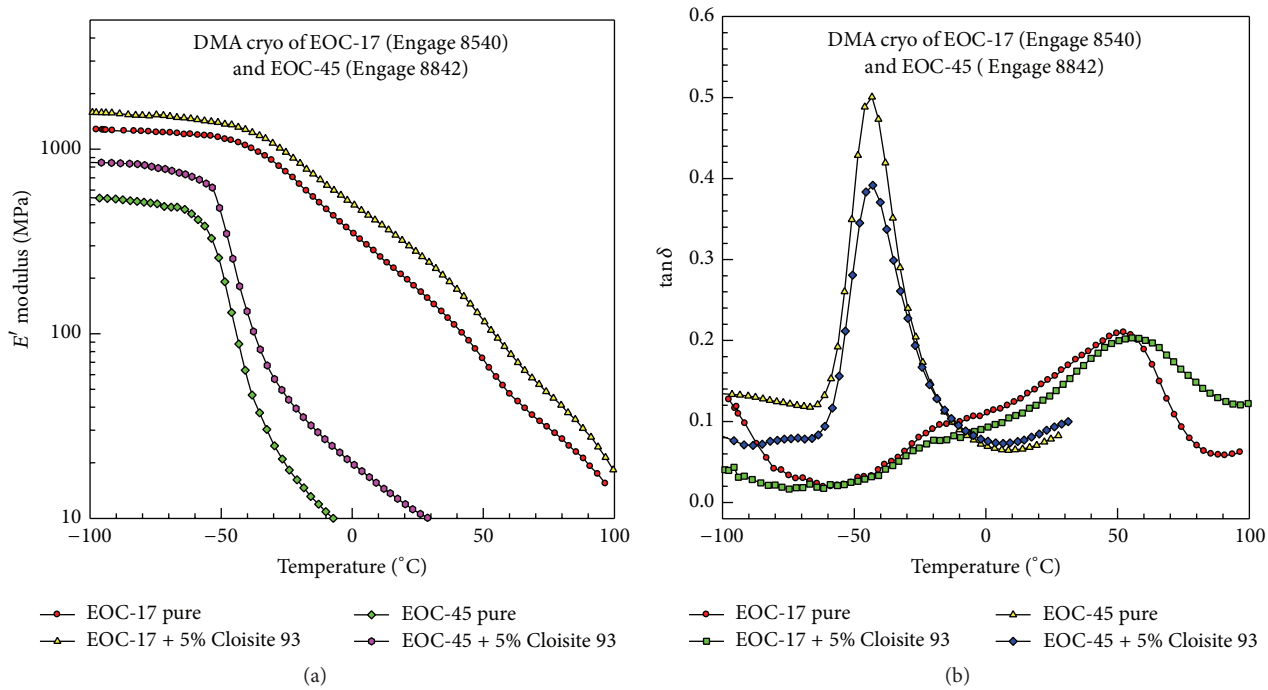

Figure 5: DMA graphs temperature dependencies: EOC-17 (Engage 8540) with 5 wt.% Cloisite 93 and EOC-45 (Engage 8842) with 5 wt.% Cloisite 93: (a) $\log E'$ modulus and (b) $\tan\delta$.

but the maximal increase at peak point is higher than EOC-17. Another difference is visible when close to melting point temperatures: the volume of side chains does change the effect of Cloisite 93 on EOC behavior.

Curves can be influenced by the low thermal conductivity of polymer samples. The E' modulus values were higher for the nanocomposites at all temperatures.

With increasing temperature the E' modulus decreases for all samples, especially above −50°C, nanofiller increases the modulus greatly at temperatures above T_m which is at this graph visible only for EOC-45 (with T_m around 50°C).

Figure 5(b) illustrates decrease from 0.5 to 0.39. The position of T_g (the first peak) did not change in case of EOC-17; nevertheless above +50°C the presence of nanoclay significantly increased the $\tan\delta$ value which can be interpreted as worse elasticity above this temperature for the nanocomposites. At lower temperatures the $\tan\delta$ values are lower for the nanocomposites which means better elasticity. The worse elasticity at temperature approaching melting point is caused by a flow of the material during mechanical testing which is not prevented by crosslinking (see Figure 5(b)). The nanofiller prevents return of the sample from elongated state at elevated temperatures and thus $\tan\delta$ for the nanocomposites is higher.

3.3. Barrier Properties. As mentioned above, the ethylene-octene copolymer can be used in packaging industry. Therefore, this study also covers the values of permeability for N_2, O_2, and CO_2, which are mediums that should be prevented from penetrating through the film, for example, in the case of food wrapping. In this instance, films pressed on the manual and hydraulic presses were used as the samples for the measurement.

The evaluation of gas transmission rate and oxygen transmission rate (see Table 5 and Figure 6) is shown for EOC-17 and EOC-45 copolymer/clay nanocomposites. As the results show permeability, pure materials (EOC-17 and EOC-45) have inferior properties compared to filled materials. The best combination seems to be of EOC + 5% Cloisite 93.

In a comparison of both used ethylene-octene copolymers, EOC-17 shows significantly better properties for all gases. This may be due to lower content of octene groups and higher crystallinity.

It can be concluded that the nanofiller Cloisite 93 can improve the polymer matrix EOC. When applied in EOC matrix the permeability of gases decreases. This may be due to a better distribution and dispersion of filler, or better exfoliation MMT nanolayers in the polymer matrix. It is known that during the pressing of samples it is not possible to suppose an achievement of a perfect orientation of MMT platelets.

Hot plates are pressed in a press machine into very thin films. The thickness of the pressed film is about 50 μm, and the size of MMT platelets is on the similar level; thus the orientation of MMT leaves, in this case, is not excluded.

3.4. Analysis of the Morphology by XRD. In order to discover the level of montmorillonite exfoliation in used matrices. XRD patterns have been taken. For easier comparison graphs with the curve of neat EOC matrix, of original MMT nanofiller and their mixture, have been summarized (Figure 7).

Table 5: The gas transmission rate for N_2, O_2, and CO_2.

Composition	Thickness (mm)	GTR for N_2 (cm^3 (STP)/m^2·den. 0.1 MPa)	GTR for O_2 (cm^3 (STP)/m^2·den. 0.1 MPa)	GTR for CO_2 (cm^3 (STP)/m^2·den. 0.1 MPa)
EOC-17 pure	0.52	509	1372	5361
EOC-17 + 3% Cloisite 93	0.52	295	789	2765
EOC-17 + 5% Cloisite 93	0.53	264	734	2619
EOC-17 + 7% Cloisite 93	0.53	386	940	3541
EOC-45 pure	0.53	3055	8060	33369
EOC-45 + 3% Cloisite 93	0.53	1792	4265	17874
EOC-45 + 5% Cloisite 93	0.53	1683	4113	16664
EOC-45 + 7% Cloisite 93	0.52	2065	5391	25878

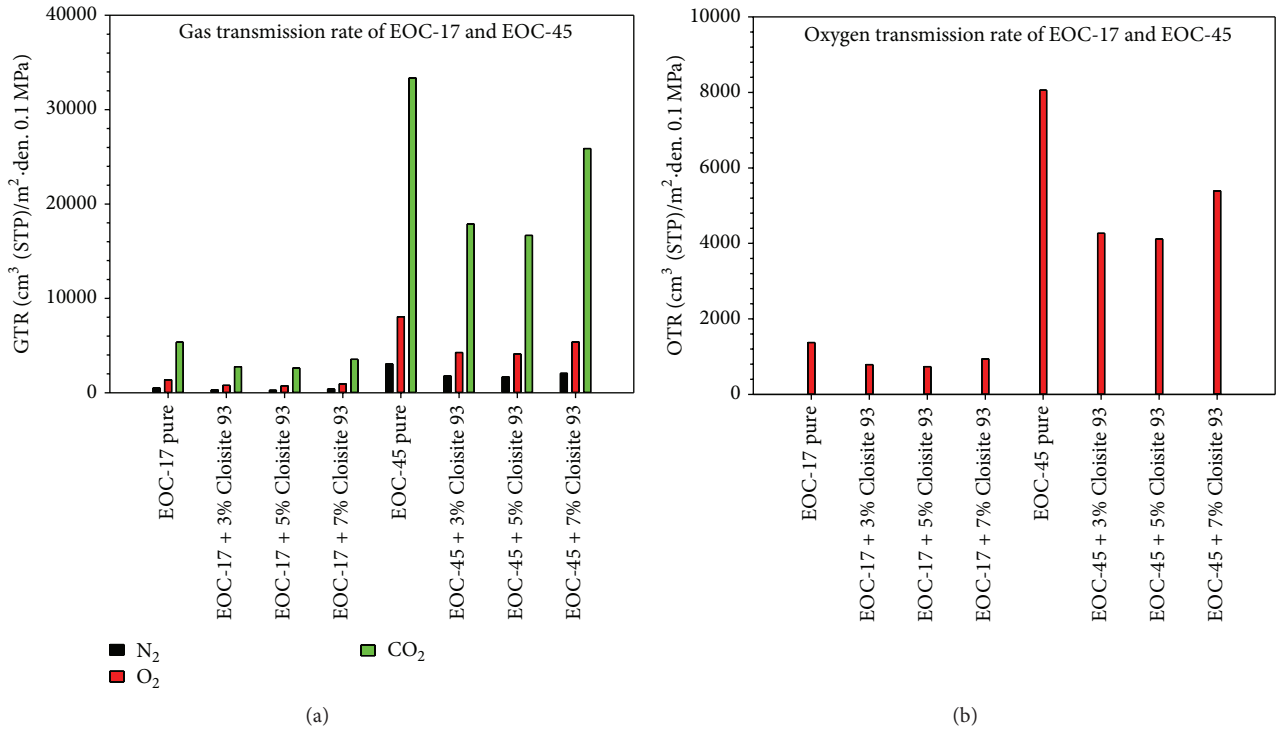

Figure 6: Barrier properties of EOC-17 (Engage 8540) and EOC-45 (Engage 8842): (a) gas transmission rate and (b) oxygen transmission rate.

According to the recorded results, it is possible to observe that incomplete montmorillonite exfoliation has taken place, but as discussed below, despite the incomplete exfoliation shown by XRD measurement, a certain improvement of some qualities observed has been proved.

Better results in X-ray diffraction can be observed in the case of EOC-45, where curves of filled materials compared with pure EOC sample are almost identical, with no significantly different peaks in the area of Cloisite 93A. In contrary, the curve of a composite of EOC-17 exhibits very noticeable peak, almost the same, like origin Cloisite 93A. This can be connected with the different EOC sample structure.

Figure 7(a) illustrates a small shift in diffraction angle towards lower value corresponding to small increase of *D*-spacing (see Table 6) from 2.56 to 2.72 nm in case of EOC-17 nanocomposite. This could be interpreted as intercalation.

Table 6: *D*-spacing of clay and filled EOC-17.

Composotion	*D*-spacing (nm)
EOC-17 + 5% Cloisite 93	2.728
Cloisite 93	2.562

Quite different scenario is recorded for EOC-45 nanocomposite in Figure 7(b). The peak has almost completely disappeared which can be interpreted as exfoliation. The presence of a small peak at 4.2° corresponding to *D*-spacing being 2.21 nm can be explained by a distribution of *D*-spacing in original Cloisite 93 ranging from 2.2 to 2.7 nm. During the melt-mixing the clay with larger *D*-spacing (2.3~2.7 nm) got exfoliated while small amount of clay with *D*-spacing 2.2 nm remained.

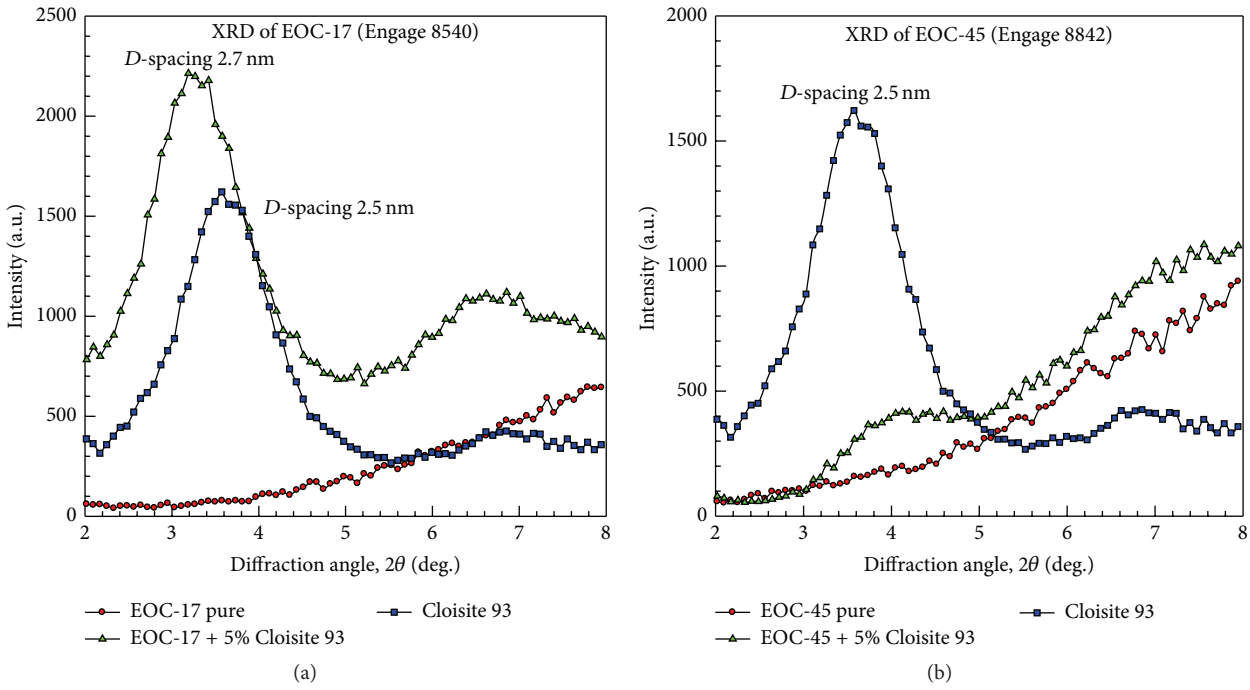

Figure 7: XRD graphs of EOC: (a) EOC-17 (Engage 8540) with 5 wt.% Cloisite 93 and (b) EOC-45 (Engage 8842) with 5 wt.% Cloisite 93.

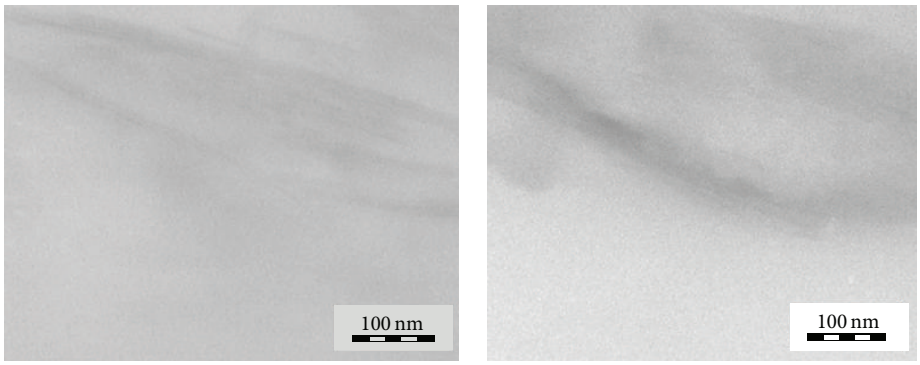

Figure 8: TEM pictures of (a) EOC-45 (Engage 8842) with 5 wt.% Cloisite 93 and (b) EOC-45 (Engage 8842) with 7 wt.% Cloisite 93.

3.5. Analysis of the Morphology by Transmission Electron Microscopy (TEM). The mixing was quite successful for both EOCs as it comes from results of TEM analysis. In Figures 8 and 9 a comparison of the distribution of nanofiller in a matrix of EOC-17 with different contents of clay can be seen. Distribution in both cases is about the same, but images suggest that in the case of EOC-17 with 5 and 7 wt.% nanofiller in polymer matrix the exfoliation is worse.

TEM results confirm previous conclusions from XRD indicating better exfoliation of nanofiller in case of EOC-45.

The similar situation is also shown in Figure 9. The distribution and exfoliation of nanofiller in the polymer matrix is correct, but only for 5 wt.% Cloisite 93.

According to our experience with filled polymers, 5 wt.% nanofiller filling is optimal in the polymer matrix.

This concentration leads to the exfoliation of the filler particles in the polymer. While when 7 wt.% nanofiller is used, not only the exfoliation is not good but even agglomerates can be formed.

3.6. Differential Scanning Calorimetry (DSC). Previous tests show that the best performance is at about 5% of nanofiller in the polymer matrix. In further tests, such as the DSC and FTIR, the samples are compared in particular with a 5 wt.% concentration.

DSC curve of pure EOC-17 (see Figure 10(a)) shows melting temperature of 108.3°C 5% of Cloisite causes the melting point to drop slightly to 106.2°C. The peak occurring at 126°C (after Cloisite 93 addition) could be assigned to the PE-MA

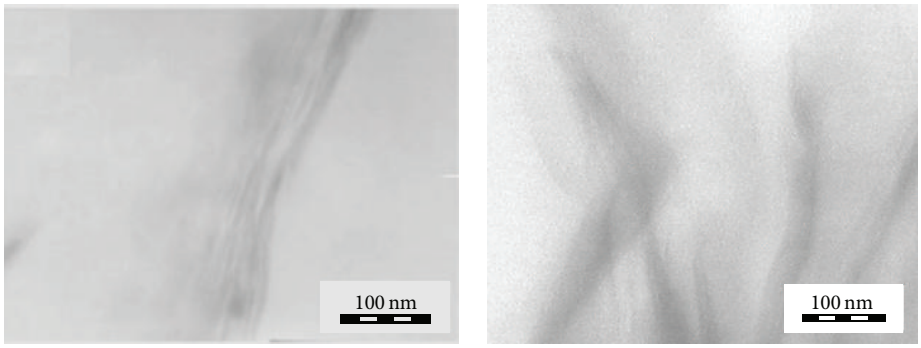

(a) (b)

Figure 9: TEM pictures of (a) EOC-17 (Engage 8540) with 5 wt.% Cloisite 93 and (b) EOC-17 (Engage 8540) with 7 wt.% Cloisite 93.

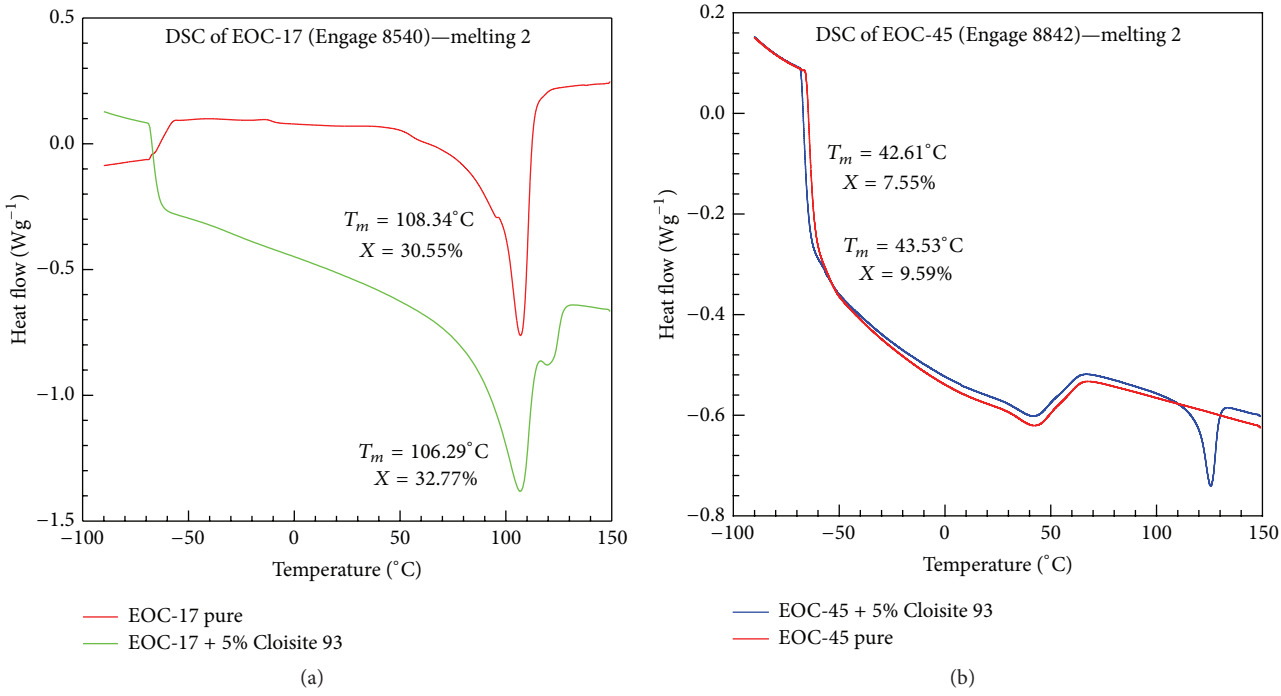

(a) (b)

Figure 10: DSC graph of (a) EOC-17 (Engage 8540) with 5 wt.% Cloisite 93—melting 2 and (b) EOC-45 (Engage 8842) with 5 wt.% Cloisite 93—melting 2.

presence. However, crystallization curves differ significantly; pure EOC crystallizes at 88.3°C, blending Cloisite 93 into EOC leads to the higher crystallization temperature of 89.4°C, and additional peak occurs at 105°C. The reason for two crystallization peaks is a low percentage of octene units. Cloisite 93 causes a shift in crystallization peaks which explains two peaks of a blend compared to two peaks of pure EOC. We can speculate that Cloisite 93 can influence crystallization ability of long base ethylene chains but does not affect short octene chains.

The exfoliation of nanoclay in EOC-17 was not perfect (shown by XRD and TEM), and some aggregates of clay remained. These aggregates acted most likely as nucleating agents. Therefore, the crystallization temperature increased about 2°C.

This effect is much more visible in a second nanocomposite, EOC-45 with Cloisite 93 (Figures 10(b) and 11(b))—in this case, pure polymer melts at 43.5°C, Cloisite 93 causes shift peak at 42.6°C of pure EOC-45, and additional peak at 126°C is visible (comes probably from PE-MA compatibilizer). Pure EOC-45 crystallizes at temperature 18.8°C and filled at 16.1°C; peak at 120°C (PE-MA) remains.

Due to mentioned effect at crystallization and a higher octene content of EOC-45, peak appearance could be caused by a combination of both factors. Melting curves show that similar behavior of Cloisite 93 causes forming of the additional peak at high temperature and a slight drop in a melting temperature. The percent crystallinity was calculated using a value of $\Delta H^{\circ}_{m} = 290\ \mathrm{Jg}^{-1}$ for the heat of fusion of 100% crystalline polyethylene [32].

Table 7: FTIR measurement and comparison of the peak area before UV degradation and peak area after 46 days of UV degradation.

Composition	Peak area 1810.920–1508.135 cm^{-1}	Peak area 46 days 1810.920–1508.135 cm^{-1}	Peak height at 1720 cm^{-1} 46 days (absorbance)
EOC-17 pure	1.347	6.828	0.111
EOC-17 + 5% Cloisite 93	1.517	4.367	0.112
EOC-45 pure	1.437	5.273	0.133
EOC-45 + 5% Cloisite 93	1.242	3.476	0.102

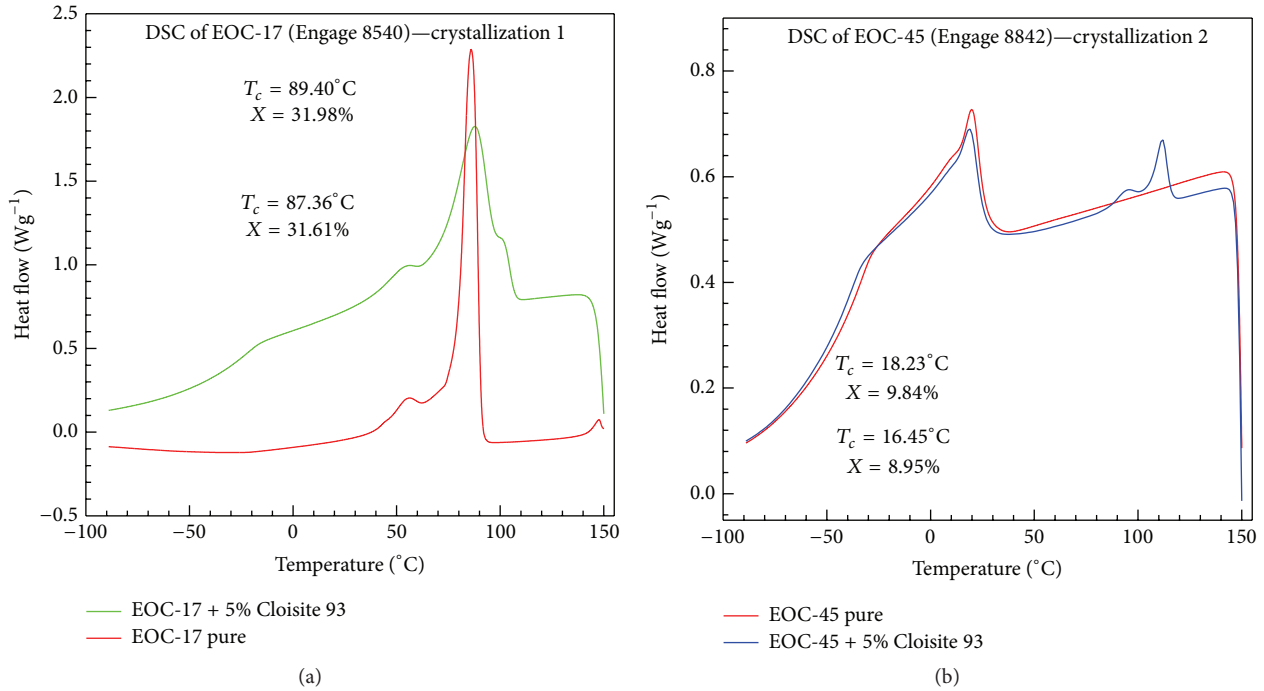

Figure 11: DSC graph of (a) EOC-17 (Engage 8540) with 5 wt.% Cloisite 93—crystallization 2 and (b) EOC-45 (Engage 8842) with 5 wt.% Cloisite 93—crystallization 2.

As shown by XRD and TEM the exfoliation of nanoclay in EOC-45 was better. This influenced rather broad melting peak and lower crystallization temperature. This time, there were no aggregates that could serve as nucleating agents.

3.7. Accelerated Weathering Test and FTIR. The samples underwent UV degradation in the device Xenotest Alpha for the period 46 days. At the beginning of the degradation test and at the end of degradation test FTIR analysis of all the measured samples was performed.

EOC chain is composed only of CH_3 and CH_2 groups. Typical peaks (see Figures 12 and 13) for these groups are in 2962 cm^{-1} for CH_3 asymmetric valence (as. v.). 2872 cm^{-1} for CH_3 symmetric valence (s. v.) and 2926 cm^{-1} for CH_2 asymmetric valence (as. v.). 2853 cm^{-1} for CH_2 symmetric valence (s. v.).

By FTIR analysis change in the area of 1810 cm^{-1} to 1681 cm^{-1} was monitored. This maximum corresponds to the vibration of C=O bonds that are generated in the degradation processes. The results show that the largest increase in the area of the pure samples EOC-17 and EOC-45 was recorded. The higher change of EOC-17 pure was observed. Filled specimens show a smaller percentage of degradation of the matrix (see Table 7). During sample degradation probably molecular weight decreases and leads to the breaking of chains.

Filling 5 wt.% of the modified Cloisite 93 has improved observed characteristics, especially in the longer term. In this case, the impact modifier can be expected during the course of degradation.

The difference between the materials in the curves may be caused by different densities of both the EOC and various contents of octene groups. The protection against UV degradation was better in the case of EOC-45 nanocomposite most likely due to a better dispersion of clay.

The presence of the filler (Cloisite 93) in the EOC-45 matrix reduces degradation of the nanocomposite in comparison to pure EOC-45, which may be due to a higher level of exfoliation of the MMT platelets in polymer matrix because these exfoliated filler particles can protect EOC's polymer chain against the degradation impacts. Table 7 shows peak height at 1720 cm^{-1} 46 days (absorbance) and Figure 13

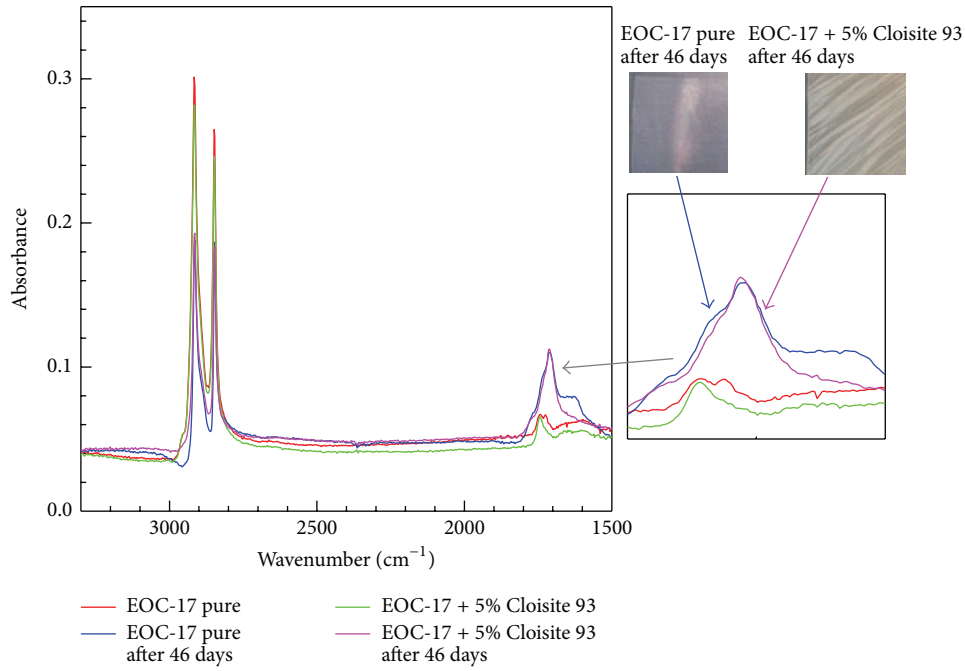

Figure 12: FTIR graph of EOC-17 (Engage 8540) pure and EOC-17 with 5 wt.% Cloisite 93 and details of area 1810 to 1681 cm^{-1}. Picture of change of EOC-17 pure after 46 days of UV degradation. EOC-17 + 5% Cloisite 93 after 46 days of UV degradation.

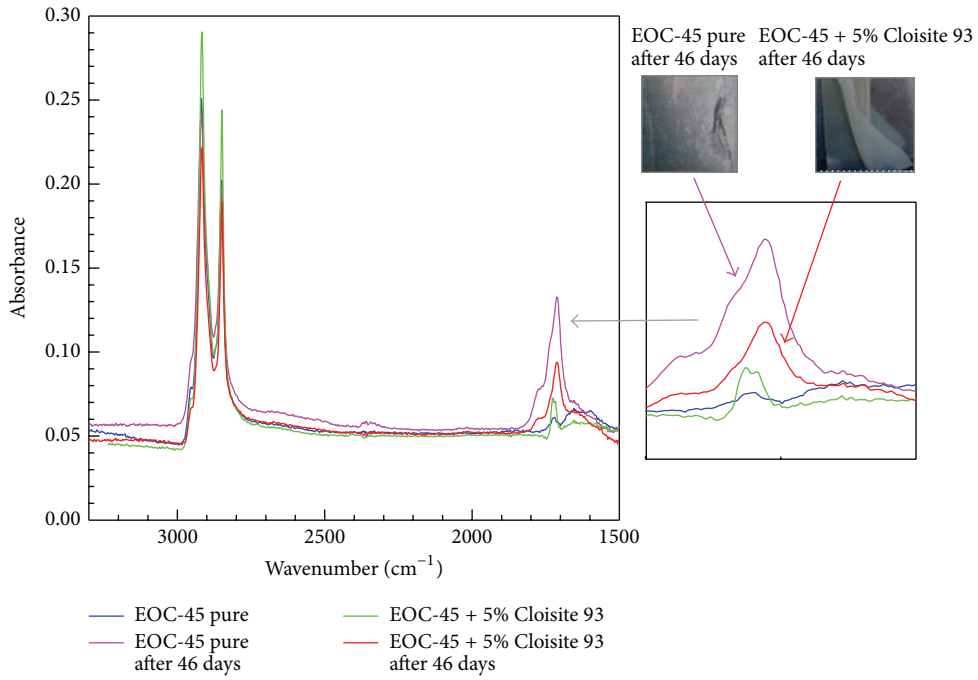

Figure 13: FTIR graph of EOC-45 (Engage 8842) pure and EOC-45 with 5 wt.% Cloisite 93 and details of area 1810 to 1681 cm^{-1}. Picture of change of EOC-45 pure after 46 days of UV degradation. EOC-45 + 5% Cloisite 93 after 46 days of UV degradation.

shows decrease from 0.133 for pure EOC-45 to 0.102 for EOC-45 with 5 wt.% Cloisite 93.

The results of FTIR confirm the tests of the DMA, XRD, TEM, and DCS for better exfoliation of nanofiller in polymer matrix EOC-45. The perfect exfoliation of nanofiller in the polymer matrix may be caused by higher content octene units.

4. Conclusion

Ethylene-octene copolymer matrices with one type of commercial nanofiller with different concentration were prepared and observed. Because of using mentioned materials for food packaging, the mechanical properties of prepared samples, barrier, morphological, thermal, and UV degradation properties were checked.

Comparison of mechanical properties and exfoliation of the nanofiller in the polymer matrix was observed. Strengthening effect of Cloisite is stronger in the EOC-45 mixture when compared to EOC-17. In addition to increased modulus, glass transmission and melting temperature are slightly shifted to higher temperatures. The very good result in the case of mechanical and barrier properties were found, especially for EOC matrix with 5 wt.% Cloisite 93. The EOC reaches the maximum value EOC-45 with 5 wt.% Cloisite 93, on the opposite side of the lowest values in the EOC-17 + 3% Cloisite 93 for mechanical properties. EOC-17 pure and its blends with Cloisite 93 show a linear decrease of tan delta ($\tan \delta$) with increasing frequency. The addition of Cloisite 93 causes $\tan \delta$ to drop significantly at high frequencies whereas the low frequencies are affected only
marginally.

Filling 5 wt.% of the modified Cloisite 93 has improved FTIR observed characteristics, especially in the longer term. In this case, the impact modifier can be expected during the course of degradation. Platelets of montmorillonite can overlap and may cause deterioration of the desired properties. The goal of the production of polymer nanocomposites is to achieve the full exfoliation. It was found that nanofillers in polymer matrix mechanics affect polymer properties. It is possible to state that good exfoliation of fillers can improve mechanical properties of nanocomposites. Nevertheless, the degree of exfoliation and orientation of the platelets is the most critical parameter.

Conflict of Interests

The authors declare that there is no conflict of interests regarding the publication of this paper.

Acknowledgments

This paper (specified by the fact) was written with the support by the Projects TA03010799 and IGA/FT/2015/007 TBU in Zlin.

References

[1] F. Bertini, M. Canetti, G. Audisio, G. Costa, and L. Falqui, "Characterization and thermal degradation of polypropylene-montmorillonite nanocomposites," *Polymer Degradation and Stability*, vol. 91, no. 3, pp. 600–605, 2006.

[2] S. P. Zhu, J. Y. Chen, H. L. Li, and Y. Cao, "Effect of polymer matrix/montmorillonite compatibility on morphology and melt rheology of polypropylene nanocomposites," *Journal of Applied Polymer Science*, vol. 128, no. 6, pp. 3876–3884, 2013.

[3] F. Lei, S. Yang, M. T. Yang, J. Li, and S. Y. Guo, "Exfoliation of organic montmorillonite in iPP free of compatibilizer through the multistage stretching extrusion," *Polymer Bulletin*, vol. 71, no. 12, pp. 3261–3273, 2014.

[4] L. B. Fitaroni, J. A. de Lima, S. A. Cruz, and W. R. Waldman, "Thermal stability of polypropylene-montmorillonite clay nanocomposites: limitation of the thermogravimetric analysis," *Polymer Degradation and Stability*, vol. 111, pp. 102–108, 2015.

[5] X. Yin and G. S. Hu, "Effects of organic montmorillonite with different interlayer spacing on mechanical properties, crystallization and morphology of polyamide 1010/nanometer calcium carbonate nanocomposites," *Fibers and Polymers*, vol. 16, no. 1, pp. 120–128, 2015.

[6] K.-B. Yoon, H.-D. Sung, Y.-Y. Hwang, S. K. Noh, and D.-H. Lee, "Modification of montmorillonite with oligomeric amine derivatives for polymer nanocomposite preparation," *Applied Clay Science*, vol. 38, no. 1-2, pp. 1–8, 2007.

[7] L. B. Manfredi, D. Puglia, A. Tomasucci, J. M. Kenny, and A. Vázquez, "Influence of clay modification on the properties of resol nanocomposites," *Macromolecular Materials and Engineering*, vol. 293, no. 11, pp. 878–886, 2008.

[8] Z. Qian, S. Zhang, and M. Yang, "Effect of clay modification on photo-oxidation of polyethylene/clay nanocomposites," *Polymers and Polymer Composites*, vol. 16, no. 8, pp. 535–546, 2008.

[9] X. Y. Meng, Z. Wang, X. H. Du, Y. H. Wang, and T. Tang, "Exfoliation of organically modified montmorillonite driven by molecular diffusion in maleated polypropylene," *Journal of Applied Polymer Science*, vol. 113, no. 1, pp. 678–684, 2009.

[10] J. Soulestin, B. J. Rashmi, S. Bourbigot, M.-F. Lacrampe, and P. Krawczak, "Mechanical and optical properties of polyamide 6/clay nanocomposite cast films: influence of the degree of exfoliation," *Macromolecular Materials and Engineering*, vol. 297, no. 5, pp. 444–454, 2012.

[11] T. Kuila, T. Tripathy, and J. H. Lee, "Polyolefin-based polymer nanocomposites," in *Advances in Polymer Nanocomposites: Types and Applications*, pp. 181–215, Woodhead Publishing, 2012.

[12] F. Zandi, M. Rezaei, and A. Kasiri, "Effect of nanoclay on the physical-mechanical and thermal properties and microstructure of extruded noncross-linked LDPE nanocomposite foams," *Composite Science and Technology*, vol. 471-472, pp. 751–756, 2011.

[13] P. Santamaría, J. I. Eguiazabal, and J. Nazabal, "Dispersion and mechanical properties of a nanocomposite with an organoclay in an ionomer-compatibilized LDPE matrix," *Journal of Applied Polymer Science*, vol. 119, no. 3, pp. 1762–1770, 2011.

[14] R. Theravalappil, P. Svoboda, J. Vilcakova, S. Poongavalappil, P. Slobodian, and D. Svobodova, "A comparative study on the electrical, thermal and mechanical properties of ethylene-octene copolymer based composites with carbon fillers," *Materials & Design*, vol. 60, pp. 458–467, 2014.

[15] C. Grein, M. Gahleitner, and K. Bernreitner, "Mechanical and optical effects of elastomer interaction in polypropylene modification: ethylene-propylene rubber, poly-(ethylene-co-octene) and styrene-butadiene elastomers," *Express Polymer Letters*, vol. 6, no. 9, pp. 688–696, 2012.

[16] R. Rajeshbabu, U. Gohs, K. Naskar, V. Thakur, U. Wagenknecht, and G. Heinrich, "Preparation of polypropylene (PP)/ethylene octene copolymer (EOC) thermoplastic vulcanizates (TPVs) by high energy electron reactive processing," *Radiation Physics and Chemistry*, vol. 80, no. 12, pp. 1398–1405, 2011.

[17] P. Svoboda, R. Theravalappil, D. Svobodova et al., "Elastic properties of polypropylene/ethylene-octene copolymer blends," *Polymer Testing*, vol. 29, no. 6, pp. 742–748, 2010.

[18] R. R. Babu, N. K. Singha, and K. Naskar, "Dynamically vulcanized blends of polypropylene and ethylene octene copolymer: influence of various coagents on mechanical and morphological characteristics," *Journal of Applied Polymer Science*, vol. 113, no. 5, pp. 3207–3221, 2009.

[19] D. Pizele, V. Kalkis, R. M. Meri, T. Ivanova, and J. Zicans, "On the mechanical and thermomechanical properties of low-density polyethylene/ethylene-α-octene copolymer blends," *Mechanics of Composite Materials*, vol. 44, no. 2, pp. 191–196, 2008.

[20] M. Jaziri, N. Mnif, V. Massardier-Nageotte, and H. Perier-Camby, "Rheological, thermal, and morphological properties of blends based on poly(propylene), ethylene propylene rubber, and ethylene-1-octene copolymer that could result from end of life vehicles: effect of maleic anhydride grafted poly(propylene)," *Polymer Engineering and Science*, vol. 47, no. 7, pp. 1009–1015, 2007.

[21] M. J. O. C. Guimarães, F. M. B. Coutinho, M. C. G. Rocha, M. Farah, and R. E. S. Bretas, "Effect of molecular weight and long chain branching of metallocene elastomers on the properties of high density polyethylene blends," *Polymer Testing*, vol. 22, no. 8, pp. 843–847, 2003.

[22] A. L. N. Silva, M. C. G. Rocha, and F. M. B. Coutinho, "Study of rheological behavior of elastomer/polypropylene blends," *Polymer Testing*, vol. 21, no. 3, pp. 289–293, 2002.

[23] R. R. Babu, N. K. Singha, and K. Naskar, "Phase morphology and melt rheological behavior of uncrosslinked and dynamically crosslinked polyolefin blends: role of macromolecular structure," *Polymer Bulletin*, vol. 66, no. 1, pp. 95–118, 2011.

[24] R. R. Babu, N. K. Singha, and K. Naskar, "Interrelationships of morphology, thermal and mechanical properties in uncrosslinked and dynamically crosslinked PP/EOC and PP/EPDM blends," *Express Polymer Letters*, vol. 4, no. 4, pp. 197–209, 2010.

[25] X. Yan, X. Xu, T. Zhu, C. Zhang, N. Song, and L. Zhu, "Phase morphological evolution and rheological properties of polypropylene/ethylene-octene copolymer blends," *Materials Science and Engineering A*, vol. 476, no. 1-2, pp. 120–125, 2008.

[26] N. Tortorella and C. L. Beatty, "Morphology and mechanical properties of impact modified polypropylene blends," *Polymer Engineering and Science*, vol. 48, no. 11, pp. 2098–2110, 2008.

[27] W.-Y. Guo and B. Peng, "Rheology, morphology, and mechanical and thermal properties of blends of propylene based plastomer and ethylene/1-octene copolymer," *Journal of Elastomers and Plastics*, vol. 40, no. 1, pp. 61–76, 2008.

[28] K. Wang, F. Addiego, N. Bahlouli, S. Ahzi, Y. Rémond, and V. Toniazzo, "Impact response of recycled polypropylene-based composites under a wide range of temperature: effect of filler content and recycling," *Composites Science and Technology*, vol. 95, pp. 89–99, 2014.

[29] O. Saravari, H. Waipunya, and S. Chuayjuljit, "Effects of ethylene octene copolymer and ultrafine wollastonite on the properties and morphology of polypropylene-based composites," *Journal of Elastomers and Plastics*, vol. 46, no. 2, pp. 175–186, 2014.

[30] I. Bochkov, R. M. Meri, J. Zicans, T. Ivanova, and J. Grabis, "Multi-component composites based on polypropylene. Ethylene-octene copolymer and zinc oxide," *Engineering Materials & Tribology XXII*, vol. 604, pp. 130–133, 2014.

[31] S. Bagheri-Kazemabad, D. Fox, Y. H. Chen, H. Z. Zhang, and B. Q. Chen, "Morphology and properties of polypropylene/ethylene-octene copolymer/clay nanocomposites with double compatibilizers," *Polymers for Advanced Technologies*, vol. 25, no. 10, pp. 1116–1121, 2014.

[32] P. Dias, Y. J. Lin, B. Poon, H. Y. Chen, A. Hiltner, and E. Baer, "Adhesion of statistical and blocky ethylene–octene copolymers to polypropylene," *Polymer*, vol. 49, no. 12, pp. 2937–2946, 2008.

PAPER II

Influence of Clay Nanofillers on Properties of Ethylene-Octene Copolymers

Alice Tesaříková, Dagmar Měřínská, Jiří Kalous, Petr Svoboda

Polymer Composites, 2017, DOI: 10.1002/pc.24568

Influence of Clay Nanofillers on Properties of Ethylene-Octene Copolymers

Alice Tesarikova, Dagmar Merinska, Jiri Kalous, Petr Svoboda
Department of Polymer Engineering, Faculty of Technology, Tomas, Bata University in Zlin, Vavreckova 275, Zlin, Czech Republic 762 72

The article deals with preparation, properties and usage of ethylene-octene copolymers/clay films. Different properties of two types of ethylene-octene copolymers (Engage 8540 and Engage 8842) with 17 and 45 wt% of octene (EOC-17 and EOC-45) were compared in nanocomposites with two types of clays—Cloisite 93A and Dellite 67. The aim was to evaluate the influence of (nano)filler type on ethylene-octene nanocomposites properties. Mechanical and thermal properties, morphology, and UV radiation degradation were observed. Furthermore, permeability of three different gasses was determined. EOC nanocomposites perform a higher elongation at break, especially EOC-45. Dynamic Mechanical Analysis (DMA) showed an increase of E' modulus of all nanocomposites in a wide range of temperatures compared to pure EOC. Intercalation of nanofillers was studied by transmission electron microscopy (TEM) and X-ray diffraction (XRD). It has been proved that EOC-45 has a better dispersion EOC-17. DSC analysis showed a shift in a crystallization temperature for EOC-17, where the nanofiller acted as a nucleation agent due to the worse dispersion. Barrier properties were improved by almost 100% by addition of organoclay for all measured gasses; they were best for EOC-17 nanocomposites due to a higher crystallinity. XRD together with transmission electron microscopy (TEM) showed much better dispersion for EOC-45 nanocomposites. Fourier transform infrared spectroscopy (FTIR) and accelerated UV aging showed C═O peaks for EOC nanocomposites. POLYM. COMPOS., 00:000–000, 2017.

INTRODUCTION

Packaging films are polymer products used in daily terms. There are a lot of different types of polymer films based on the usage purpose ranging from simple polyethylene (PE) bags to complicated multilayered bags designed for special purposes, such as barrier films [1–3].

Ethylene-octene copolymer (EOC) is a polyolefin elastomer newly developed by Dow Chemical Company (Delaware) and metallocene stereospecific catalysts are applied in a polymerization process. This copolymer has been extensively studied because of its extremely favorable properties [4–9]. EOC is an ethylene based elastomer, thus it shows an excellent compatibility with polyolefins, such as polyethylene and polypropylene (PP) [10–13]. The presence of octene comonomer in EOC does not allow crystallinity typical for PE or PP homopolymers which causes higher flexibility. Octene content in the copolymer is usually under 20 wt% [14, 15]. Blends of PP/EOC can exhibit enhanced impact properties. It is possible to find them in extruded or molded automotive exterior and interior parts, housing appliances, and other low-temperature applications. Pelletized EOC provides easy handling, mixing, and processability. Regarding these properties, EOC has been currently used as an impact modifier for PP to replace EPR (ethylene-propylene rubber) and EPDM (ethylene-propylene-dien-monomer rubber) [16–18].

As it has been described, EOC noticeably improves the impact strength. Conversely, it causes a decrease of PP tensile strength and stiffness [19–21]. Therefore, PP/EOC/mineral filler-based composites have been studied to enhance PP toughness and stiffness. These mixtures are immiscible [22–24]. Mineral fillers with a high aspect ratio, such as clay nanofillers, are presumed to be able to increase stiffness and strength of the thermoplastic polyolefins. They provide a greater possibility of energy transfer from one phase to another [25–28].

Polymer nanocomposites have been studied for a longer period of time. They are systems where polymer matrix is mixed with a certain type of nanofiller. Layered silicate mineral is nanofiller with the thickness of individual leaves in nanometers. Montmorillonite (MMT) has been extensively used nanoclay [29–35]. It is a layered clay mineral with octahedral and tetrahedral nets in the ratio of 2:1. Because of the exfoliation of its layer in polymeric matrix, MMT is modified by the intercalation, the insertion of a suitable organic compound, into MMT interlayer [30, 36–38]. This process allows broadening of d-spacing together with a reduction of dispersing forces

Correspondence to: A. Tesarikova; e-mail: atesarikova@ft.utb.cz or D. Merinska; e-mail: merinska@ft.utb.cz
PACS: 82.35.Np Nanoparticles in polymers
DOI 10.1002/pc.24568
Published online in Wiley Online Library (wileyonlinelibrary.com).

TABLE 1. List of applied polymer and clay materials – data sheet of Engage 8540, Engage 8842, Cloisite 93A and Dellite 67G.

Name	Abbreviation	Octene content (wt%)	Density (g/cm^3)	T_m (°C)	Melt flow index 190°C/2.16kg
Engage 8540	EOC-17	17	0.908	104	1.0 g/10 min
Engage 8842	EOC-45	45	0.857	38	1.0 g/10 min
	Organic modifier[a]	Moisture content (%)	Density (g/cm3)	Loss on ignition (%)	Size of particle (μm)
Cloisite 93A	MDHT	</=2	1.6	40	2–13
Dellite 67G	DMDHT	3	1.7	40–42	7–9

[a]MDHT = methyl, dehydrogenated tallow ammonium, DMDHT = dimethyl, dehydrogenated tallow ammonium (high modifier content).

between the individual montmorillonite platelets. MMT nanoplatelets play various roles in polymer matrix, especially the improvement of mechanical properties [39–42] should be considered.

Nanofillers reach this improvement by significantly lower loading in comparison with common fillers, such as calcium carbonate. These layers also perform as gas barriers. Therefore, the gas permeability is lower. It is conditioned by the orientation of long thick platelets in polymer matrix during compounding, mainly the extrusion or blowing.

However, detailed evaluation of mechanical and thermal properties of composites dealing with PP, EOC, and mineral fillers has been limited [43–45]. Similarly, the evaluation of barrier properties has not been studied properly yet.

Therefore, the aim of this work was to gain more information about the properties of EOC copolymer with two types of clay nanofillers and to evaluate the influence of applied nanofiller and its concentration on EOC copolymers.

Possibility of using the EOC with nanofillers, such as packaging materials for special purposes, has also been considered.

EXPERIMENTAL

Materials

Two ethylene-octene copolymers: Engage 8842 and Engage 8540 (both from The Dow Chemical Company, Gales Ferry, CT) - linear formula $(CH_2CH_2)_x[CH_2CH[(CH_2)_5CH_3]]_y$ as a polymer matrix were used.

Engage 8540 (EOC-17) is a polyolefin elastomer well suited for foam applications and it offers excellent performance for profile extrusion of tubing and hoses.

Engage 8842 (EOC-45) is an ultra-low density copolymer offering exceptional properties of an ultra-low density elastomer with the added potential of handing this polymer in pellet form (Table 1).

Maleic anhydride grafted polyethylene (PE-*g*-MA) Priex 12043 (ADDCOMP Holland BV) in 5% concentration was used to increase compatibility between the polymer matrix and the filler.

Organically modified montmorillonite (MMT) with tradename Cloisite 93A (Southern Clay Products) and Dellite 67G (Lavoisa Chimica Mineraria S.p.a) were used; these are recommended for nonpolar polymer matrices.

The quantity of mentioned nanofiller added to polymeric matrix was 5 wt%.

Samples Preparation

Ethylene-octene copolymers with clay fillers were compounded in a twin-screw extruder Scientific LTE 20–40 with a screw diameter of 20 mm and L/D ratio of 40/1. Temperatures of individual heating zones and extrusion head were from 170°C to 205°C. Rotation speed of the screws was 300 rpm and rotation speed of the volumetric feeding screw was 20 rpm. Extruded strands were air cooled and then transferred using a knife mill back to a pelletizer Scherr SGS - 50E.

Specimens for properties measurement were prepared by compression molding and die cutting. Nanocomposite in the form of pellets was placed between two PET sheets preventing the contact with air and thus oxidative degradation. Material was pressed into a mold with a size of 125 × 125 × 2 mm (for slabs). Pressing time was 5 min for slabs (thickness approximately 2 mm) and 3 min for films (thickness about 50 μm); pellets were molded without a frame, only between two plates of the machine. Afterwards, mold with the material was placed into a water-cooled hydraulic press and cooled down to room temperature.

Samples Evaluation

Mechanical Properties. Tensile tests were perfomed on a tensile testing machine Tensometer 2000. The initial speed was −1 mm/min for the module of 2% then it was increased to 100 mm/min until the rupture according to ISO 527–3. Tensile strength, elongation at break, and tensile modulus were evaluated.

Dynamic Mechanical Analysis. Dynamic mechanical analysis (DMA) measurements were conducted on the samples of a size of 20 × 5 × 2 mm made from premolded slabs on DMA Perkin Elmer. E' modulus and tan δ (tan delta = E''/E') for room temperature in the range of 1–200 Hz with a step of 2 Hz and for temperatures in the range from −100°C to +100°C at a frequency of 1 Hz and amplitude of 50 μm were measured.

DOI 10.1002/pc

TABLE 2. Tensile tests.

Composition	Tensile strength	Strain at break
	(MPa)	(%)
EOC-17 pure	27.950	997
EOC-17 + 5% Cloisite 93	30.658	991
EOC-17 + 5% Dellite 67	28.400	875
EOC-45 pure	5.740	> 1000
EOC-45 + 5% Cloisite 93	7.400	> 1000
EOC-45 + 5% Dellite 67	7.912	> 1000

Thermal Analysis – Differential Scanning Calorimetry. Differential scanning calorimetry (DSC) test was performed on Mettler Toledo DSC 1 with an external cooling unit while purging the chamber with nitrogen at 25 ml/min. Specimens with weight of about 7 mg were heated or cooled, and the heat flow changes were recorded. The rates of cooling and heating were 5, 10, 15, and 20°C per minute and the temperature range was from −90°C to 140°C.

Melt Flow Index. The melt flow index (MFI) measurement was performed on a capillary extrusion plastometer according to standard CSN 64 0861. The load of the piston was −2.16 kg and a diameter of the piston was −9.0 mm. The length of the capillary was −8 mm with a diameter of −2.1 mm.

X-ray Diffraction Analysis. X-ray diffraction analysis (XRD) was also performed. Diffractometric URD 6 was used. Measurements were done in the reflection mode in the range of 2 – 8° at a voltage of 40 kV and a current of 30 mA with a step size of 0.0263°.

Transmission Electron Microscopy (TEM). Transmission electron microscopy on JEM 200 CX at an accelerated voltage of 100 kV was conducted. Ultrathin sections prepared on Ultra-cryo-microtome LEICA at −100°C were used as the samples, the temperature of the knife was −50° C and the thickness was about 50 nm.

Gas and Oxygen Barrier Properties (GTR, OTR). Prepared nanocomposite pressed films with the thickness of about 50 μm and a diameter of 80 mm were measured. The pressure of 2 bar and a temperature of 35°C were set for the measurement of N_2. O_2 and CO_2 permeability were determined by a method of a constant volume on Julabo TW8 according to CSN 64 0115.

Accelerated Weathering Test. Measurement conditions (as defined in EN ISO 4892 - 2nd ingestion device) were set at the temperature of 38°C, irradiance of 60 Wh/m^2 filters simulating daylight and 50% RH. Accelerated UV degradation test by Xenotest Alpha was performed. One measurement cycle lasted for 46 days simulating one-year degradation.

Fourier Transform Infrared Spectroscopy (FTIR). The test on FTIR spectrometer AVATAR 320 (Nicolet) in the range of waves of 4,000 to 500 cm^{-1} was performed. Wave numbers from 1,810 cm^{-1} to 1,681 cm^{-1} were monitored. The measurement by ATR (attenuated reflection method) was conducted.

RESULTS AND DISSCUSION

Mechanical Properties

Table 2 presents mechanical properties of two types of EOC and nanofiller (Cloisite 93 and Dellite 67) in polymer matrix. As can be seen, the values of the tensile strength of EOC-45 with 5% Cloisite 93 (∼30%) and 5% Dellite 67 (∼40%) increased in comparison with pure EOC-45 material. However, the tensile strength is greater

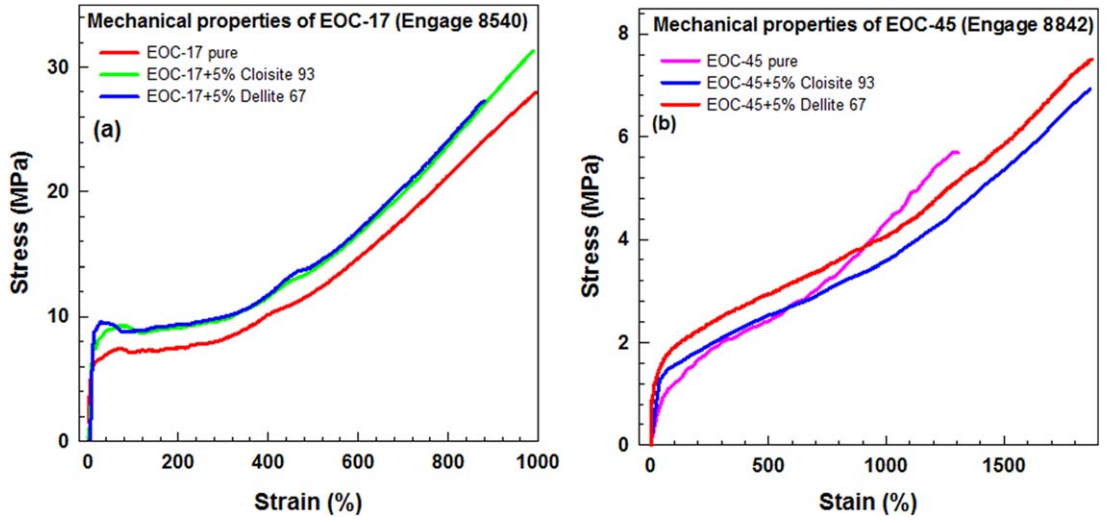

FIG. 1. Tensile properties of EOC-17 (Engage 8540) and EOC-45 (Engage 8842). [Color figure can be viewed at wileyonlinelibrary.com]

TABLE 3. Residual strain of pure EOC-17. EOC-45 and filled EOC-17.

Composition	l_0 (mm)	l_1 (mm)	l_2 (mm)	l_3 (mm)
EOC-17 pure	10	80	60.9	60.1
EOC-17 + 5% Cloisite 93	10	90	70.5	60.5
EOC-17 + 5% Dellite 67	10	80	60.8	60.0
EOC-45 pure	10	140	40.0	30.2
EOC-45 + 5% Cloisite 93	10	145	40.1	30.5
EOC-45 + 5% Dellite 67	10	140	40.5	30.5

EOC-45 with 5 wt% of nanoclay Cloisite 93 and Dellite 67. Measuring distance: l_0 = initial distance. l_1 = distance at maximum extension. l_2 = distance after 1 h of relaxation. l_3 = distance after 24 h of relaxation.

for EOC-17 most likely caused by higher crystallinity. Strain at break is almost identical for EOC-17 + 5% Cloisite 93 and it decreased by about 20% regarding Dellite 67.

Figure 1 illustrates tensile stress as a function of strain for pure EOC-17 (45) and EOC with 5% of Cloisite 93 and Dellite 67. EOC-17 exhibits the yield point and higher values of stress. The yield point has been caused by the presence of lamellar crystals. Clay increases the stress at the yield point for Cloisite 93 and also Dellite 67 nanocomposites by about 20% (Fig. 1a).

Higher content of octene groups in EOC-45 lowered the crystal presence. The crystals are not lamellar but small, spot-like [46, 47]. EOC-45 samples have not broken due to the size of test specimens and because of reaching the machine limit.

This unusual morphology is responsible for a lower modulus (higher softness), the absence of the yield point and better elasticity (Fig. 1). During the tensile test, the crystal orientation caused a stress increase in all samples [37].

The presence of nanoclay has risen the stress value; in the case of EOC-17 during the whole test and in the case of EOC-45 at a higher elongation.

Residual strain was measured during and after the tensile test (Table 2). EOC-45 samples exhibited better elasticity (a lower value of residual strain). As can been seen in Table 3, the composites showed slightly worse elasticity (higher values of residual strain). The most significant change occurred during the first hour of relaxation (EOC-45 ~300%, EOC-17 ~25%). The small relaxation of EOC-17 sample may be affected by the copolymer structure. Lamellas were oriented.

Dynamic Mechanical Analysis

Frequency sweep at room temperature was performed on pure EOC-17 and its blends with Cloisite 93 and Dellite 67 and pure EOC-45 with Cloisite 93 and Dellite 67. Overall trend of EOC-17 tan δ curves can be seen in Fig. 2a. Tan δ drops rapidly in the region of a frequency lower than 10 Hz. After reaching 10 Hz, all three samples lose their tan δ at a much smaller rate, but pure EOC-17 has a higher tan δ value if compared with both EOC with Cloisite 93 and Dellite 67. Differences between EOC-17 with Cloisite 93 and Dellite 67 are negligible. When the frequency approaches 200 Hz, tan δ of pure EOC-17 begins to increase but tan δ of filled EOCs does not. EOC-45 behaves differently when compared with EOC-17. Initially, in the low-frequency area, tan δ decreases very slowly for all three samples, but tan δ of pure EOC-45 increases rapidly after reaching the area of 100 Hz (Fig. 2b). However, tan δ of both EOCs with additives increases at a much lower rate. In both cases, fillers do strongly influence the frequency dependent on tan δ behaviour. Higher content of octene chains strongly influences tan δ behaviour but the effect is moderated by the

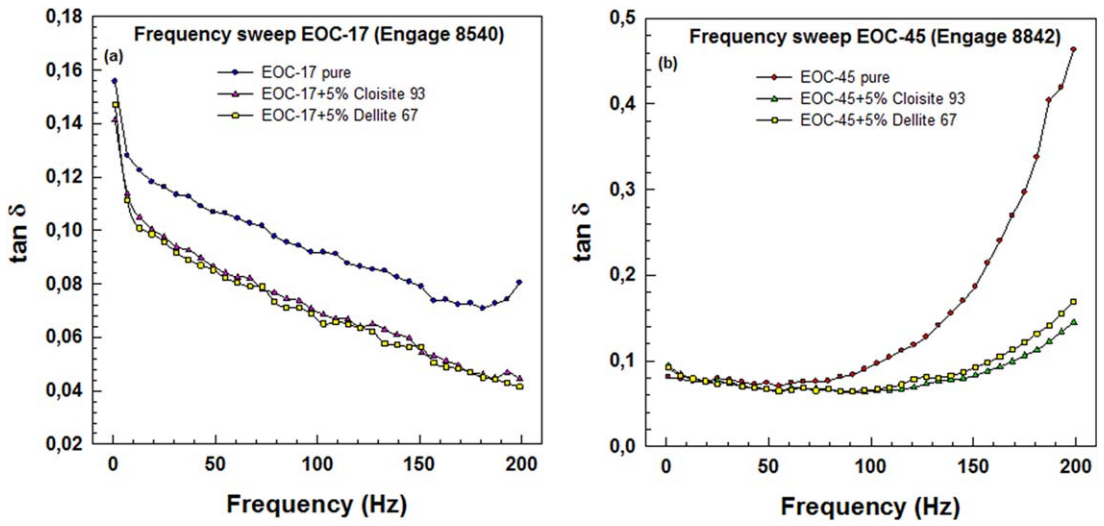

FIG. 2. Tensile stress as a function of strain for pure EOC-17 (45) and EOC with 5% of Cloisite 93 and Dellite 67. [Color figure can be viewed at wileyonlinelibrary.com]

 DOI 10.1002/pc

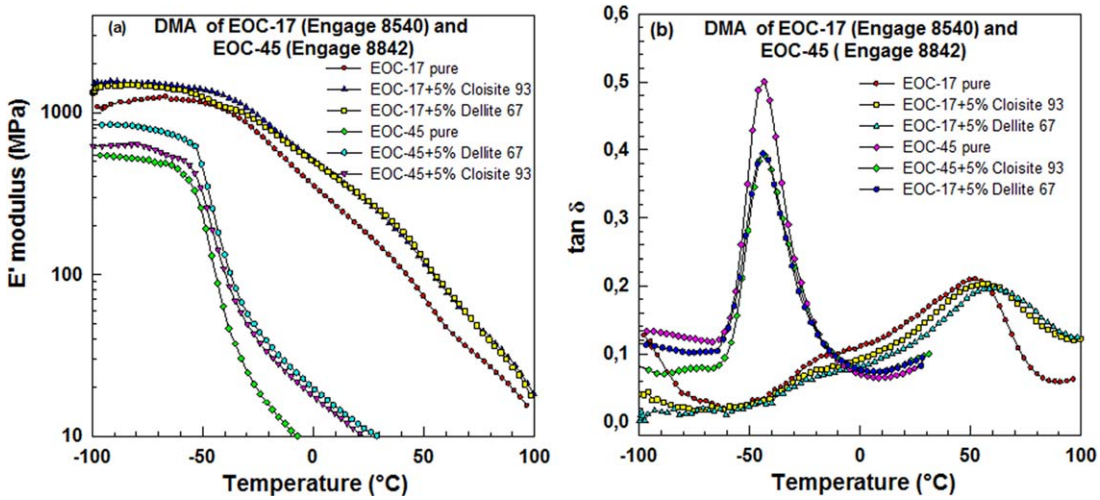

FIG. 3. DMA graphs temperature dependencies: EOC-17 (Engage 8540) with 5% Cloisite 93 and Dellite 67, EOC-45 (Engage 8842) with 5% Cloisite 93 and Dellite 67: (a) E' modulus, (b) tan δ. [Color figure can be viewed at wileyonlinelibrary.com]

filler addition. Both nanofillers have decreased tan δ leading to better elasticity of nanocomposites. The value of tan δ at a frequency of 100 Hz dropped by 25% for EOC-17 with Cloisite 93 and by 30% for EOC-17 with Dellite 67.

The value of tan δ is the highest for pure EOC-45 at high frequencies, the addition of Cloisite 93 and Dellite 67 reduces tan δ. This pattern is stronger for EOC-45 which could be explained by larger percentage of octene side chains leading to a stronger interaction between filler and matrix and to a smaller deformation. High tan δ of EOC-45 is caused by low crystallinity and "spot-like" crystals [46, 47]. A rise of tan δ in high frequencies is the disability of macromolecules to gain their original shapes. While filled samples are more elastic at high frequencies, pure EOCs are more viscous.

DMA curves of E' modulus and tan δ dependencies on temperature are shown in Fig. 3. Both EOCs behave similarly. E' drops after reaching a glass transition temperature. However, the drop is much sharper for pure EOC-45 and both composites. EOC-17 has a slightly higher modulus and its decrease with a rising temperature is more moderate if compared with EOC-45. Strengthening effect of additives is more significant for EOC-17. It also shifts E' to higher values.

This dependency may be caused by the unusual volume of side chains and thus different interactions with nanofillers. As nanocomposites perform two times higher E' modulus, the influence of nanoclays on the elastic modulus is significant.

Pure EOC-45 has E' value of 4.01 MPa at 30°C, filled EOC-45 has a modulus of 8.78 MPa (Cloisite 93) and 9.79 MPa (Dellite 67) at the same temperature. Impact of nanofillers falls with temperatures below 0°C and below T_g.

EOC-45 has a lower modulus and nanoclay fillers increase its modulus more than EOC-17 which shows a higher modulus with a smaller effect of the fillers.

The addition of nanofillers to EOCs decreases tan δ values if compared with pure EOC. When the melting temperature of polymer mixture is reached, nanofillers causes tan δ to retain some of its value. The decrease of tan δ before reaching the glass transition temperature is more significant for EOC-17. However, EOC-45 retains more of tan δ when the temperature approaches the melting point. EOC-45 and its nanocomposite mixtures behave similarly until the glass transition temperature is exceeded. Unlike EOC-17 and its nanocomposite mixtures, which shows similar behaviour in the temperatures outside a glass transition region.

Nevertheless, pure EOC-17 possesses rather higher tan δ in the area of glass transition. Curves can be influenced by low thermal conductivity of the samples. Pure EOC-45 reached the peak of tan δ of 0.5 and nanofillers addition lowered it to 0.39 while T_g values remained the same. This has proven that filled EOC exhibits better elasticity. However, EOC-17 with nanofillers performed a slightly higher tan δ at 90°C (0.05 for pure, 0.12 for nanocomposites).

Tan δ values showed linear dependency on the temperature, it rises with an increasing temperature. This is caused by a measured sample flow during mechanical testing at higher temperatures which leads to polymer chains elongation. Polymer chain return to its original shape is hindered by a nanofiller. These findings correspond with the studies of nanofiller behavior in other polymer matrix [46–48].

Differential Scanning Calorimetry

According to previous tests, nanofillers offer the best performance at 5% filling. Thus, DSC and FTIR measurement results focused on 5 wt% concentration.

DSC analysis results of pure EOC-17 and EOC-17 with both nanofillers are shown in Figs. 4 and 5 and in

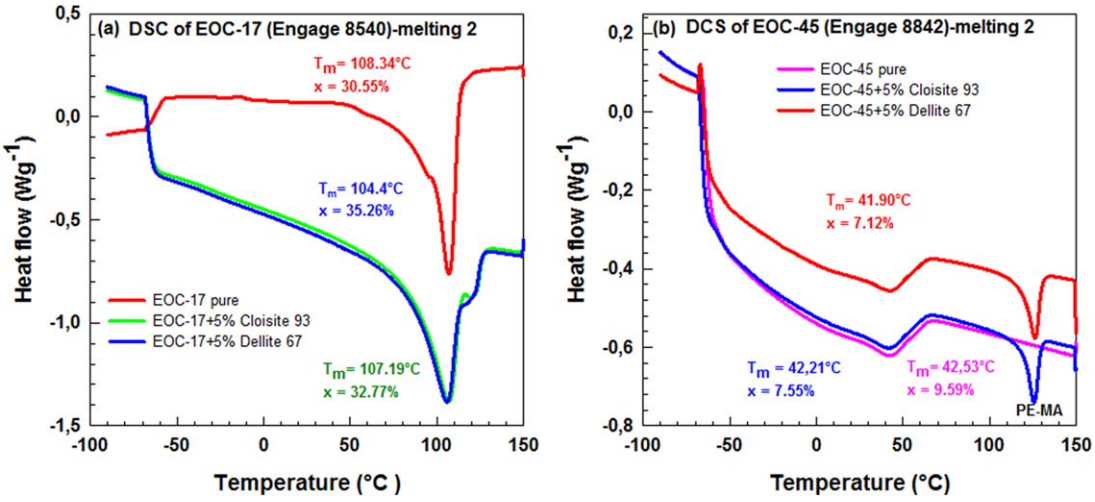

FIG. 4. DSC graph of melting 2: (a) EOC-17 (Engage 8540) and (b) EOC-45 (Engage 8842); with 5% Cloisite 93, Dellite 67 – heating rate 15°C/min. [Color figure can be viewed at wileyonlinelibrary.com]

Table 4. Melting temperature of pure EOC-17 is 108.34°C. The addition of Cloisite 93 decreases melting temperature to 107.14°C and Dellite 67 causes a drop of the melting point to 104.4°C. The peak occurring at the temperature of 126°C for nanocomposites is a consequence of the presence of maleinized PE (Fig. 4).

What is more, crystallinity is also dependent on the nanofillers presence. Crystallinity grows higher after nanofillers addition to EOC-17. Crystallinity increase is higher for Dellite 67, specifically from 30.55 to 35.26%, and Cloisite 93 addition leads to the crystallinity of 32.77%. Melting temperatures of EOC-45 have also altered with Cloisite 93 performing temperature change to 42.21°C and nanofiller Dellite 67 from 42.53°C to 41.90°C.

The influence on crystallinity is significant for EOC-17. Crystallinity and crystallization temperatures are higher within EOC-17 with nanofillers. Cloisite 93 increases the temperature of crystallization from 88.12 to 90.25°C while Dellite 67 alters it to 91.25°C (Fig. 5a).

Similarly with the composites, pure EOC-17 performs a crystallinity of 31.61%, Cloisite increases it to 32.14% and Dellite even to 33.21%.

Difference between crystallization temperatures is probably due to a lower mobility of polymer chains after the addition of nanofillers. Initial crystallization temperatures have also been influenced. They are higher for filled samples, specifically they shifted from 95°C for pure EOC to 110°C for filled samples. It can be assumed that nanofillers act as nucleation agents. However, both nanofillers in EOC-45 have affected crystallization temperatures and crystallinity only marginally.

Opposite to EOC-17, nanofillers in EOC-45 shift crystallization temperatures to higher values. Pure EOC-45

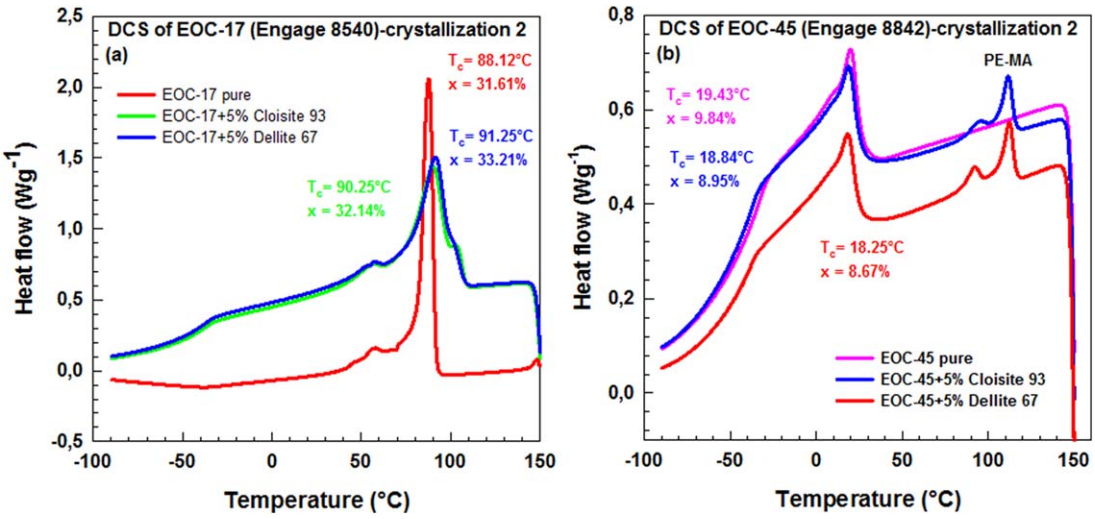

FIG. 5. DSC graph of crystallization 2: (a) EOC-17 (Engage 8540) and (b) EOC-45 (Engage 8842); with 5% Cloisite 93, Dellite 67 – cooling rate −15°C/min. [Color figure can be viewed at wileyonlinelibrary.com]

 DOI 10.1002/pc

TABLE 4. Melting 2 (crystallinity and peak) and crystallization 2 (crystallinity and peak) of pure EOC and filled EOC.

Melting 2		
Composition	Crystallinity (%)	Peak (°C)
EOC-17 pure	30.55	108.34
EOC-17 + 5% Cloisite 93	32.77	107.19
EOC-17 + 5% Dellite 67	35.26	106.41
EOC-45 pure	9.59	42.53
EOC-45 + 5% Cloisite 93	7.55	42.21
EOC-45 + 5% Dellite 67	7.12	41.90
Crystallization 2		
Composition	Crystallinity (%)	Peak (°C)
EOC-17 pure	31.61	88.12
EOC-17 + 5% Cloisite 93	32.14	90.25
EOC-17 + 5% Dellite 67	33.21	91.25
EOC-45 pure	9.84	19.43
EOC-45 + 5% Cloisite 93	8.95	18.84
EOC-45 + 5% Dellite 67	8.67	18.25

crystallizes at 19.43°C, whilst with Cloisite at 18.84°C and with Dellite at 18.25°C. TEM analysis for EOC-45 shows no nanofiller aggregates which could serve as nucleation agents. Additional peaks at temperatures above 100°C are caused by PE-g-MA compatibilizer crystallization. Crystallinity percentage was calculated by using a value of $\Delta H_m^0 = 290\text{J g}^{-1}$ for the heat of 100% crystalline polyethylene fusion [46–48].

As shown by XRD and TEM, the exfoliation of nanoclay in EOC-45 was more significant causing rather broad melting peak and a lower crystallization temperature. There were no aggregates that could serve as nucleating agents.

Different melting rate was used during heating to evaluate the influence of heating on melting temperatures

TABLE 5. Dependence of heating rate on the temperature of pure EOC and filled EOC.

Heating Rate (°C/min)				
	20	15	10	5
Composition T_m (°C)				
EOC-17 pure	110.83	108.34	106.16	105.66
EOC-17 + 5% Cloisite 93	109.38	107.19	105.53	104.86
EOC-17 + 5% Dellite 67	108.25	106.41	104.09	103.39
EOC-45 pure	43.85	42.53	41.55	40.28
EOC-45 + 5% Cloisite 93	43.18	42.21	41.28	41.08
EOC-45 + 5% Dellite 67	42.85	41.90	41.08	40.03

(Fig. 6 and Table 5). Increasing heating rate has led to higher melting temperatures. The most significant difference is between 20°C/min and 10°C/min.

Both nanofillers slightly decrease final melting temperatures, but the trend has been preserved. Crystallization temperatures are lower for higher cooling rates. The addition of nanofillers has caused a drop of crystallization temperatures for EOC-45 but an increase for EOC-17.

Side chains with the interaction of nanofillers affect the crystallization temperatures. EOC-45 has been influenced less than EOC-17 with the highest difference between 10°C/min and 5°C/min. The effect of filler on the initial T_m has been less significant for EOC-45.

Melt Flow Index

The comparison of MFI with the available data does not indicate the MFI change of filled EOC materials in comparison with pure EOC materials tested.

The measurement results of pure EOC-17 (45) have achieved approximately the same values as reported in data sheet (Table 1). A slight decrease of MFI for EOC samples with Cloisite 93 and Dellite 67 has been

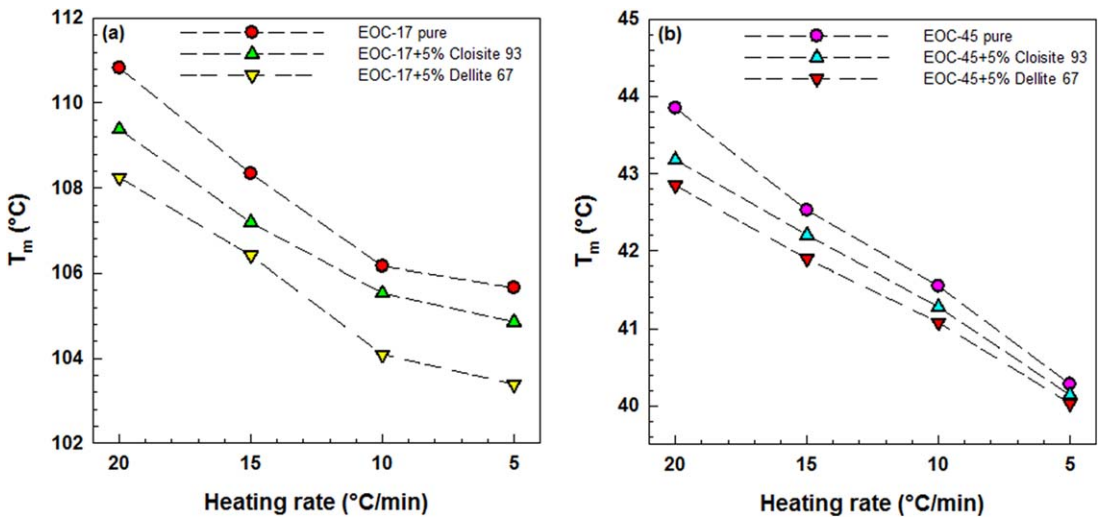

FIG. 6. Change of melting temperature of (a) EOC-17 (Engage 8540) and (b) EOC-45 (Engage 8842); with 5% Cloisite 93, Dellite 67 – heating rate from 20 to 5°C/min. [Color figure can be viewed at wileyonlinelibrary.com]

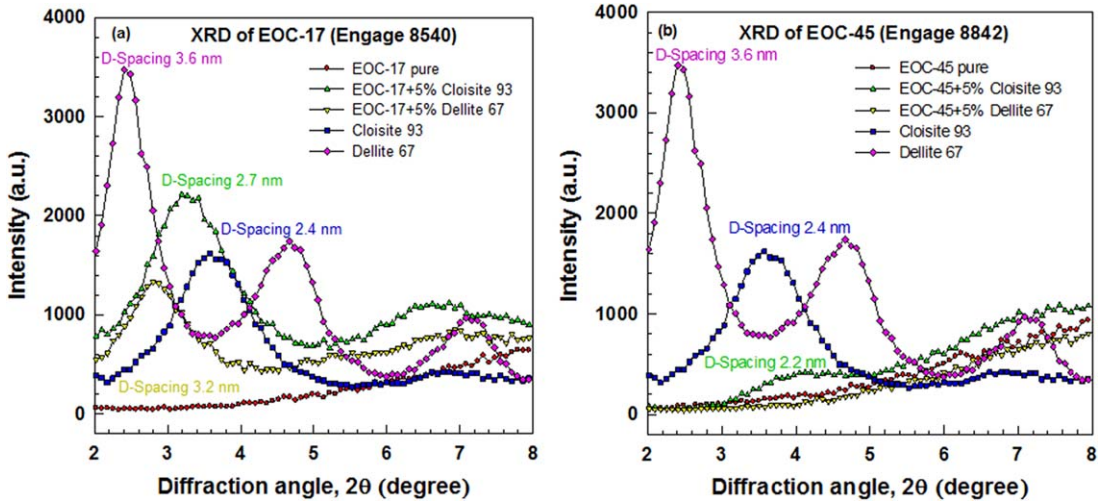

FIG. 7. XRD graphs of: (a) EOC-17 (Engage 8540) with 5% Cloisite 93 and Dellite 67, (b) EOC-45 (Engage 8842) with 5% Cloisite 93 and Dellite 67. [Color figure can be viewed at wileyonlinelibrary.com]

observed, but fillers in EOC matrices have not significantly altered the MFI value in comparison with pure EOC. The viscosity has increased with the addition of nanofillers from 0.8 g/10 min to 0.62 g/10 min for EOC-17 and from 0.8 g/10 min to 0.64 g/10 min for EOC-45 matrix, but MFI is not significantly changed depending on the content of nanofiller in the polymer matrix.

X-ray Diffraction

XRD patterns have been taken to determine the level of montmorillonite exfoliation in EOC matrices. Graphs with the curve of neat EOC matrix, original MMT nanofiller, and their mixture have been compared (Fig. 7).

Recorded results have proven incomplete montmorillonite exfoliation. Despite this incomplete exfoliation showed by XRD measurement, certain improvement of observed qualities has been detected.

Better results of X-ray diffraction can be observed for EOC-45 where the curves of filled materials compared with pure EOC sample are almost identical with no significantly different peaks in the area of Cloisite 93. Conversely, the curve of EOC-17 composite has exhibited a noticeable peak, almost the same as for Cloisite 93A. This can be connected with different EOC sample structure.

Figure 7a illustrates a small shift in a diffraction angle towards lower values corresponding to a small increase of D-spacing (Table 6) from 2.36 to 2.72 nm for EOC-17 + 5% Cloisite 93 nanocomposite. Partial intercalation and exfoliation can be pronounced for EOC-17. A sample of EOC-17 + 5% Cloisite 93 has shown the intercalation from 2.4 to 2.7 nm and platelets of EOC-17 + 5% Dellite 67 from 3.6 to 3.2 nm. There is a general pattern that plates with a greater distance are presumed to peel and exfoliate while the plates with a smaller distance will remain together.

Rather different scenario has been recorded for EOC-45 nanocomposite shown in Fig. 7b. Tensile strength of EOC-45 + 5% Dellite 67 has increased (see the mechanical properties). Platelets with a greater distance have performed the exfoliation (TEM, XRD). Platelets of EOC-45 + 5% of Cloisite 93 with larger distances have exfoliated as well. Other platelets have been separated only at a distance of 2.2 nm.

Transmission Electron Microscopy

TEM analysis results suggest that mixing has been successful for both EOCs. Figures 8 and 9 depict a comparison of nanofiller distribution in EOC-17 matrix with various types of clay. Even though the distributions are comparable, the exfoliation has been slightly better for EOC 17 with 5 wt% of Dellite 67 in polymer matrix.

TEM results have confirmed XRD conclusions indicating more significant exfoliation of nanofiller for EOC-45.

Similarly, Fig. 9 shows the distribution and exfoliation of nanofiller in polymer matrix, acceptable only for 5 wt% Dellite 67. To sum up, the best result in MMT exfoliation has been achieved for a mixture of EOC-45 and 5% of Dellite 67.

These results have revealed that 5 wt% of nanofiller in polymer matrix is optimal.

TABLE 6. D - Spacing of clays Cloisite 93, Dellite 67 and filled EOC.

Composition	D - Spacing (nm)
EOC-17 + 5% Cloisite 93	2.72
EOC-17 + 5% Dellite 67	3.16
EOC-45 + 5% Cloisite 93	2.18
EOC-45 + 5% Dellite 67	—
Cloisite 93	2.36
Dellite 67	3.60

DOI 10.1002/pc

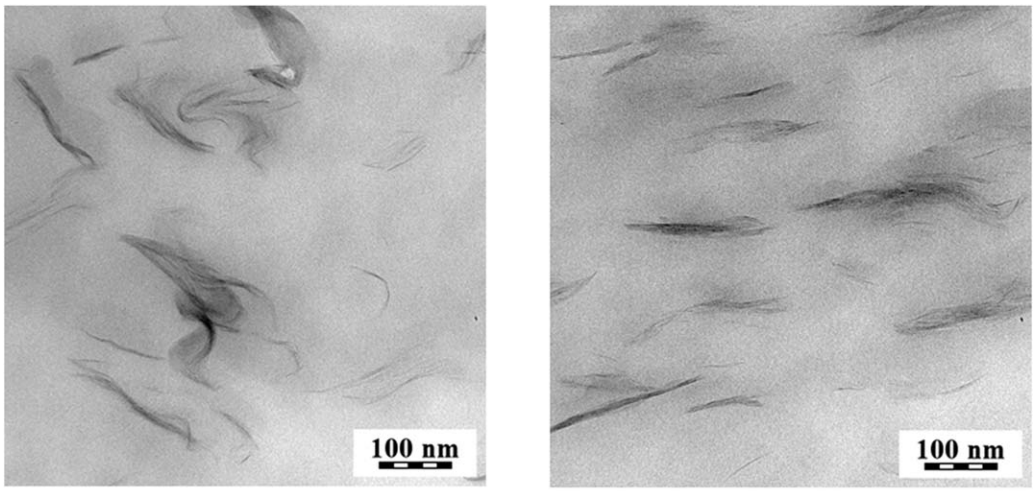

FIG. 8. TEM Pictures of EOC-17 (Engage 8540) with: (a) 5% Cloisite 93 and (b) 5% Dellite 67.

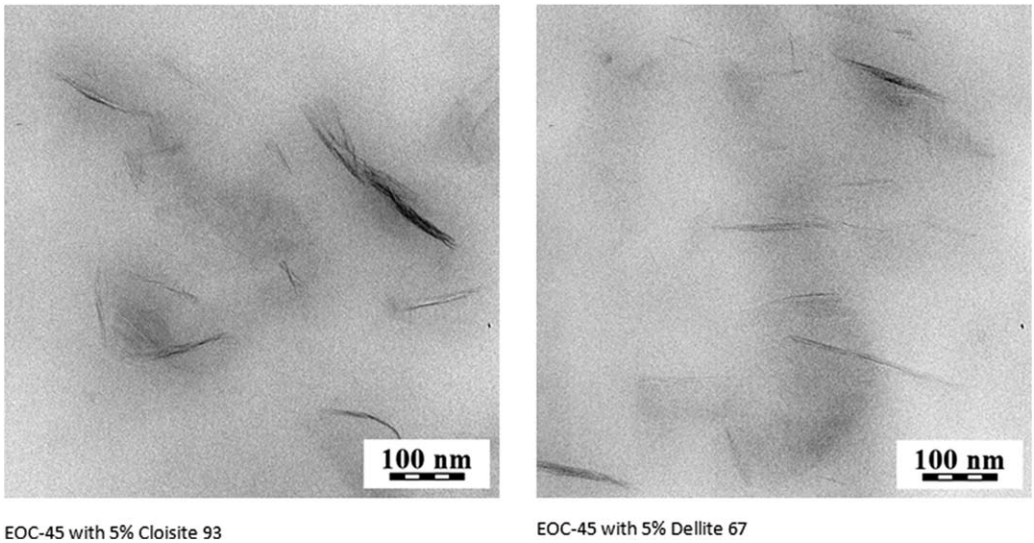

FIG. 9. TEM Pictures of EOC-45 (Engage 8842) with: (a) 5% Cloisite 93 and (b) 5% Dellite 67.

Barrier Properties of N_2, O_2, and CO_2

As mentioned above, ethylene-octene copolymers may be used as packaging materials for various packaging applications. Therefore, this study has also studied permeability for N_2, O_2, and CO_2, gases which should be prevented from penetrating through the film determined food wrapping. Platelets between hot plates were shaped into thin films in a press machine. The thickness of the

TABLE 7. The gas transmission rate for N_2, O_2 and CO_2.

Composition	Thickness (mm)	GTR pro N_2 (cm^3(STP)/m^2.den .0.1MPa)	GTR pro O_2 (cm^3(STP)/m^2.den .0.1MPa)	GTR pro CO_2 (cm^3(STP)/m^2.den .0.1MPa)
EOC-17 pure	0.52	509	1372	5361
EOC-17 + 5% Cloisite93	0.53	264	734	2619
EOC-17 + 5% Dellite 67	0.53	346	719	2627
EOC-45 pure	0.53	3055	8060	33369
EOC-45 + 5%Cloisite93	0.53	1683	4113	16664
EOC-45 + 5% Dellite 67	0.52	2033	4863	20701

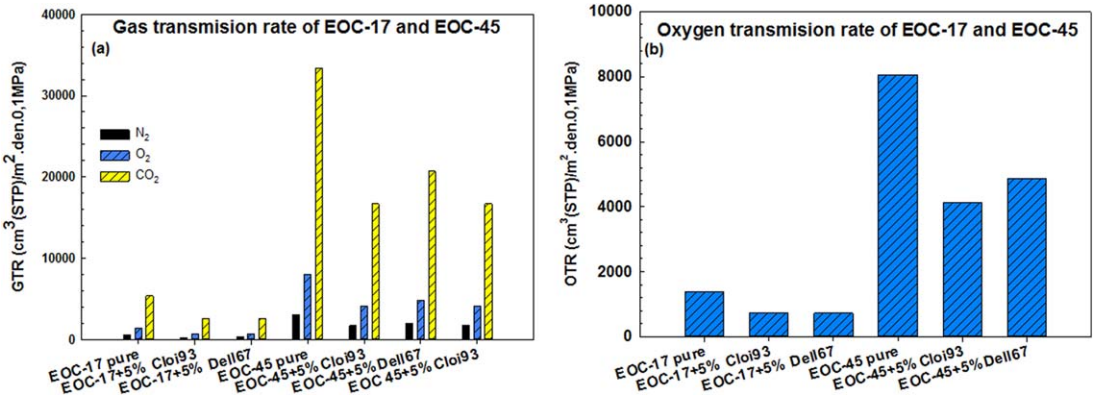

FIG. 10. Barrier properties of EOC-17 (Engage 8540) and EOC-45 (Engage 8842): (a) gas transmission rate (GTR), (b) oxygen transmission rate (OTR). [Color figure can be viewed at wileyonlinelibrary.com]

pressed film was about 50 μm and the size of MMT platelets was similar. That is why MMT leaves orientation has not been considered.

As the results demonstrate (Table 7), pure materials (EOC-17 and EOC-45) perform inferior properties compared with filled materials. The best combination seems to be EOC-17 + 5% Cloisite 93 and Dellite 67. Permeability decreased by 50% which may be due to a lower content of octene groups and higher crystallinity. Changed values of filled EOC-45 permeability are also illustrated in Fig. 10 (decreased by about 50% for Cloisite 93 and 40% for Dellite 67).

It can be concluded that nanofillers, specifically Cloisite 93 and Dellite 67, may improve EOC polymer matrix properties. If nanofillers are properly mixed in EOC matrix, gases permeability decreases. This may be caused by the distribution and dispersion of the nanofiller or by better exfoliation of MMT nanolayers in polymer matrix. It has been generally known that it is impossible to achieve a perfect orientation of MMT platelets during the samples pressing.

Accelerated Weathering Test and FTIR Analysis

FTIR analysis test has been performed for all the samples at the beginning and the end of the degradation.

EOC chain is composed only of CH_3 and CH_2 groups in 2,800 – 3,000 cm^{-1} area (Fig. 11). The change in the area from 1,811 cm^{-1} to 1,508 cm^{-1} was monitored by FTIR analysis. Maximum corresponds with the vibration of C—O bonds generated in degradation processes (Figs. 12 and 13). The largest increase has been monitored in the area of pure samples EOC-17 and EOC-45.

A substantial change of EOC-17 pure and EOC-45 + 5% Dellite 67 has been observed. Filled specimens have shown a smaller percentage of matrix degradation (Table 8). Chain disintegration has probably led to a molecular weight decrease during the sample degradation.

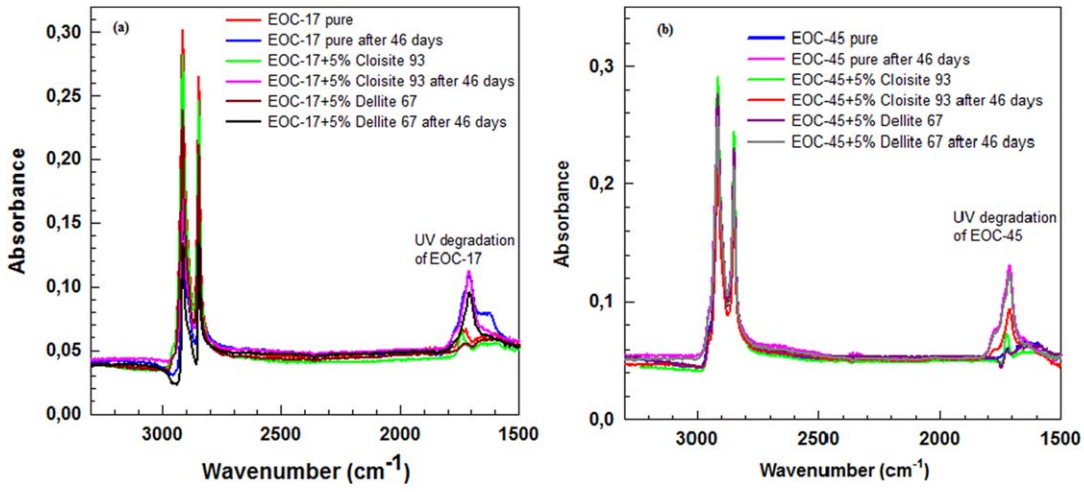

FIG. 11. FTIR graph of: (a) EOC-17(Engage 8540) pure and EOC17 with 5% Cloisite 93 and Dellite 67, (b) EOC 45(Engage 8842) pure and EOC 45 with 5% Cloisite 93 and Dellite 67. Pictures of change of EOC pure after 46 days of UV degradation, EOC +5% Cloisite 93 and Dellite 67 after 46 days of UV degradation. [Color figure can be viewed at wileyonlinelibrary.com]

 DOI 10.1002/pc

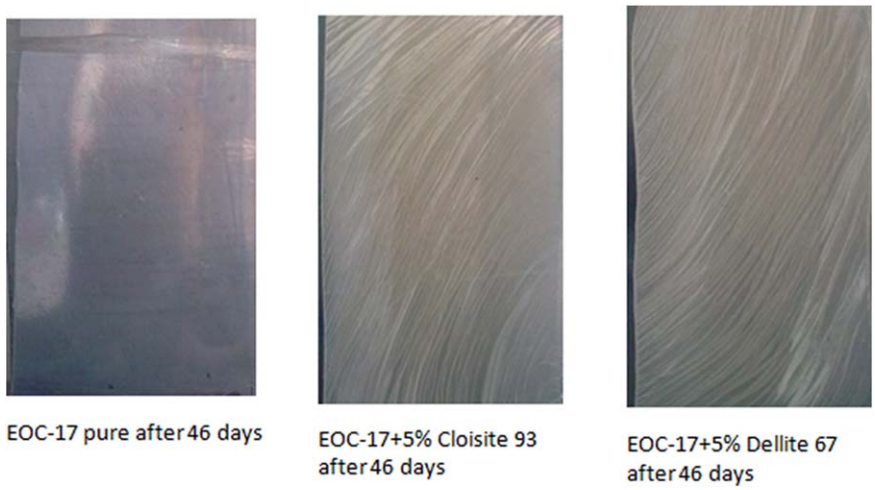

FIG. 12. Detailed photographs of EOC-17 pure, EOC-17 + 5% Cloisite 93 and Dellite 67 after 46 days of UV degradation. [Color figure can be viewed at wileyonlinelibrary.com]

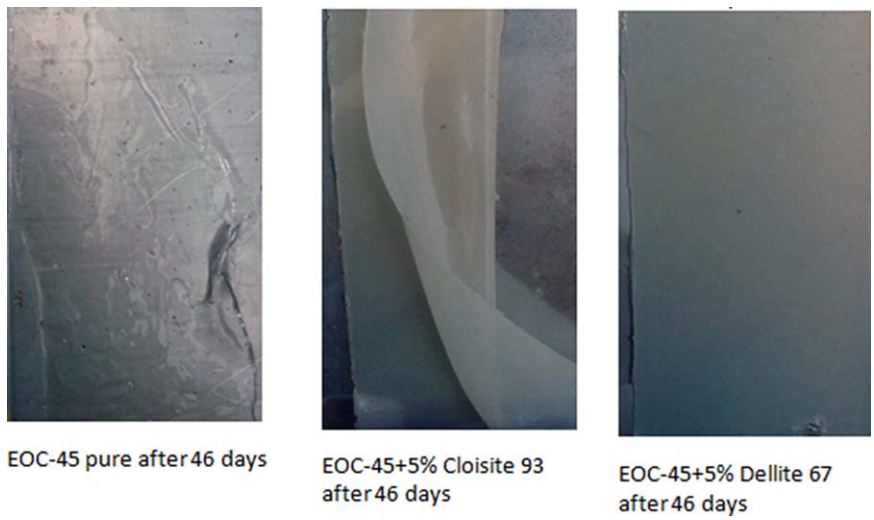

FIG. 13. Detailed photographs of EOC-45 pure, EOC-17 + 5% Cloisite 93 and Dellite 67 after 46 days of UV degradation. [Color figure can be viewed at wileyonlinelibrary.com]

The peaks of 1,720 cm^{-1} for pure materials have moved to lower wavenumbers and then expanded. The area may express the upper limit of ester groups (RCOOR, 1,750–1,725 cm^{-1}. HCOOR, 1,730–1,715 cm^{-1}) and ether bonds (C = OR, 1,720–1,700 cm^{-1}). Five percent of filling of the modified Cloisite 93 and Dellite 67 has improved observed characteristics, especially in longer term.

Divergences in the curves may be caused by different EOC densities and by various content of octene groups. Protection against the UV degradation has been more

TABLE 8. FTIR measurement of the peak area.

Composition	Peak area 1811–1508 cm–1	Peak area 46 days 1811–1508 cm–1	Peak height at 1720 cm^{-1} (Absorbance)	Peak height at 1720 cm^{-1} - 46 days (Absorbance)
EOC 17 pure	1.347	6.828	0.011	0.062
EOC 17 + 5% Cloisite 93	1.517	4.367	0.018	0.057
EOC 17 + 5% Dellite 67	1.158	3.717	0.004	0.046
EOC 45 pure	1.437	5.273	0.061	0.079
EOC 45 + 5% Cloisite 93	1.242	3.476	0.022	0.042
EOC 45 + 5% Dellite 67	0.714	4.518	0.006	0.072

effective in EOC-45 nanocomposite due to the perfect clay dispersion (Figs. 12 and 13).

CONCLUSIONS

Ethylene-octene copolymer matrices with two types of commercial nanofillers, specifically Cloisite 93, Dellite 67, of 5 wt% concentration have been observed. Nanocomposites may be applied in packaging and they may also serve as one layer in special multilayer packaging films; therefore, mechanical, barrier, morphological, thermal, and UV degradation properties have been studied.

As the content of octene groups of the EOC nanofiller also affect the viscosity of the resulting material. This may result in improving the improvement of certain properties. Strengthening effect of Cloisite has been stronger in EOC-45 mixture if compared with EOC-17. It was also demonstrated by the measurement of mechanical properties. Both EOC occurred on increase of tensile strength of about 20%. In addition to increased modulus, glass transition and melting temperature have been slightly shifted to higher temperatures as well. DMA results show nanofiller influence on mechanical properties; while tan δ has been decreased in a wide range of conditions, E' value has been higher for both added mixtures. From the results of DSC measurement is obvious that nanofillers have increased crystallinity for EOC-17 and EOC-45 and also influenced crystallization and melting temperatures. TEM micrographs have revealed homogeneity in MMT dispersion showing exfoliated platelets in EOC matrix. The best result of the MMT dispersion has been achieved in a mixture of EOC-45 and 5% of Dellite 67. The processing conditions have leads to improved dispersion nanoparticle in the EOC matrix. This was further supported by XRD study which shows a better dispersion of nanoparticles particles in case of EOC-45. Cloisite 93 and Dellite 67 have improved FTIR characteristics, especially in the long term. What is more, MMT has shown their capacity to enhance gasses barrier properties. GTR for all measured gases decrease about 50%, especially OTR decrease which would be very useful for the packaging material. The reducing the permeability for oxygen of the material can extend the shelf life of some packaged foods.

This study clarifies suitability of nanocomposites as packaging materials since nanoclay in polymeric EOC matrix may enhance desired film properties.

ACKNOWLEDGMENT

This article was written with the support of the project TA03010799, FR-TI 4/623, and IGA/FT/2017/007 TBU in Zlin.

REFERENCES

1. X.J. Gao, L.Q. Huang, and X. Li, *Adv. Print. Packag. Technol.*, **262**, 581 (2013).
2. H.B. Mu, W. Gao, Z.S. Chang, G.L. Wang, and G.J. Zhang, *IEEE Conf. on Electrical Insulation and Dielectric Phenomena (CEIDP)*, 160 (2013).
3. R.J. Xu, X.D. Chen, J.Y. Xie, Q. Cai, and C.H. Lei, *Ind. Eng. Chem. Res.*, **54**, 2991 (2015).
4. R. Theravalappil, P. Svoboda, J. Vilcakova, S. Poongavalappil, P. Slobodian, and D. Svobodova, *Mater. Des.*, **60**, 458 (2014).
5. C. Grein, M. Gahleitner, and K. Bernreitner, *Express Polym. Lett.*, **6**, 688 (2012).
6. R. Rajeshbabu, U. Gohs, K. Naskar, V. Thakur, U. Wagenknecht, and G. Heinrich, *Radiat. Phys. Chem.*, **80**, 1398 (2011).
7. R. Dangtungee, S.S. Desai, S. Tantayanon, and P. Supaphol, *Polym. Test.*, **25**, 888 (2006).
8. P. Doshev, D. Tomova, A. Wutzler, and H.J. Radusch, *J. Polym. Eng.*, **25**, 375 (2005).
9. P. Svoboda, *Polym. Bull.*, **74**, 121 (2017).
10. Y.B. Fu, D.L. Li, and W.C. Xu, *Thirteenth National Conf. on Packaging Engineering, TNCPE 13*, 129 (2010).
11. Z. Najarzadeh, A. Ajji, and J.B. Bruchet, *Rheol. Acta*, **54**, 377 (2015).
12. R. Shemesh, M. Krepker, D. Goldman, Y. Danin-Poleg, Y. Kashi, N. Nitzan, A. Vaxman, and E. Segal, *Polym. Adv. Technol.*, **26**, 110 (2015).
13. P.M. Wood-Adams, J.M. Dealy, A.W. deGroot, and O.D. Redwine, *Macromolecules*, **33**, 7489 (2000).
14. M.W.C. Guimaraes, F.M.B. Coutinho, M.C.G. Rocha, A. Farah, and R.E.S. Bretas, *Polym. Test.*, **22**, 843 (2003).
15. A.L.N. Silva, M.C.G. Rocha, and F.M.B. Coutinho, *Polym. Test.*, **21**, 289 (2002).
16. R.R. Babu, N.K. Singha, and K. Naskar, *Polym. Bull.*, **66**, 95 (2011).
17. R.R. Babu, N.K. Singha, and K. Naskar, *Express Polym. Lett.*, **4**, 197 (2010).
18. D. Pizele, V. Kalkis, R.M. Meri, T. Ivanova, and J. Zicans, *Mech. Compos. Mater.*, **44**, 191 (2008).
19. X.L. Yan, X.H. Xu, T.B. Zhu, C.H. Zhang, N. Song, and L. Zhu, *Mater. Sci. Eng. A-Struct.*, **476**, 120 (2008).
20. N. Tortorella and C.L. Beatty, *Polym. Eng. Sci.*, **48**, 2098 (2008).
21. W.Y. Guo and B. Peng, *J. Elastom. Plast.*, **40**, 61 (2008).
22. A. Grigalovica, R.M. Merijs, and J. Zicans, *Eng. Mater. Tribol.*, **Xxii**, 114 (2014).
23. M. Jaziri, N. Mnif, V. Massardier-Nageotte, and H. Perier-Camby, *Polym. Eng. Sci.*, **47**, 1009 (2007).
24. H.L. Kim, D. Rana, H. Kwag, and S. Choe, *J. Ind. Eng. Chem.*, **6**, 115 (2000).
25. K. Wang, F. Addiego, N. Bahlouli, S. Ahzi, Y. Remond, and V. Toniazzo, *Compos. Sci. Technol.*, **95**, 89 (2014).
26. O. Saravari, H. Waipunya, and S. Chuayjuljit, *J. Elastom. Plast.*, **46**, 175 (2014).
27. I. Bochkov, R.M. Meri, J. Zicans, T. Ivanova, and J. Grabis, *Eng. Mater. Tribol.*, **Xxii**, 130 (2014).
28. S. Bagheri-Kazemabad, D. Fox, Y.H. Chen, H.Z. Zhang, and B.Q. Chen, *Polym. Adv. Technol.*, **25**, 1116 (2014).
29. S.H.K. Devi, G.M. Shashidhara, and A.K. Ghosh, *Compos. Interface*, **17**, 217 (2010).

30. J. Golebiewski, A. Rozanski, and A. Galeski, *Polimery*, **51**, 374 (2006).
31. R.S. Chauhan, R. Chaturvedi, and P.K. Gutch, *Def. Sci. J.*, **56**, 649 (2006).
32. Kusmono, Z.A.M. Ishak, W.S. Chow, and T. Takeichi, *Express Polym. Lett.*, **2**, 655 (2008).
33. B.N. Narayanan, R. Koodathil, T. Gangadharan, Z. Yaakob, F.K. Saidu, and S. Chandralayam, *Mater. Sci. Eng. B-Adv.*, **168**, 242 (2010).
34. N. Hasegawa, H. Okamoto, M. Kato, and A. Usuki, *J. Appl. Polym. Sci.*, **78**, 1918 (2000).
35. P. Svoboda, C.C. Zeng, H. Wang, L.J. Lee, and D.L. Tomasko, *J. Appl. Polym. Sci.*, **85**, 1562 (2002).
36. F. Bellucci, A. Terenzi, A. Leuteritz, D. Pospiech, A. Frache, G. Traverso, and G. Camino, *Polym. Adv. Technol.*, **19**, 547 (2008).
37. W.R. Caseri, *Mater. Sci. Technol.-Lond.*, **22**, 807 (2006).
38. L.B. Manfredi, D. Puglia, A. Tomasucci, J.M. Kenny, and A. Vazquez, *Macromol. Mater. Eng.*, **293**, 878 (2008).
39. J. Soulestin, B.J. Rashmi, S. Bourbigot, M.F. Lacrampe, and P. Krawczak, *Macromol. Mater. Eng.*, **297**, 444 (2012).
40. T. Kuila, T. Tripathy, and J.H. Lee, *Conf. On Woodhead Publication in Materials*, 181 (2012).
41. F. Zandi, M. Rezaei, and A. Kasiri, *Compos. Sci. Technol.*, Pts 1 and 2, **471–472**, 751 (2011).
42. P. Santamaria, J.I. Eguiazabal, and J. Nazabal, *J. Appl. Polym. Sci.*, **119**, 1762 (2011).
43. C.S. Reddy, P.K. Patra, and C.K. Das, *Macromol. Symp.*, **277**, 119 (2009).
44. M. Maiti, S. Sadhu, and A.K. Bhowmick, *J. Appl. Polym. Sci.*, **101**, 603 (2006).
45. H.R. Dennis, D.L. Hunter, D. Chang, S. Kim, J.L. White, J.W. Cho, and D.R. Paul, *Polymer*, **42**, 9513 (2001).
46. P. Svoboda, R. Theravalappil, D. Svobodova, P. Mokrejs, K. Kolomaznik, K. Mori, T. Ougizawa, and T. Inoue, *Polym. Test.*, **29**, 742 (2010).
47. P.S. Chum, C.I. Kao, and G.W. Knight, *Plast. Eng.*, **51**, 21 (1995).
48. K.R. Mahest, H.N. Murthy, B.E. Kumaraswamy, N. Raghavendra, R. Sridhar, M. Krishna, N. Pattar, R. Pall, and B.S. Sherigara, *Front. Chem. China*, **6**, 153 (2011).

PAPER III

Basic Properties of PVC/PVB Pure and Recycled Material Blends and Their Preparation

Alice Tesaříková, Dagmar Měřínská, Jiří Kalous, Jana Orsavová, Michael Tupý, Jaroslav Císař

Manuscript

Basic Properties of PVC/PVB Pure and Recycled Material Blends and Their Preparation

A. Tesarikova[a*], D. Merinska[a], J. Kalous[a], J. Orsavova[b], M. Tupy[c], J. Cisar[c]

[a]Department of Polymer Engineering.
Faculty of Technology,
Tomas Bata University in Zlin, Nam. T. G. Masaryka 275, 762 72 Zlin.
CZECH REPUBLIC

[b]Language Centre.
Faculty of Humanities,
Tomas Bata University in Zlin, Nam. T. G. Masaryka 275, 762 72 Zlin.
CZECH REPUBLIC

[c]Fatra, a.s.
třída Tomáše Bati 1541
763 61 Napajedla
CZECH REPUBLIC

---

*corresponding author: Tel. +420 576 031331, Fax +420 577 210 172, atesarikova@ft.utb.cz

Abstract

This article deals with preparation, properties and usage of plasticized poly(vinyl chloride) (PVC) with poly(vinyl butyral) (PVB) blends. Binary blends of poly(vinyl chloride) (PVC) and poly(vinyl butyral) (PVB) were prepared by melt blending. The possibility of using PVB recycled from windshield disposal was also examined. The main aim was to prepare, compare and evaluate mechanical properties of PVC/pure PVB (PVC/PVB) and PVC/recycled PVB (PVC/R-PVB) blends. Selected properties of each blend containing from 0 to 100 % of pure or recycled PVB were compared. Immiscibility of PVC/PVB blends was determined by DSC method. Stability of mechanical properties in blends containing between 60-100 % of PVB may be caused by high molecular weight of PVB. Tan δ values at 1 Hz rose with PVB concentrations of 50% and more. The highest hardness value was established in pure PVC (86 ShoA). Shore A values decreased with PVB content ranging from 10% to 40% (70 ShoA). Afterwards, they started to grow again after reaching 100% of PVB matrix (84 ShoA). The trend of resilience values contrasted with the results of mechanical properties and hardness.
The study strongly recommends practical applications of these blends, such as in flooring, glue production and in the civil engineering and automotive industry.

Keywords **—** poly(vinylchloride), poly(vinylbutyral)**,** blends, mechanical properties, polymer waste, hardness

1. INTRODUCTION

Poly(vinyl butyral) is a low cost polymer of good recyclability, clarity, toughness, flexibility, and excellent adhesion properties[1]. PVB is one of a few polymers conceivable to mix with a plasticizer to obtain specific materials applicable in the automotive glass production, where they enhance and optimize occupants safety, or materials which could be employed in the building industry[2]. As a result of a worldwide usage of these materials, there is a consistently growing amount of PVB waste originating from safety glasses to be handled. Unfortunately,

because of the lack of verified methods of the re-use of these materials in safety glasses in the automotive industry, PVB films have mostly been stored in waste disposal sites.
Poly(vinyl chloride) (PVC) may also be combined with the plasticizer to obtain material with enhanced properties and a wider range of applications. PVC shows specific properties, such as a significantly low flammability[3] and good resistance to nonpolar solutions. On the other hand, it performs rather poor thermal and light (UV) stability[4-9]. Therefore, thermal stabilizers are commonly added. In spite of its thermal instability, plasticized PVC has been widely used and, similarly to PVB, it also forms a considerable amount of polymeric waste.

Even though the PVC re-use has already been studied[10-13], processing of recycled PVB into safety glasses has been rather complicated because of residual glass fragments. That is why, further alternatives of PVB waste re-use must be investigated[14, 15].

Based on the fact that both PVB and PVC are possible to be plasticized, preparing mixtures[16-18] of them may be one of the alternatives to treat the waste. As has been already dealt in several studies, it seems to be feasible with introducing new materials of specific properties[15, 19-23].

The main aim of this work was to examine optimal conditions of PVB/PVC blend preparation in order to develop further ways to treat PBV waste originating from safety glasses. To do so, it has focused on setting the optimal proportions and ratios of PVC and PVB mixing, on technological mixing conditions and on defining of reprocessing with the possible lowest material degradation. The novelty of this research lies in the comparison of properties of original and waste PVB film to emphasize that PVB waste may be considered as a valuable material.

2. EXPERIMENTAL AND METHODS

2.1. Materials

Suspension type of PVC Ongrovil S 5070 with K value of 70 was fluidly mixed with 38% of diisononylphthalate (DINP). Thermal stabilizer was added (0.5 % w/w to PVC) to obtain the final product of PVC powder with adsorbed additives. Molecular weight of PVC of 75 kg/mol was estimated according to K value.
Pure PVB (PVB) was plasticized with 28 % of triethylene glycol, bis(2-ethylhexanoate) (3GO). Commercially available PVB sheets were supplied by Kuraray Europe Moravia.
Recycled PVB (R-PVB) sheets were provided by Praktik group *(Czech Republic)*. Particles of PVB sheets were of a size of 1-5 cm^2 and contained less than 1.0 % (w/w) of impurities, such as glass and sand.

2.2. Sample preparation

First, optimal proportions of PVB and R-PVB to form PVC mixtures were investigated. Samples were prepared in Brabender kneader with two blunders W50 and friction of 2:3. The constant amount of 40 g of PVC/PVB was placed into a chamber and processed for 10 minutes at temperature of 150 °C and rotation speed of 50 rpm.
The initial tests have shown that blends may be mixed in any concentrations from 0 to 100% of PVB dispersed in PVC mixtures.
Blends of PVC/PVB and PVC/R–PVB applied to determine mechanical properties of each PVB/PVC ratio were prepared in the total amount of 2 kg in a continual BUSS extruder with two kneading chambers with friction. Processing time was from 6 to 8 minutes. The conditions

in the first (blending) chamber were set to temperatures of 130 / 140 / 150 / 160 / 160 / 160 °C and rotation speed of 250 rpm. In the second (transport) chamber, temperature was 160 °C and rotation speed 55 rpm. Extruded string was cut and granulated and blend particles were then mixed in a bag. Granules were kneaded by BUSS extruder, thereafter cut and granulated again to homogenize polymers.
Blends in a form of pellets were placed in between two PET sheets preventing the contact with the air and thus oxidative degradation. Mixtures were pressed in a mold of 125 x 125 x 2 mm. Temperature was set to 170 °C and pressing time was 5 minutes for platelets with thickness of approximately 2 mm. Afterwards, mold containing examined material was placed into a water-cooled hydraulic press and cooled down to room temperature.

2.3. Evaluation of prepared samples

2.3.1. Mechanical properties

Tensile tests were performed in the laboratories of FT UTB Zlin, using a tensile testing machine Quasar 25. Two speeds of tearing with the initial speed were used according to EN ISO 527-3, 1 mm/min to the module of 2%, then it was increased to 100 mm/min until causing the rupture. Tensile strength, elongation at break and tensile modulus were measured and evaluated.

2.3.2. DMA

DMA measurements were performed with the samples of a size of 20 x 5 mm prepared from pre-molded panels using DMA Perkin Elmer. E' modulus and tan δ (tan delta) damping, which is tangent of the phase angle and the ratio of E"/E' for room temperature in the range of 1-200 Hz with a step of 2 Hz, were measured and evaluated.

2.3.3. DSC

Glass transition temperature and melting behavior of composites were investigated by differential scanning calorimetry (DSC) using 200PC Phox NETZSCH operating under nitrogen flow. Samples of approximately 10 mg were weighed and sealed in aluminium sample pans. Prior to heating and cooling scans, composites were melted at 150 °C and maintained at this temperature for 5 min in order to erase the thermal history of the tested material. Subsequently, they were cooled from 150 to -80 °C at a rate of 10 °C/min and then heated from -80 to 160 °C at 10°C/min. Transition temperatures were expressed as the inflection points of calorimetric curves.

2.3.4. Hardness

Hardness test was performed using hardness test equipment Shore A (ShoA) in accordance with EN ISO 868. First, samples were kept at defined conditions for 24 hours to be stabilized. Afterwards, they were measured at laboratory temperature of 23 °C. Sample bodies consisted of three 2-mm thick plates so their thickness was 6 mm in total. Shore testing apex is hardened steel with a diameter of 1.25 mm. The immediate value of hardness was recorded 1 s after the release of the apex. The final value was established on five measurements at different points of the tested body.

2.3.5. Resilience

The method of resilience testing according to Schobe is commonly applied for a quick testing of plasticized materials (ASTM D 1054/B). Working part is constituted of a hammer with a

bumper in the shape of a small steel ball with a diameter of 7.5 mm. The potential energy of this part was 0.5 J and the speed of fall was 2 m s^{-1}. The value of resilience in the % of falling height was measured at the backward movement of the hammer.

3. RESULTS AND DISSCUSION

3.1. Mechanical properties

Table 1 presents mechanical properties of two types of PVB (PVB = pure PVB and R-PVB = recycled PVB) in PVC polymer matrix.
As can be seen in Figure 1, blends with PVB content between 10 and 30% (10.09 MPa) showed descending tensile strength values. Then these values grew. Blends containing 60 % of PVB or more (15.96 MPa) performed similar values to pure PVC (15.78 MPa). Blends with 80% of PVB showed the highest values in the comparison with pure PVC.

Table 1.
Tensile tests of PVC/PVB blends (pure PVB, recycled PVB).

Composition	Tensile strength (MPa)	Standard deviation of t. s.	Strain at break (%)	Composition	Tensile strength (MPa)	Standard deviation of t. s.	Strain at break (%)
PVC 100%	15.78	0.49	352.82	PVC 100%	15.78	0.49	352.82
PVC/PVB 10%	11.87	0.92	242.26	PVC/R-PVB 10%	12.54	0.99	240.79
PVC/PVB 20%	10.44	1.11	192.48	PVC/R-PVB 20%	10.62	0.81	186.63
PVC/PVB 30%	10.09	0.45	185.68	PVC/R-PVB 30%	10.75	0.98	185.61
PVC/PVB 40%	12.43	0.49	183.10	PVC/R-PVB 40%	11.13	1.00	181.06
PVC/PVB 50%	13.62	0.86	210.64	PVC/R-PVB 50%	13.92	1.03	201.42
PVC/PVB 60%	15.96	1.05	227.62	PVC/R-PVB 60%	15.41	0.95	216.35
PVC/PVB 70%	17.27	0.99	231.12	PVC/R-PVB 70%	17.29	0.85	217.17
PVC/PVB 80%	18.57	1.06	236.92	PVC/R-PVB 80%	18.83	1.02	221.50
PVC/PVB 90%	17.89	1.07	228.38	PVC/R-PVB 90%	17.21	0.78	199.41
PVB 100%	18.37	1.21	218.22	R-PVB 100%	17.84	1.12	178.65

Considering recycled PVB systems, the same trend has been recorded, only with slightly lower values.
Pure PVC performed the highest values of tensile strain (352%) which may be explained by the presence of only one type of plasticizer. The values of tensile strain decreased to the content 40% PVB. Then they began to rise again. The best results were obtained for 10-% PVB (240%) and 80-% PVB (221%).
Observable fluctuation of mechanical properties was dependent on PVB concentration in polymer blends. The course of recorded values may be explained by a certain degree of polymer immiscibility. In general, noticeable binodal character is due to a different chemical polymer composition as well as significantly varying polymer chain length.

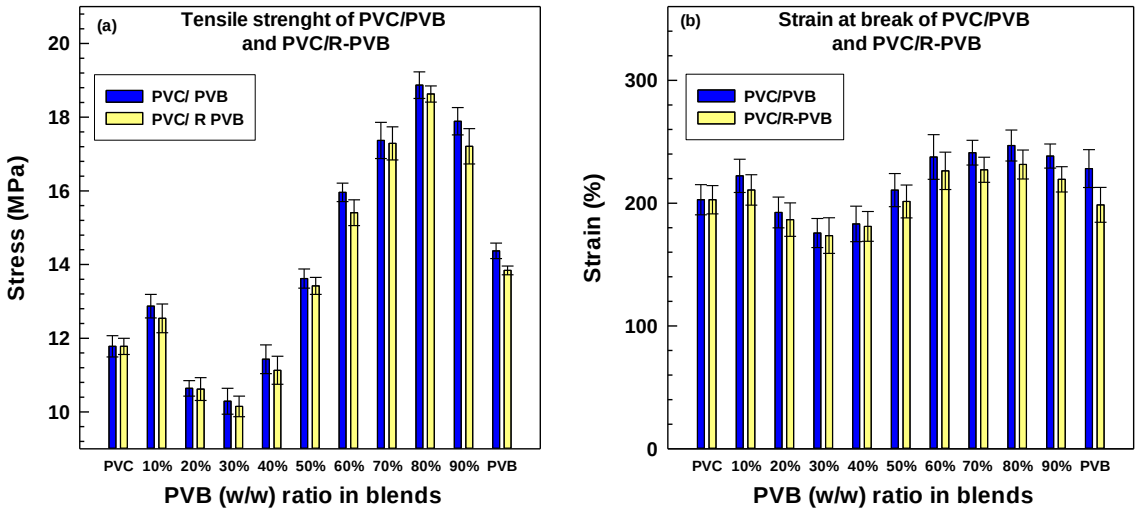

Fig. 1. Tensile properties of PVC/PVB blends, (a) tensile strength, (b) strain at break.

The miscible theory of tested polymers was estimated by Gibbs energy of blending. Entropy of blending depended on polymer morphology defined by particular molecular weight of blended polymers. What is more, the bimodal curve was significantly affected by applied mechanical (stirring) energy supporting the blending process. The enthalpy of Gibbs law was expressed by the interaction between PVB and PVC. Similarity of density of cohesive energies (polymer polarity) between PVB and PVC also positively influenced the blending process. Their difference determined the enthalpy ΔH. PVC and PVB values were very similar. Regarding PVB, density of cohesive energy value were adjusted by an amount of residual vinyl alcohol units. Gibbs energy (ΔG) [J/mol] may be determined according to the equation (1):

$$\Delta G = \Delta H - T\Delta S \qquad (1)$$

where ΔG is Gibbs energy of the blending process, ΔH is the enthalpy of the polymers used in the blending process, T is the temperature of the blending process and ΔS is the entropy, a degree of system disorderliness. The entropy was based on the system of amorphous PVB and PVC macromolecules and the presence of both plasticizers. However, as it was mentioned above, the entropy (ΔS) values were primarily determined by molecular weight of the blended polymers. The average molecular weight (M_w) of PVC was 75 kg/mol and the molecular weight of PVB was 410 kg/mol. PVB molecular weight is approximately 5.5 times higher than PVC molecular weight. Therefore, the amount of PVB macromolecules has to be 5.5 times smaller than the amount of PVC macromolecules in the unit volume. Gibbs energy values proved that the mixture with PVB content between 10 and 70 % (w/w) could be blended to a particular extent and that may cause a reduction in material strength.
The miscibility of the polymers was evaluated by differential scanning calorimetry (DSC) as described in chapter 3.2.

3.2. DSC

DSC analysis was conducted to determine polymer miscibility. Glass transition temperatures (T_g) of pure (non-blended) plasticized PVC and PVB were established. T_g of plasticized PVC was -29.5 °C and T_g of PVB was 16.8 °C. Obtained curves are shown in Fig. 2.

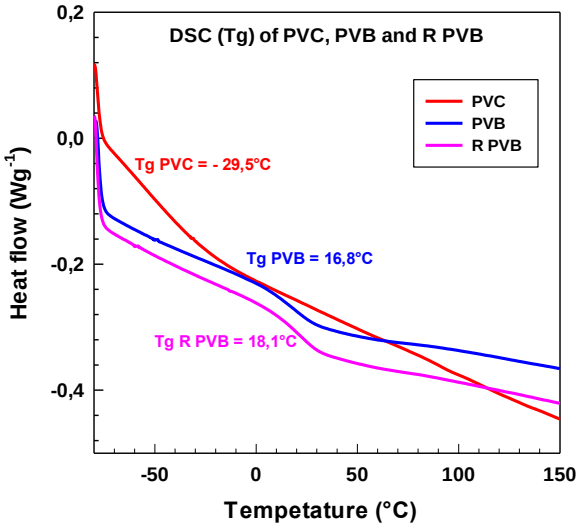

Fig.2: Glass transition temperatures of pure PVC, PVB and recycled R PVB polymers determined by DSC analysis.

Furher experiments focused on T_g values of selected blends. Polymer immiscibility was determined by two glass transition points, at a ratio of 20% and 80% of PVB. As shown in Fig. 3a and 3b, glass transitions at temperatures of -40.6 °C (PVC part) and 28.2 °C (PVB part) were determined in a blend containing 20% of pure PVB and -29.6 °C (PVC part) and 18.1 °C (PVB part) in a blend consisting of 80% of pure PVB.

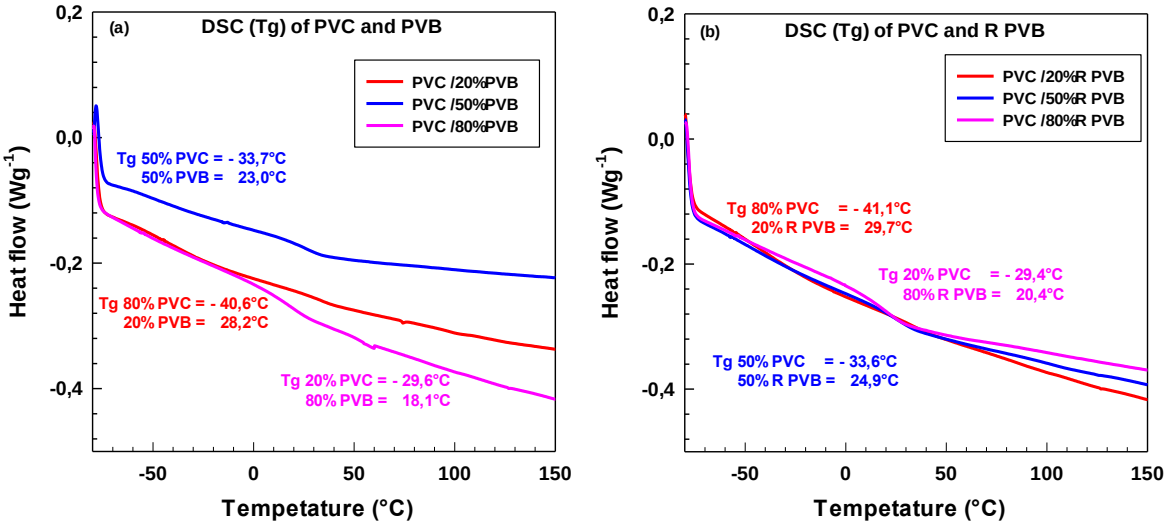

Fig. 3 DSC evaluation of blends of (a) 20%, 50% and 80% of PVB, (b) 20%, 50% and 80% of recycled R PVB.

3.3. DMA

Pure PVC showed a slight increase of tan δ with a rising frequency (Fig. 4). The addition of 10% of PVB and R-PVB caused the resonation peak at approximately 100 Hz. After reaching 150 Hz, tan δ values of both mixtures soared. An increase of PVB content to 20% affected the behavior of PVB and R-PVB. Non-recycled PVB maintained a resonation peak at approximately 100 Hz and a sharp increase of tan δ after exceeding 150 Hz. However, R-PVB did not perform a resonation peak and it fluctuated around the value of 0.36 after the initial drop

of tan δ value. Additional increase of PVB and R-PVB to 30% shifted a resonation peak of each mixture to different regions of frequencies; PVB resonated at 150 Hz whereas R-PVB started to resonate at 130 Hz and its peak was broader. After exceeding 170 Hz, tan δ of PVB fell slightly while tan δ of R-PVB showed an upward trend.

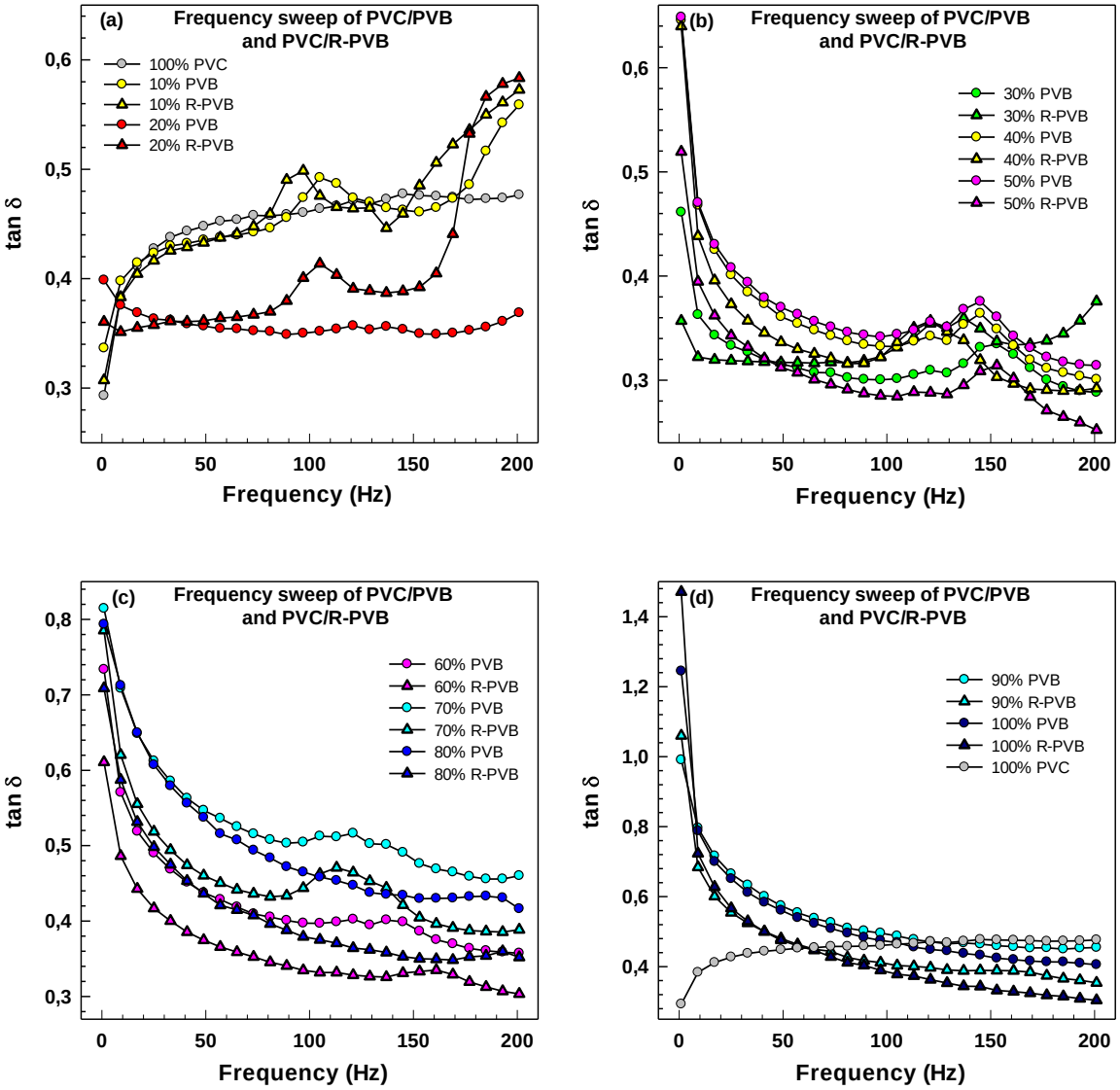

Fig. 4. DMA graphs (a-d), frequency sweep (tan δ) of PVC/PVB blends (pure and recycled PVB) at room temperature.

Considering 40% of PVB and R-PVB (Fig. 4b), resonation peaks were recorded in both mixtures but their frequencies differed. It was lower in the case of R-PVB. Even though further increase of PVB content to 50% caused a significant difference between tan δ of PVB and R-PVB, the overall trend was almost the same for both mixtures showing resonation peaks at around 150 Hz. PVB performed considerably higher tan δ if compared with R-PVB. Resonation peaks were much wider and shallower in the mixtures containing 60% of PVB than in 50-% mixtures albeit the trend was similar. When PVB and R-PVB concentrations were increased to 70%, the peak of R-PVB became narrower and higher than within the mixture of 60% of R-PVB. However, both peaks vanished at the concentration of 80% and a similar trend may be observed at the concentration of 90% of PVB. But in that case, the difference of tan δ between

PVB and R-PVB was lower (Fig. 4c). Pure PVB behaved very similarly in 90% mixtures, although its tan δ dropped faster at the frequencies above 100 Hz (Fig. 4d).
With PVB content of 50% and more, tan δ values at 1 Hz reached higher values. However, a rapid decline of tan δ value in a low frequency area from 1 to 20 Hz was monitored at PVB concentrations between 30% and 100%. Recycled PVB performed lower tan δ at the concentration reaching 40% if compared with PVB.
Frequency sweep of elastic modulus of PVC and its mixtures with PVB and R-PVB is shown in Fig. 5. Pure PVC displayed low E', which rose with an increasing frequency. After adding 10% of PVB and R-PVB, E' value grew. However, after reaching the certain frequency (120 Hz for R-PVB and 160 Hz for PVB) it plummeted. The increase of E' value was even more significant after the addition of 20% of PVB since E' did not slump at higher frequencies as it was recorded for pure PVB. Drops in E' values were affected by resonation of a sample during the measurement. If the content of PVB was increased to 30%, it caused further growth in E' value and rapid falls were not observed. At 30% of PVB and lower, PVB addition increased E' more substantially if compared with the addition of R-PVB.
This effect changed at the point of the concentration of 40%; PVB addition increased E' value much less effectively. The mixture with 50% of R-PVB performed significantly higher E' value (Fig. 5b) than 40% of R-PVB but the mixture with 50% of PVB decreased E' value slightly in comparison with 40% of PVB. Further growth of PVB content to concentrations of 60, 70 and 80% led to a lower E' value (Fig 5c). The mixture with 70% and to some extent also the mixture with 60% of PVB showed resonation peaks at higher frequencies. If concentration reached 90%, strengthening effect was recorded again and E' gained higher values than in the mixtures with 50% of PVB.

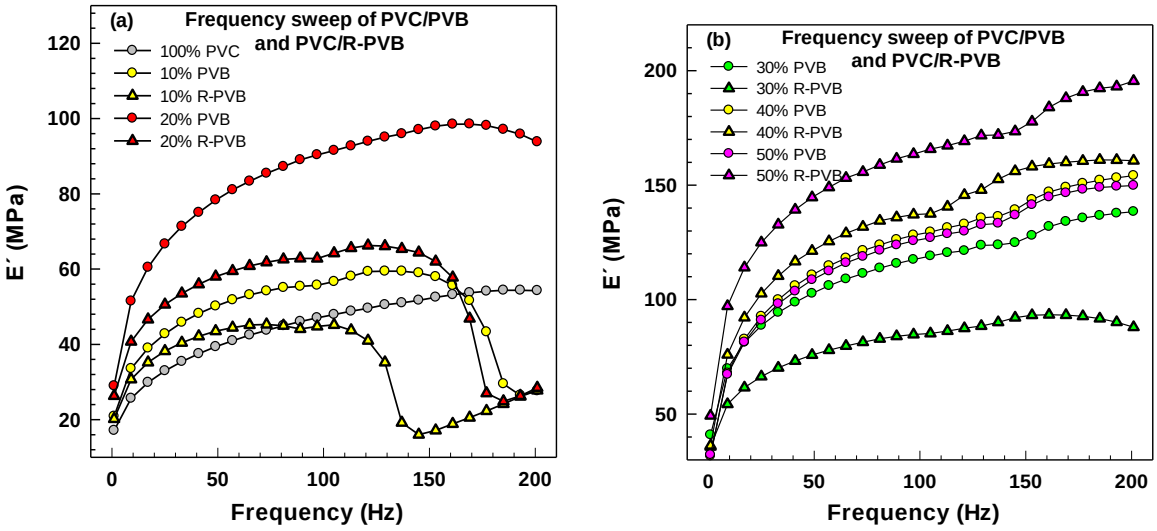

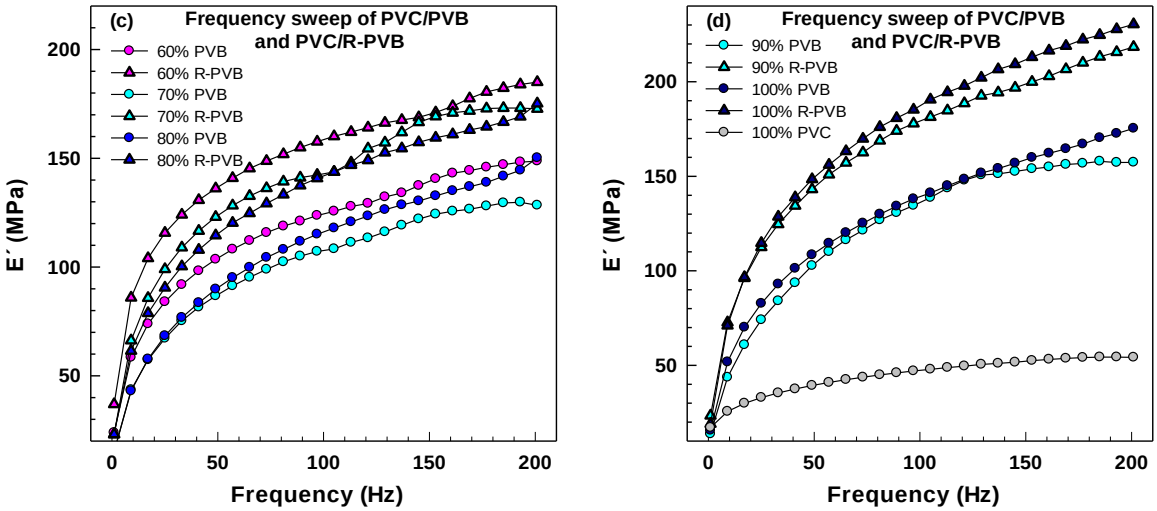

Fig. 5. DMA graphs (a-d), frequency sweep (E´) of PVC/PVB blends (pure and recycled PVB) at room temperature.

A few trends in E'- tan δ dependency may be observed. The behavior was dependent on PVB/R-PVB content. Concentrations may be divided into four different regions. The first region covered from 0 to 30% of PVB filling. In this region, PVB addition increased E' more than R-PVB. In the second region with PVB concentrations between 30 and 50%, R-PVB increased E' value more than PVB. Thus higher PVB concentrations led to higher E' values in both regions. Reversed effect of PVB on E' value is specific for the third region with PVB concentrations between 50 and 80%. Finally, strengthening effect appeared in the fourth region with PVB concentrations of 90% and more (Fig.5d).
Not only has tan δ measurement been performed, resonation frequencies were also examined. However, the effect of PVB concentration on E' was rather less significant if compared with tan δ values, with the only exception of a low PVB content.

3.4. Hardness

Hardness was subtracted from the instant value (ShoA) and pressing force F was calculated using the formula:

$F = 550 + H_{A,w}$,

where F is the contact force (mN) and H_A is the value of hardness on Hardness tester A (ShoA). Measured values of hardness and contact force F calculated afterwards are listed in Table 2. Graph 4 depicts dependency with a similar trend to the one recorded for mechanical properties. The highest value of hardness was reached by pure PVC (86 ShoA). The values of Shore A decreased in the area between 10% and 40% of PVB (70 ShoA), and then they grew until reaching 100% of PVB matrix (84 ShoA). The same tendency was maintained with calculated contact force values.

Table 2.
Test of hardness of PVC/PVB blends (pure PVB, recycled PVB) at room temperature.

Composition	Strength F (mN)	ShA H_A	Standard deviation	Composition	Strength F (mN)	ShA H_A	Standard deviation
PVC 100%	625	76,0000	1,1700	PVC 100%	624	74,0000	1,2700
PVC/PVB 10%	626	78,0000	1,4100	PVC/R-PVB 10%	625	76,0000	0,8200
PVC/PVB 20%	625	75,0000	0,9800	PVC/R-PVB 20%	624	74,0000	0,9500
PVC/PVB 30%	623	73,0000	1,2700	PVC/R-PVB 30%	621	71,0000	1,4600
PVC/PVB 40%	620	70,0000	1,0800	PVC/R-PVB 40%	615	69,0000	1,4100
PVC/PVB 50%	626	76,0000	1,1500	PVC/R-PVB 50%	621	71,0000	1,4100
PVC/PVB 60%	627	77,0000	1,4000	PVC/R-PVB 60%	622	72,0000	1,1000
PVC/PVB 70%	628	78,0000	1,6300	PVC/R-PVB 70%	625	75,0000	1,4000
PVC/PVB 80%	631	81,0000	1,7300	PVC/R-PVB 80%	625	76,0000	0,9800
PVC/PVB 90%	632	82,0000	1,2700	PVC/R-PVB 90%	630	80,0000	1,0700
PVB 100%	630	80,0000	1,5400	R-PVB 100%	628	78,0000	0,9500

The values of Shore A for recycled PVB followed the same dependency on the filler content (%) as pure PVB. Only a very small difference of Shore A values was possible to monitor in the region of 40% R-PVB with the obtained results 10% lower than values recorded for PVB matrix (Fig. 4). Similar trend of physical and mechanical properties is described in Fig.1.

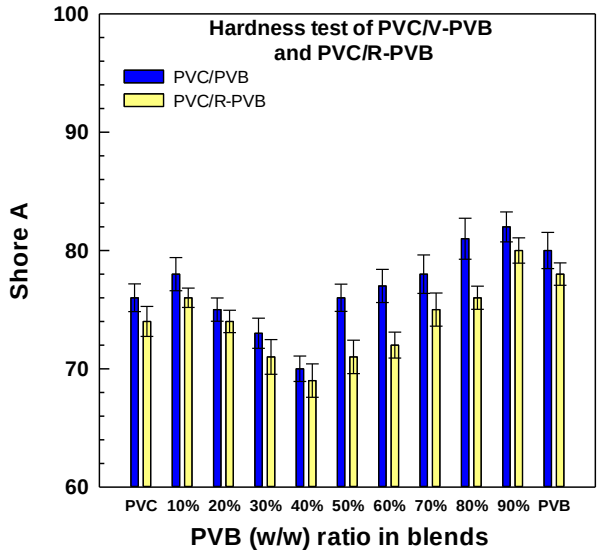

Fig. 6. Graph of Shore A of PVC/PVB blends.

As Fig. 6 shows, the effect of hardness characteristics dependency on PVB content stemmed from polymer immiscibility in a given PVB ratio. Immiscibility was observed even though both vinyl polymers showed similar values of cohesive energy and enthalpy blending ΔH_{blend} promoted positive conditions for their blending. This may be caused by different molecular weights of blended PVC and PVB; PVC molecular weight was approximately 70 $Kg.mol^{-1}$ and PVB molecular weight was around 410 $Kg.mol^{-1}$. It resulted in high entropy with a negative effect to Gibbs energy of blending.

While a smaller miscibility led to lower hardness and tensile strength, opposite effect was observed within resilience of polymer blends. Resilience growth was affected by polymer softening together with PVC and PVB immiscibility. Non-miscible effect was determined by differential scanning calorimetry.

3.5. Resilience

Resilience values were calculated from the formula:

$R = \frac{h}{H} \cdot 100,$

where R is the ratio of energy returned to the energy delivered during an impact (%), h is the height of reflection of the pendulum bumper after an impact (mm) and H is the lifting height of the pendulum bumper in the starting position (mm), H = 1.

Table 3.
Resilience test of PVC/PVB blends (pure PVB, recycled PVB) at room temperature.

Composition	R (%)	Composition	R (%)
PVC 100%	10	PVC 100%	10
PVC/PVB 10%	11	PVC/R-PVB 10%	11
PVC/PVB 20%	15	PVC/R-PVB 20%	14
PVC/PVB 30%	16	PVC/R-PVB 30%	15
PVC/PVB 40%	17	PVC/R-PVB 40%	16
PVC/PVB 50%	17	PVC/R-PVB 50%	16
PVC/PVB 60%	18	PVC/R-PVB 60%	17
PVC/PVB 70%	18	PVC/R-PVB 70%	18
PVC/ PVB 80%	19	PVC/R-PVB 80%	18
PVC/ PVB 90%	17	PVC/R-PVB 90%	16
PVB 100%	14	R-PVB 100%	13

The resilience was measured in the same conditions as hardness at room temperature without any heating. Tendency of the values (Table 3, Fig. 7) was in contrast with the results of mechanical properties and hardness measurement.

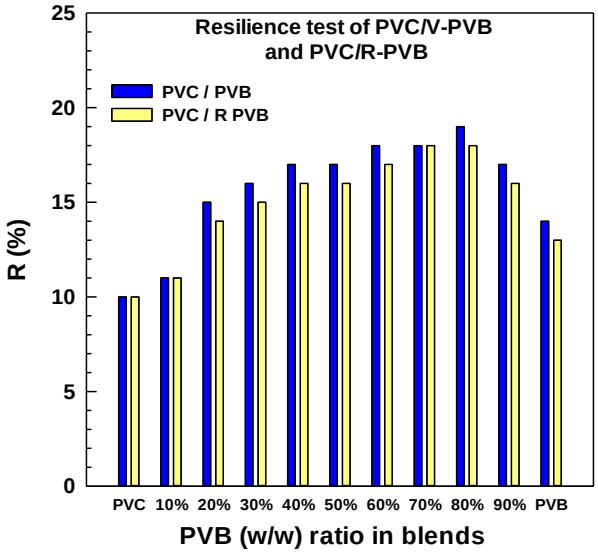

Fig. 7. Graph of resilience test of PVC/PVB blends.

From the starting point of 10% for pure PVC values for filled blends in the range from 10% to 40% of PVB increased from 11% to 17%. Then they levelled off in the region from 40% to 70% and thereafter fell to 14 % for the blends with PVB concentrations between 70 % and 100%.

Recycled PVB showed the same trend with the values lower by 1-2%.

4. CONCLUSION

PVC with different concentrations of PVB and recycled PVB in its matrix have been prepared and observed. All experiments have confirmed that recycled PVB may be considered as a valuable material applicable in the industry, especially in the form of polymer blends with plasticized PVC. Furthermore, miscibility of specific polymer ratios and possible immiscibility effects on material properties have been tested.

Examined polymers showed significantly similar polarity of macromolecules and employed plasticizers. Even though these polymers should be miscible, measurements of mechanical properties and differential scanning calorimetry confirmed considerably decreased strength and strain of blends, particularly within PVB concentration between 10 and 60 %. It was caused by PVB molecular weight 5.5 times higher than PVC molecular weight resulting in an increase of the enthalpy of Gibb's energy of the blending process. High PVB molecular weight probably contributed to the stability of mechanical properties within PVB concentrations in the range from 60 to 100 as well.

Pure PVC performed low E' values which rose with an increasing frequency. On the other hand, growing PVB concentration led to lower E' values.

As far as PVB is concerned, Shore A values depended on filler content (%) equally as pure PVB. Only a very slight difference of Shore A values was possible to record in R-PVB concentrations of 40% and more. This behavior was dependent on PVB content in the particular polymer blend. Final spinodal characteristics showed a similar trend as tensile strength.

Resilience values rose for the blends of PVB concentrations between 10% and 40%. Thereafter they maintained the same in the region of concentrations from 40% to 70% and decreased after reaching 70% of PVB or more. Less miscible polymer system resulted in lower hardness and tensile strength. However, it performed higher resilience.

This study clarifies suitability of the application of recycled PVB in the industry, especially in PVC blends. Not only is recycled PVB possible to be acquired at the acceptable cost, unlike PVB, it also performs decent mechanical properties and is not degraded during its lifetime.

ACKNOWLEGEMENT

This article was written with the support by the project TH 01030054, and IGA/FT/2017/007 TBU in Zlin.

REFERENCES

1 X. H. Zhang, H. Hao, Y. C. Shi and J. Cui, *Constr Build Mater* **93:**404-415 (2015).
2 F. Pelayo, M. J. Lamela-Rey, M. Muniz-Calvente, M. Lopez-Aenlle, A. Alvarez-Vazquez and A. Fernandez-Canteli, *Thin Wall Struct* **119:**324-331 (2017).
3 M. M. Hirschler, *Fire Mater* **41:**993-1006 (2017).
4 Y. C. Yang and P. H. Geil, *J Macromol Sci Phys* **B22:**463-488 (1983).
5 A. Aboutaybi, J. Bouzon, J. L. Taverdet and J. M. Vergnaud, *Abstr Pap Am Chem S* **197:**52-Poly (1989).
6 M. Gilbert and Z. Lui, *Plast Rub Proc Appl* **9:**67-72 (1988).
7 L. C. Uitenham and P. H. Geil, *J Macromol Sci Phys* **B20:**593-622 (1981).
8 F. R. Kulas and N. P. Thorshaug, *J Appl Polym Sci* **23:**1781-1794 (1979).

9 A. Royaux, I. Fabre-Francke, N. Balcar, G. Barabant, C. Bollard, B. Lavedrine and S. Cantin, *Polym Degrad Stabil* **137:**109-121 (2017).
10 M. Sadat-Shojai and G. R. Bakhshandeh, *Polym Degrad Stabil* **96:**404-415 (2011).
11 I. Spacek and J. Kotovicova, *Mendelnet 2010* 625-633 (2010).
12 X. Cui, F. M. Jin, G. Y. Zhang and X. K. Duan, *2nd International Symposium on Aqua Science, Water Resource and Low Carbon Energy* **1251:**256-259 (2010).
13 J. M. Lusinchi, Y. Pietrasanta, J. J. Robin and B. Boutevin, *J Appl Polym Sci* **69:**657-665 (1998).
14 S. Zarinabadi, *Bulg Chem Commun* **48:**112-118 (2016).
15 A. R. Zanjanijam, S. Hakim and H. Azizi, *Rsc Adv* **6:**44673-44686 (2016).
16 L. N. Chi, J. Wang, T. S. Chu, Y. J. Qian, Z. J. Yu, D. Y. Wu, Z. J. Zhang, Z. Jiang and J. O. Leckie, *Rsc Adv* **6:**28038-28046 (2016).
17 M. Asian, D. Weingarth, P. Herbeck-Engel, I. Grobelsek and V. Presser, *J Power Sources* **279:**323-333 (2015).
18 A. Bendaoud, C. Carrot, J. Charbonnier and C. Pillon, *Macromol Mater Eng* **298:**1259-1268 (2013).
19 P. J. Bora, N. Shahidsha, G. Madras, Kishore and P. C. Ramamurthy, *International Conference on Condensed Matter and Applied Physics (Icc 2015)* **1728:**(2016).
20 X. F. Wang, B. Jin, R. F. Peng, Q. C. Zhang, W. L. Gong, H. J. Huang, S. J. Chu and H. S. Dong, *J Polym Res* **22:**1-11 (2015).
21 S. H. Jiang, J. Wang, J. Wu, H. Z. Zhou and C. W. Jiang, *J Mater Res* **30:**2688-2701 (2015).
22 K. Aouachria, G. Quintard, V. Massardier-Nageotte and N. Belhaneche-Bensemra, *Polimeros* **24:**428-433 (2014).
23 K. Song, Y. Zhang and M. L. Minus. *Macromol. Chem. Phys*. **216**: 1313-1320 (2015).

PAPER IV

Mechanical Properties of PE, PP, Surlyn and EVA/Clay Nanocomposites for Packaging Films

Alice Tesaříková, Dagmar Měřínská

Book of conference 7th International Conference on Times of Polymers and Composites (TOP), Ischia, ITALY, Jun 22-26, 2014
Book Series: AIP Conference Proceedings, 2014, vol. 1599, p. 178-181

Mechanical Properties of PE, PP, Surlyn and EVA/Clay Nanocomposites for packaging films

A. Tesarikova[a] and D. Merinska[ab]

[a]Department of Polymer Engineering,
Faculty of Technology, Tomas
Bata University in Zlin, Nam. T. G. Masaryka 275, 762 72 Zlin,
CZECH REPUBLIC

[b]Centre of Polymer Systems,
University Institute, Tomas Bata
University in Zlin, Nad Ovcirnou 3685, 760 01 Zlin,
CZECH REPUBLIC

Abstract: The article deals with the preparation, properties and the usage of polymer barrier films. The problem of exfoliation and dispersion of the filler in the polymer matrix and mechanical properties of barrier films is discussed. This problem is connected with the use of nanofiller either in the polymer matrix or on the surface of prepared films. Together the evaluating comparison of used nanofillers is done. Polypropylene, polyethylene, EVA copolymer and Surlyn were used like polymer matrices. Organically modified montmorillonite (Cloisite 93A, 30B, 10A, Dellite 67) were used like nanofillers. Morphology (TEM, XRD) and mechanical properties were observed.

Keywords: nanocomposites, nanofillers, clays, montmorillonite, polymers, mechanical properties,
PACS: 82.35.Np Nanoparticles in polymers

INTRODUCTION

A new trend in chemical engineering is the development of new technologies and new types of active nanocomposites contain as the active ingredient nanomaterials. Such materials, especially packaging films are still on the market in limited quantities. Goal is to develop new technologies and materials that help to eliminate causes problems of production and technical limits of current commercial materials. Nanocomposites -, significantly affects their structure. Polymers with improved properties must have some degree of polarity, the resistance against gases (polar groups that enable the polymer to absorb moisture from the surrounding environment), good interaction between chains and a high glass transition temperature. To compare the improved properties of nanocomposites used for example of mechanical resistance, exfoliation, determination or comparison of morphology and more [1- 4].

Nanocomposites are materials comprising a polymer matrix, a nanofiller. To obtain nanocomposite with the required properties, especially in case of nonpolar ones it is necessary to apply a modification of clay nanofiller leading to the "organofilization" of filler. Nanocomposites differ from traditional plastic composites by providing improvements with minimal impact on density and do it without processing penalty. This article builds on our research in the area of packaging films. In this section, the mechanical properties of polyethylene, polypropylene, EVA and Surlyn nanocomposites are studied [5, 6].

This article is focused on the preparation and comparison of polymer nanocomposites supposed to be used in the packaging industry.

Times of Polymers (TOP) and Composites 2014
AIP Conf. Proc. 1599, 178-181 (2014); doi: 10.1063/1.4876807

EXPERIMENTAL

The polymer matrix used as carrier materials were Polyethylene (Borealis RB 707 CF fy Borealis AG) and Polyethylen (Bralen RB 03-23, fy Slovnaft Petrochemicalis Bratislava), EVA (Ultra FL 00218) and Surlyn A (8940). To increase compatibility between the polymer matrix and the filler was used for maleinized PP polypropylene (PP - MA) Exxelor PO 1015 K 1,909,201 1 3 EXXON and PE maleinized polyethylene (PE - Ma) AMPLIFY GR 216

Were used organically modified montmorillonites with tradenames Cloisite 93A, 30B, 10A (fa Southern Clay Products, Inc.), and Dellite 67G (fa Laviosa Chimica Mineraria S. p A.).

Polymers with the fillers (mass fraction 5 %) were compounded in a twin screw extruder ZE Berstdorff 25, screw diameter was 2 x 28 mm and a L / D ratio of 38 The temperature of the individual heating zones and the extrusion head was set at 210 ° C for PP and PE, 160 ° C for EVA and 200 ° C for the Surlyn A rotation speed was 15 per minute. The extruded wire was cooled in a water bath and then transferred using a knife mill back to granulate the unit Scherr SGS - 50E. On the laboratory blow line TVR - C9S - 7EX (UTB) connected to the extruder single screw unit Brabender OHG Duisburg were prepared from granules blown film. From the prepared granules were pressed plates of dimension 125 x 125 x 2 mm. The temperature for molding the PP and PE was 210 ° C, 150 ° C for EVA and for Surlyn 220 ° C. The pressing time was 3 minutes for all the polymers and the cooling period was from 7 to 15 minutes. To prepare the solution for deposition of the filler onto the surface of the polymer matrix was used a solvent consisting of ethyl acetate and ethanol, which is a normal part of the polymer printing inks used for printing on transparencies. 150 g of solvent was added 10 wt% (15 g), polyvinyl butyral (PVB) and 5 wt% (7.5 g) nanofiller. The solution was prepared separately for nanofiller Cloisite 93A and for Dellite 67.

The structure was studied using an URD-6 Diffractometer in the reflection mode in the range from 0.8000 to 11.9870 ° 2 θ at a voltage of 40 kV and 30 mA with a step size of 0.0263 °. The dispersion of the clays in polymer matrix and nanostructures were observed through microscopic investigations.

Samples of 40 x 20 mm made from molded plates were sent to the IMC Prague, where it was performed TEM. As samples were used ultrathin sections prepared on special Ultra - cryomikrotomu LEICA at -100 ° C, temperature of the knife - 50 ° C and a thickness of about 50 nm. Transmission electron microscopy was performed on a JEM 200 CX at an accelerated voltage of 100 kV.

Tensile tests were measured at the Faculty of Technology in UTB Demo Room ALPHA Technologies Ltd. On tensile testing machine TENSOMETR 2000. EN ISO 527-3 (64 0604) was used the speed of the tearing 2 - initial speed was 1 mm / min to the module 2%, then the speed was increased to 100 mm / min until rupture. For tensile tensile strength, elongation et break, tensile-Chor modulus and yield stress were measured and evaluated.

RESULT AND DISCUSSION

Polymer/clay nanocomposites have been studied for longer period as materials possible used in packaging industry. Therefore, this work is particularly interested in the mechanical properties. Table 1 and 2 presents the mechanical properties of polymers with nanofillers and the inside surface of the polymeric matrix.

In the table 1, it is possible to see the effect of fillers on tensile strength, tensile modulus and elongation. As it can be see, the values of net PP, PE and Surlyn are higher than the same materials enriched by fillers. Especially PP samples with fillers show significantly lower tensile strength. It can be assumed that the presence of filler in samples, compared to the net ones, has not a significant effect on tensile strength. However interesting is the fact that filled Surlyn had lower tensile strength, despite the fact that according to X-ray and TEM achieves the highest degree of exfoliation. Tensile modulus values were higher in samples filled with PE and Surlyn [7-10].

TABLE 1. Tensile tests - filler within the polymer matrix

Composition	Stress at break (MPa)	Elongation at break (%)	Yield stress (MPa)	Tensile modulus (MPa)
PP/93A	8,601	601,08	22,34	307,67
PP/67	8,657	619,08	21,01	313,97
PP	28,592	948,48	20,32	320,57
PE/10A	13,323	862,04	9,76	142,37

PE/30B	13,261	833,74	10,08	145,74
PE	15,903	790,30	9,73	117,37
EVA/93	20,580	1171,00	0,00	42,15
EVA/67	20,071	1112,10	0,00	38,60
EVA	19,51	1173,40	0,00	26,92
SRL/93	22,65	461,94	13,72	206,67
SRL/67	23,14	449,78	13,36	206,97
SRL	30,45	555,94	12,75	167,85
SRL/93	22,65	461,94	13,72	206,67
SRL/67	23,14	449,78	13,36	206,97

TABLE 2. Tensile tests - filler on the surface of the polymer matrix

Composition	Stress at break (MPa)	Elongation at break (%)	Tensile modulus (MPa)
EVA/93	16,58	1189,80	40,07
EVA/67	17,49	1254,30	34,26
EVA	19,51	1173,40	26,917
SRL/93	26,25	736,10	197,69
SRL/67	27,09	565,27	192,77
SRL	30,45	555,94	167,85

In the table 2, we can see that the filler material surface showed almost the same values as the pure material. The problem was that during tensile tests with the deposition of filler on the surface began to tear sooner than the blades.

The surface layer tore already at 12% elongation in almost all cases. Changing the properties in the case of the filler on the surface of the polymer matrix may also be caused by disruption of the surface of the blades during the deposition of filler (solvent effect). Tensile modulus at EVA filler surface and Surlyn with the filler surface slightly improved. The same fact was also observed for the filler within the polymer matrix. As shown by mechanical testing - the filler achieves a high degree of exfoliation, there is no difference in the imposition of filler - in a polymer matrix or at the surface [9-11, 13].

The exfoliation was very successful for Surlyn as it comes from results of TEM analysis. In Figure 1 it can be seen comparison of the distribution of nanofiller in a matrix of EVA and Surlyn. Distribution in both cases is about the same, but images suggest that in the case of EVA matrix the exfoliation is worse [11-14].

A) SURLYN+MMT 93A 5% B) EVA+MMT 93A 5%

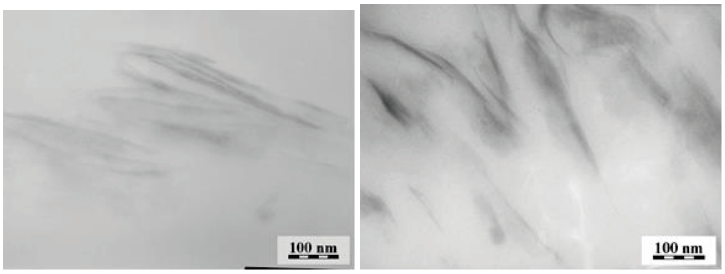

FIGURE 1. TEM Pictures of Surlyn a EVA Nanocomposites

Best resultsin X-ray diffraction can be observed Surlyn, where curves of both filled materials are compared with pure sample and they are almost identical, with no peaks. It can be stated that only filled Surlyn probably occurred highest grade of exfoliation when comparing the prepared samples [13-15].

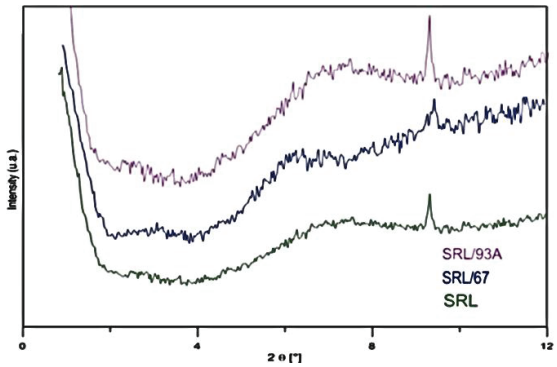

FIGURE 2. XRD Surlyn nanofillers, pure Surlyn, surlyn +MMT 93A 5% and surlyn + MMT 67 5%

CONCLUSION

Comparison of mechanical properties and exfoliation of the nanofiller in the polymer matrix was observed. Platelets of montmorillonite overlaped and may cause deterioration of the desired properties. The goal of the production of polymer nanocomposites is to achieve the full exfoliation. Important is the observation that nanofillers within the polymer matrix or on the surface of the polymer matrix mechanics affect polymer properties. We can say that good exfoliation of fillers can improve mechanical properties of nanocomposites. Nevertheless, the degree of exfoliation and orientation of the platelets is the most critical parameter .

ACKNOWLEDGMENTS

This article (specify by the fact) was written with support of Operational Program Research and Development for Innovations co-funded by the European Regional Development Fund (ERDF) and national budget of Czech Republic, within the framework of project Centre of Polymer Systems (reg. number: CZ.1.05/2.1.00/03.0111) and by the project TA03010799. Some of presented data were already published

Special acknowledgement is dedicated to Ing. Miroslav Pastorek for X-ray analysis.

REFERENCES

1. G. Zehetmeyer, J. M. Scheibel and R. M. D. Soares, et al. , *Polymer bulletin*, **70** (8), 2181-2191 (2013)
2. D. Merinska, H. Kubisova and A. Kalendova et al., *Journal of Thermal Analysis and Calorimetry*, **25** (1), 115-131 (2012)
3. J. Ma,; Z. Duan,and CH. Xue,; et al., *Journal of Thermoplastic Composite Materials*, **26 (** 4) , 555-569 (2013)
4. T. Seyidoglu and U. Yilmazer, *Journal of Applied Polymer Science* , **127** (2) 1257-1267 (2013)
5. S. Rodriguez-Llamazares, B. L. Rivas and M. Perez, et al., *Journal of Applied Polymer Science*, **122** (3) , 2013-2025 (2011)
6. Y. Y. Su, S. P. Rwei and W. J. Gou.; et al, *Journal of Thermoplastic Composite Materials* , **25** (8), 987-1003 (2012)
7. Q. P. Ran, H. Y. Hua and Y. Tian, et al., *Polymers & Polymer Composites*, **14** (3) 301-306 (2006)
8. M. H. Abdolrasouli, E. Behzadfar and H. Nazockdast, et al., *Journal of Applied Polymer*, **125** (1) E435-E444 (2012)
9. A. Sharif-Pakdaman, J. Morshedian and Y. Jahani, *Journal of Applied Polymer*, **125** (1), E305-E313 (2012)
10. L. Xie, L. Xia-Yan and Z-J. Han, et al., *Polymer Plastic Technology and Engineering*, **51** (12) ,1251-1257 (2012)
11. B. Akbari and R. Bagheri, *Journal of Nanocomposites*, **810623** (2012)
12. V. Goodarzi, S. H. Jafari, and H. A. Khonakdar, et al., *Journal of Polymer Research*, **18** (6), 1829-1839 (2011)
13. F.- Ch. Chiu, H. – Z. Yen and Ch. – E. Lee, *Polymer Testing*, **29** (3), 397-406 (2010)
14. H. - M. Yang, O. Zheng and M. Du, *Chemical Research in Chinese Universites*, **22** (5) 651-657 (2006)
15. A. Szep, A. Szabo and N. Toth, et al. *Polymer Degradation and Stability*, **91** (3) 593-599 (2006)

Alice Tesaříková Svobodová

Polymer Special and Multifunctional Films

Polymerní speciální a multifunkční folie

Doctoral Thesis

Published by Tomas Bata University in Zlín,

Nám. T. G. Masaryka 5555, 760 01 Zlín.

Print run: printed electronically

Typesetting: Alice Tesaříková Svobodová

This publication did not pass through editiorial or stylistic revision.

Year of Publication 2018